REFERENCES

Anquetil, P.A., Yub, H., Madden, J.D., Madden, P.G., Swager, T. M., and Hunter, I. W. (2002) Thiophene-based conducting polymer molecular actuators smart. Paper presented at Smart Structures and Materials 2002: Electroactive Polymer Actuators andDevices (EAPAD), Yoseph Bar-Cohen, Editor, Proceedings of SPIE Vol.4695

Appel, G., Yfantis, A., Göpel, W., and Schmeißer, D. (1996) Highly conductive polypyrrole film on non-conductive substrates. Synthesis metal, 83, 197-200.

Brie, M., Turcu, R., Neamtu, C., Pruneanu, S. (1996) The effect of intial conductivity and doping anion on gas sensitivity of conducting polypyrrole film to NH_3. Sensor and Actuator, B 37, 119 -122.

Careem, M.A., Vidanapathirana, K.P., Skaarup, S., and West, K. (2004) Dependenc of force produced by polypyrrole-based artificial muscles on ionic species involved. Solid State Ionics, 175, 725 – 728.

Çakmak, G., Küçükyavuz, Z., Küçükyavuz, S., and Çakmak, H. (2004) Mechanical, electrical and thermal properties of carbon fiber reinforced poly(dimethylsiloxane)/polypyrrole composites. Composites: Part A, 35, 417- 421.

Chandrasekhar, P. (1999) Fundamentals and Applications of Conducting Polymers Handbook, USA: Kluwer Academic Publishers.

Erik, T., Thostensona, Z.R., Choua, T. (2001) Advances in the science and technology ofcarbon nanotubes and their composites: a review Composites Science and Technology, 61, 1899–1912.

Fan, J., Wan, M., Zhu, D., Chang, B., Pan, Z., and Xie, S. (1999) Synthesis and properties of carbon nanotube-polypyrrole composites. Synthesis Metal, 102, 1266-1267.

Fehér, J., Filipcsei , G., Szalma, J., and Zrínyi, M. (2001) Bending deformation of neutral polymer gels induced by electric fields. Colloids and Surfaces A: Physicochemical and Engineering Aspects,183–185, 505–515.

Fu, Y., Palo, D.R., Erkey, C., and Weiss, R.A. (1997) Synthesis of Conductive Polypyrrole/ Polyurethane Foams via a Supercritical Fluid Process. Macromolecules, 30, 7611-7613.

Gangopadhyay, R. and De, A. (1999) Polypyrrole–ferric oxide conducting nanocomposites I. Synthesis and characterization. European Polymer Journal, 35, 1985 – 1992.

Göliz, Ç., Zuhal, K., Savaş, K., and Hasan, Ç. (2004) Mechanical, electrical and thermal properties of carbon fiber reinforced poly(dimethylsiloxane)/polypyrrole composites. Composites: Part A, 35 ,417–421

Han, G., Yuan, J., Shi, G., and Wei, F. (2004) Electrodeposition of pyrrole/ multiwalled carbon nanotube composites films. Thin Solid Films, 474, 64-69.

Harper, A.C. (2002) Handbook of Plastic, Elastomer, and Composites. New York : Mcgraw-Hill.

He, B.L., Zhou, Y.K., Zhou, W.J., Dong, B., and Li, H.L. (2004) Preparation and characterization of ruthenium-doped polypyrrole composites for supercapacitor. Materials Science and Engineer A, 374, 322-326.

Kim, M. S., Kim, H. K., Byun, S.W., Jeong, S. H., Hong, Y.K., Joo, J.S., Song, K.T., Kim, J. K., Lee, C.J., and Lee J.Y. (2002) PET fabric/polypyrrole composite with high electrical conductivity for EMI shielding. Synthesis Metal, 126, 233 – 239.

Kornbluh, R., Joseph, J., Heydt, R., Pei, Q., Pelrine, R., and Chiba, S. (2000) High field deformation of elastomeric dielectrics for actuators. Materials Science and Engineering, C 11, 89–100.

Krause, S. and Bohan, K. (2001) Electromechanical response of electrorheological fluids and poly(dimethylsiloxane) networks. Macromolecules, 34, 7179-7189

Kumar, D., and Sharma, R.C. (1998). Advances in conductive polymers.European Polymer Journal, 34, 1053-1060.

Lee, J.Y., Kim, D.Y., and Kim, C.Y. (1995) Synthesis of soluble polypyrrole of the doped state in organic solvents. Synthetic Metal, 74, 103-106.

Li, Y., and He, G. (1998). Effect of conditions on the two doping structures of polypyrrole. Synthetic Metal, 94, 127-129.

MacDiarmid, A.G. (2001) A novel role for organic polymers. Synthetic Metals,125(1), 11-22.

Madden, J.D.W., Madden P.G.A. and Ian W. H. (2001) Polypyrrole actuators: modeling and performance, as part of the Electroactive Polymer Actuators and Devices conference, SPIE 8th Annual International Symposium on Smart Structures and Materials, Newport Beach; CA.

Malone, E. and Lipson, H. (2000) Freeform Fabrication of Electroactive Polymer Actuators and Electromechanical Devices, Mechanical and Aerospace Engineering, Cornell University evan.malone@cornell.edu

Marco, F., Suàrez, R., and Compton, G. (1999) In situ atomic force microscopy study of polypyrrole synthesis and the volume changes induced by oxidation and reduction of the polymer. Journal of Electroanalytical Chemistry, 462, 211–221.

Mitsumata, T., Sugitani, K., and Koyama, K. (2004) Electrorheological response of swollen silicone gels containing barium titanate. Polymer, 45, 3811-3817.

Omastová, M., Piontec , J., and Kośina, S. (1996) Preparation and characterization of electrically conductive polypropylene/polypyrrole composites. European Polymer Journal, 32(6), 681-689.

Onishi, K., Sewa, S., Asaka, K., Fujiwara, N., and Oguro, K. (2000) Morphology of electrodes and bending response of the polymer electrolyte actuator. Electrochimica Acta, 46, 737–743.

Pelrine, R., Kornbluh, R., Joseph, J., and. Chiba, S. (1994) Electrostriction of Polymer films for Microactuators, Journal of Application Polymer Science, 53, 79-84.

Pelrine, R., Kornbluh, R., Joseph, J., and Chiba, S. (1995) Proceedings of The First International Micromachine Symposium, Tokyo.

Prissanaroon, W., Ruangchuay, L., Sirivat, A., and Schwank, J.W. (2000) Electrical conductivity response of dodecylbenzene sulfonic acid-doped polypyrrole films to SO_2-N_2 mixtures. Synthetic Metals, 114, 65-72.

Puvanatvattana, T. (2005) Electroactive Polythiophene/Polyisoprene Elastomer Blends, MS Thesis, Petroleum and petrochemical College, Chulalongkorn University

Reece, D.A., Innis, P.C., Ralph, S.F., and Wallace, G.G. (2002) Electrohydrodynamic synthesis of polypyrrole coated polyurethane colloidal dispersions using the electrocatalyst Tiron Colloids and Surfaces. A Physicochemical and Engineering Aspects, 207, 1–12.

Ruangchuay, L., Sirivat, A., and Schwank, J. (2004) Selective conductivity of polypyrrole-based sensor on flammable chemicals. Reactive and Functional Polymers, 61, 11 – 12.

Scheinbeim, J.I., Newman, B.A., Z.Y., and Ma, J.W.L. (1992) Electrostrictive respons of elastomeric polymers. Journal of Polymer Science, 33, 385-342.

Shiga, T., Okada, A., and Kurauchi, T. (1993) Electroviscoelastic effect of polymerblends consisting of silicone elastomer and semiconducting PolymerParticles. Macromolecules, 26, 6958-6963.

Simmons, M.R., Chaloner, P.A., and Armes, S.P. (1995) Synthesis Characterization of Colloidal Polypyrrole Particles Using Reactive Polymeric Stabilizers. Langmuir, 37(13), 2743-2749.

Sommer, P. and Dr Larson. (2002) Artificial Muscles, Ris National Laboratory,Condensed Matter Physics and Chemistry Department. http://www.risoe.dk/fys- artmus/MIC-ARTI.pdf.

Song, M.K., Kim, Y.T., Kim, B.S., Kim, J., Char, K., and Rhee, H.W., (2004) Synthesis and characterization of soluble polypyrrole doped with alkylbenzenesulfonic acids. Synthetic Metals, 141 315–319

Van Vught, F.A. (2000) Transparent and conductive polymer layers by gas plasma Techniques, Ed. Mayorga, R.V: The International association of Science and Technology for Development –IASTED, The Netherlands: L.M.H. Groenewoud.

Wissler, M and Mazza, E. (2005) Modeling of a pre-strained circular actuator made of dielectric elastomers. Sensors and Actuators A, 120, 184-192

Yan, H., Tomizawa, K., Ohno, H., and Toshima, N. (2003) All-Solid Actuator Consisting of Polyaniline Film and Solid Polymer Electrolyte. Macromolecule Materials, 208, 578-584.

Yfantis, A., Appel, G., Schmeißer, D., and Yfantis, Ds. (1999) Polypyrrole doped with fluoro-metal complexes: thermal stability and strutural properties. Synthetic Metals, 106, 187-195.

Zhang, J., Wu, M.Z.., Pu, T. S., Yang Zhang, Z., Jin, R.P., Zhi, S.T., Zhu, D.Z., De X , C., Zhu, F.Y., and Cao, J.Q. (1997) Investigation of plasma deposites from pyrrole, Thin Solid Film, 307, 14-20

Zhou, D., Spinks, G.M., Wallace, G.G., MacFarlane, D.R., Forsyth, M., and Sun, J. (2003) Solid state actuators based on polypyrrole and polymer-in-ionic liquid electrolytes. Electrochimica Acta, 48, 2355-2359.

APPENDICES

Appendix A Identification of Characteristic FT-IR Spectrum of Undoped and Doped Poly(Pyrrole)

The undoped and doped Poly(pyrrole) (Ppy) were first characterized by FT-IR spectroscopy in order to identify functional groups. An · FT-IR spectrometer (Thermo Nicolet, Nexus 670) was operated in the absorption mode with 32 scans and a resolution of ± 4 cm^{-1}, covering a wavenumber range of 4000-400 cm^{-1} using a deuterated triglycine sulfate detector. Optical grade KBr (Carlo Erba Reagent) was used as the background material. The synthesized ppy was intimately mixed with dried KBr at a ratio of Ppy:KBr = 1:20.

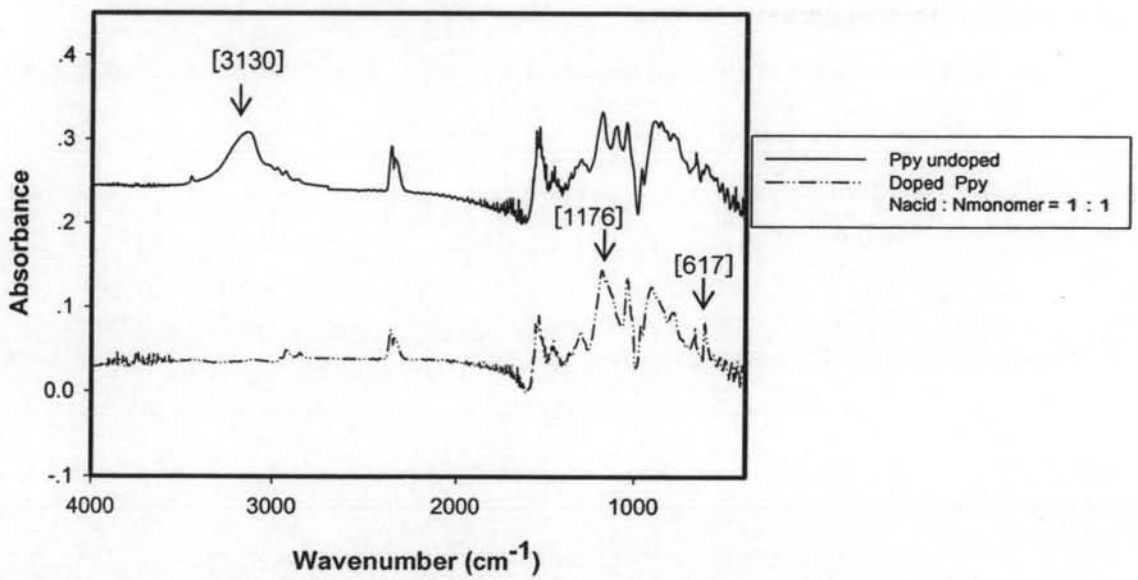

Figure A1 The FT-IR spectrum of undoped and doped Ppy.

The assignments of peaks in the spectrum are shown in Table A1. The characteristic peaks of Ppy were found between 4000 and 400 cm^{-1} and can be assigned to the stretching vibration of the C-H bond on the pyrrole ring; the peak at 3400 cm^{-1} represents the N-H stretching of pyrrole ring; the peaks at 3000-2800 cm^{-1} represent the aliphatic C-H bonds; the peaks at 1560 and 1531 cm^{-1} can be identified

as the asymmetric and the symmetric C=C /C-C stretching vibrations in pyrrole ring. After polypyrrole was doped that peak at 1183 cm^{-1} represents the S=O stretching vibration of sulfonate anion; and the peak at 620 cm^{-} indicates the characteristic vibration of DBSA. Both 1183 and 620 cm^{-1} peaks increase with increasing DBSA concentration.

Table A1 The FT-IR absorption spectrum of undoped and doped Ppy with DBSA

Wavenumber (cm^{-1})	**Assignments**	**References**
3130 [3400]	N-H stretching	Zhang *et al.* (1997)
3000-2800	C-H stretching of aliphatic	Prissanaroon *et al.* (2000)
1558 [1560]	Asymmetric C=C /C-C stretching vibration	Prissanaroon *et al.* (2000)
1541 [1531]	Symmetric C=C /C-C stretching vibration	Prissanaroon *et al.* (2000)
1176 [1183]	S=O stretching vibration	Prissanaroon *et al.* (2000)
1044,1038 [1089,1039]	C-H in plane bending	Zhang *et al.* (1997)
796 [805]	Out of plane vibration of ring	Zhang *et al.* (1997)
617 [620]	The characteristic vibration of DBSA.	Prissanaroon *et al.* (2000)

Appendix B Identification of Characteristic Peaks of Undoped and Doped Poly(Pyrrole) from UV-Visible Spectroscopy

The UV-Visible spectra of undoped and doped polypyrrole recorded with a UV-Vis absorption spectrometer (Perkin-Elmer, Lambda 10). Measurements were taken in the absorbance mode in the wavelength range of 700-300 nm. Synthesized Ppy was grinded into a fine powder, dissolved 0.05 g. in m-cresol 100 ml. and the solution was poured into the cuvett quartz cell. Scan speed was 240 mm/mi with a slit width of 2.0 nm, using a deuterium lamp as the light source.

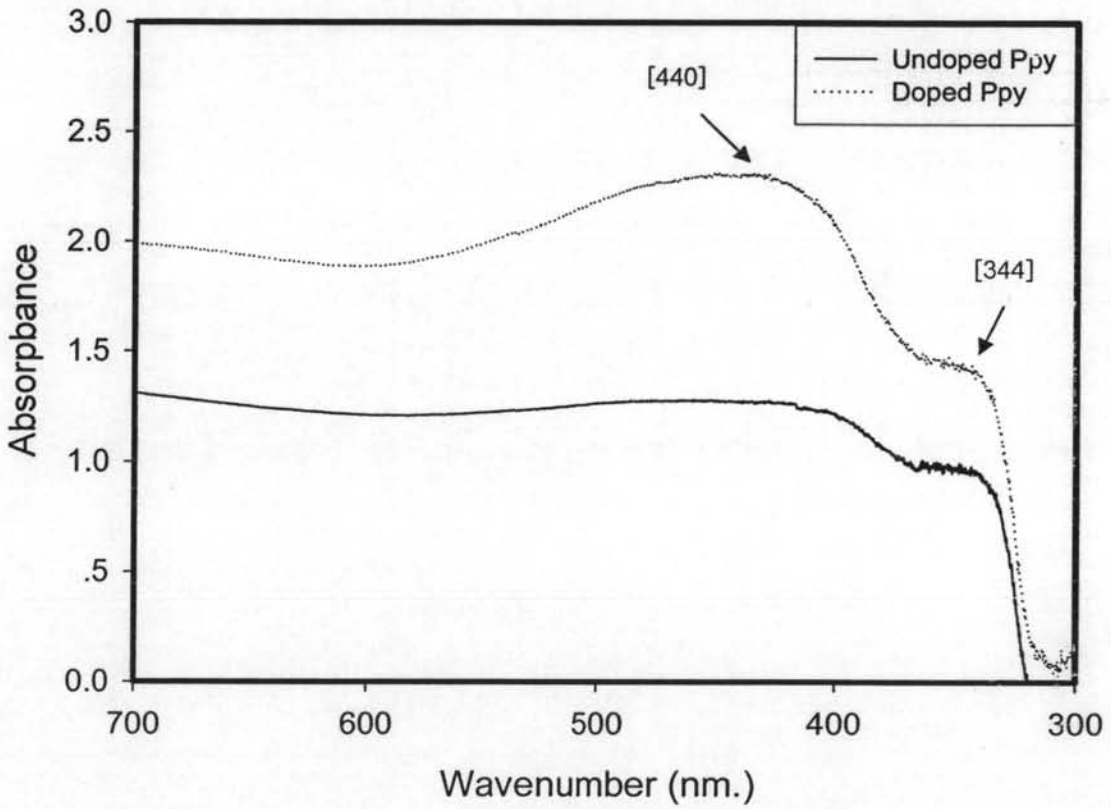

Figure B2 The UV-Visible spectra of undoped and doped Ppy.

The UV-Visible spectra of undoped and doped poly(pyrrole) from the references are shown in Table 2B. The wavelength in [] refers to the results of the assignments cites from references.

Table B2 Assignment peaks of UV-Visible peaks of undoped and doped pyrrole

Wavelength (nm)	Assignments	References
344 [345]	π-π* transitions of the electrons of neutral pyrrole trimer	Prissanaroon et al. (2000)
440 [460]	π-π* transitions of the π electrons Of the poly pyrrole in the oxidized form	Prissanaroon et al. (2000)

Appendix C Determination of Particle Sizes of Undoped and Doped Polypyrrole

Table C1 Summary of the particle diameters of Ppy_U, and Ppy_1:1

Samples	Particle diameter (μm)				
	1	2	3	Avg.	STD
Ppy_U	25.24	24.80	25.50	25.18	0.35384
Ppy_1:1	37.32	37.33	37.21	37.29	0.06658

Table C2 The raw data from particle size analysis of undoped Ppy

Size		Undoped polypyrrole (Ppy_U)					
Low (μm)	High (μm)	In%	Under%	In%	Under%	In%	Under%
0.50	1.32	0.14	0.14	0.11	0.11	0.01	0.01
1.32	1.60	1.05	1.19	0.96	1.07	0.58	0.59
1.60	1.95	1.85	3.04	1.73	2.80	1.13	1.72
1.95	2.38	2.49	5.53	2.38	5.18	1.69	3.41
2.38	2.90	3.00	8.53	2.93	8.11	2.29	5.70
2.90	3.53	3.42	11.95	3.44	11.55	2.96	8.66
3.53	4.30	3.83	15.78	3.95	15.50	3.70	12.36
4.30	5.24	4.24	20.02	4.47	19.97	4.51	16.87
5.24	6.39	4.64	24.66	4.95	24.92	5.26	22.13
6.39	7.78	4.94	29.60	5.25	30.17	5.73	27.86
7.78	9.48	5.11	34.71	5.34	35.51	5.81	33.67
9.48	11.55	5.25	39.96	5.34	40.85	5.74	39.41
11.55	14.08	5.38	45.34	5.33	46.18	5.64	45.05
14.08	17.15	5.57	50.91	5.40	51.58	5.62	50.67
17.15	20.90	5.89	56.80	5.65	57.23	5.79	56.46
20.90	25.46	6.38	63.18	6.13	63.36	6.17	62.63
25.46	31.01	6.94	70.12	6.75	70.11	6.70	69.33
31.01	37.79	7.30	77.42	7.20	77.31	7.13	76.46
37.79	46.03	7.11	84.53	7.10	84.41	7.12	83.58
46.03	56.09	6.12	90.65	6.20	90.61	6.35	89.93
56.09	68.33	4.46	95.11	4.59	95.20	4.83	94.76
68.33	83.26	2.60	97.71	2.71	97.91	2.96	97.72
83.26	101.44	1.10	98.81	1.17	99.08	1.35	99.07
101.44	123.59	0.24	99.05	0.24	99.32	0.33	99.40
123.59	150.57	0.00	99.05	0.00	99.32	0.00	99.40
150.57	183.44	0.07	99.12	0.00	99.32	0.00	99.40
183.44	223.51	0.26	99.38	0.14	99.46	0.07	99.47
223.51	272.31	0.35	99.73	0.27	99.73	0.23	99.70
272.31	331.77	0.26	99.99	0.24	99.97	0.25	99.95
331.77	404.21	0.01	100.00	0.03	100.00	0.05	100.00
404.21	492.47	0.00	100.00	0.00	100.00	0.00	100.00
492.47	600.00	0.00	100.00	0.00	100.00	0.00	100.00

Table C3 The raw data from particle size analysis of doping Ppy doping ratio 1:1 (Pth_1:1)

Size		Ppy doping ratio 1:1 (Ppy_1:1)					
Low (μm)	High (μm)	In%	Undcr%	In%	Under%	In%	Under%
0.50	1.32	0.15	0.15	0.16	0.16	0.15	0.15
1.32	1.60	0.47	0.62	0.48	0.64	0.47	0.62
1.60	1.95	0.67	1.29	0.69	1.33	0.69	1.31
1.95	2.38	0.75	2.04	0.77	2.10	0.77	2.08
2.38	2.90	0.73	2.77	0.74	2.84	0.75	2.83
2.90	3.53	0.70	3.47	0.72	3.56	0.73	3.56
3.53	4.30	0.76	4.23	0.77	4.33	0.78	4.34
4.30	5.24	0.95	5.18	0.96	5.29	0.98	5.32
5.24	6.39	1.29	6.47	1.31	6.60	1.32	6.64
6.39	7.78	1.71	8.18	1.73	8.33	1.74	8.38
7.78	9.48	2.15	10.33	2.17	10.50	2.16	10.54
9.48	11.55	2.63	12.96	2.64	13.14	2.59	13.13
11.55	14.08	3.17	16.13	3.16	16.30	3.04	16.17
14.08	17.15	3.86	19.99	3.82	20.12	3.66	19.83
17.15	20.90	4.91	24.90	4.86	24.98	4.79	24.62
20.90	25.46	6.52	31.42	6.47	31.45	6.63	31.25
25.46	31.01	8.85	40.27	8.85	40.30	9.26	40.51
31.01	37.79	11.85	52.12	11.86	52.16	12.26	52.77
37.79	46.03	14.53	66.65	14.50	66.66	14.43	67.20
46.03	56.09	14.57	81.22	14.45	81.11	14.06	81.26
56.09	68.33	10.87	92.09	10.84	91.95	10.66	91.92
68.33	83.26	5.76	97.85	5.84	97.79	5.95	97.87
83.26	101.44	2.03	99.88	2.10	99.89	2.13	100.00
101.44	123.59	0.12	100.00	0.11	100.00	0.00	100.00
123.59	150.57	0.00	100.00	0.00	100.00	0.00	100.00
150.57	183.44	0.00	100.00	0.00	100.00	0.00	100.00
183.44	223.51	0.00	100.00	0.00	100.00	0.00	100.00
223.51	272.31	0.00	100.00	0.00	100.00	0.00	100.00
272.31	331.77	0.00	100.00	0.00	100.00	0.00	100.00
331.77	404.21	0.00	100.00	0.00	100.00	0.00	100.00
404.21	492.47	0.00	100.00	0.00	100.00	0.00	100.00
492.47	600.00	0.00	100.00	0.00	100.00	0.00	100.00

Appendix D Density Measurement

The specific density (ρ_p) of poly(pyrrole) was measured by using a pyncometer. We used a 25 ml pyncometer. First step, the weight of blank pyncometer was measured and we added acetone into the pyncometer and we remeasured the weight again. The specific density of acetone at testing temperature was calculated by equation (D.1).

$$\rho_a = \frac{(a-b)}{25} \qquad \text{(D.1)}$$

where ρ_a is specific density of acetone ($g.cm^{-3}$), a is the weigth of pyncometer with water (g), and b is the weigth of blank pyncometer (g).

Second step, weight of blank pyncometer was measured again, then we added Ppy powders into the pynometer, and measured the weight changes. Then we added acetone into the pyncometer and remeasured the weight of the pyncometer. The specific density of poly(pyrrole) at testing temperature was calculated by equation (D.2) – (D.3).

$$A = \frac{(e-d)}{\rho_a} \qquad \text{(D.2)}$$

where A is the volume of acetone added into pyncometer (cm^3), ρ_a is the specific density of acetone ($g.cm^{-3}$), e is the weight of the pyncometer with acetone and Ppy powders (g). and d is the weight of Ppy powder and the pyncometer (g).

$$\rho_p = \frac{(d-b)}{25-A} \qquad \text{(D.3)}$$

where ρ_p is the specific density of Ppy ($g.cm^{-3}$), d is the weight of Ppy powder, pyncometer (g), b is the weight of the blank pyncometer (g), and A is the volume of acetone added into the pyncometer (cm^3).

Table D1 The data of the determination specific density of water and Ppy at 298K.

Specific density (g/cm^3)	Measure (g/cm^{-3})			average	SD
	1	2	3		
Acetone	0.9668	0.9664	0.9668	0.966667	0.000231
Ppy	1.272091	1.265039	1.282921	1.27335	0.009007

Appendix E Identification Thermal Property of Undoped, Doped Ppy and Pure Elastomer.

Undoped and doped poly(pyrrole) (Ppy) at various ratios of monomer to dopant unit were determined by a thermal gravimetric analyzer (DT-TGA 1790). Measurements were taken with the temperature scans from 60 to 1000°C and a heating rate of 10°C/min. The samples were weighed in the range of 1-5 mg and loaded into a platinum pan, and then were heated under N_2 flow. From figure E1, the transitions can be observed for undoped and dope poly(pyrrole). The first transition refers to the losses of residue solvent and water. The second transition refers to the Ppy_U side chain degradation, and the third transition refers to the Ppy backbone degradation. After doping, the thermal stability improved as compared to that of undoped Ppy.

Table E1 Summary of Undoped and doped Ppy degradation step

sample	Transititon temperature (^{0}C)			% Weight loss			%Residue
	1st	2nd	3rd	1st	2nd	3rd	
Ppy_U	60-172	172-312	312-1000	5.1	13.8	59.2	22.56
Ppy_1:1	60-105	105-356	356-1000	2.7	8.9	62.1	27.26

PDMS, AR, SAR, AR71, AR72HF, SIS, and SBR were also characterized by a thermal gravimetric analyzer (DT-TGA 1790). Measurements were taken with the temperature scans from 60 to 500 °C and a heating rate of 10°C/min. The samples were weighed in the range of 15-25 mg and loaded into a platinum pan, and then were heated under N_2 flow. All of elastomer matrices show only one transition that can be referred to as the backbone degradation. From Figure E2, most of materials rapidly lost their weights at about 400 ^{0}C. The degradation temperature of PDMS is higher than others.

Table E2 Summary of various elastomer degradation temperatures

Sample	Transitions temperature(C0)	% Weight loss	% Residue
AR70	365-409	72.25	3.03
AR71	365-400	78.77	1.08
AR72	363-419	71.92	8.65
PDMS	444-511	78.11	0.45
SAR	371-417	78.06	0
SBR	372-468	78.06	2.2
SIS	421-482	78.18	0

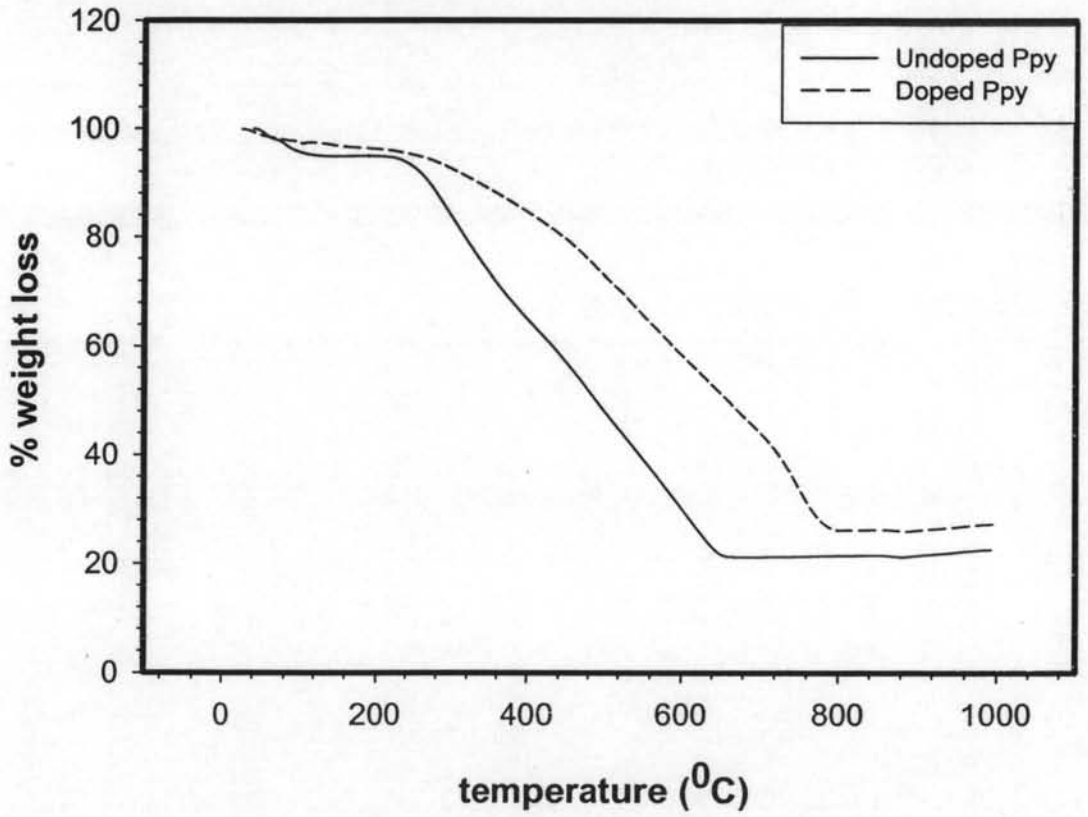

Figure E1 The TGA thermograms of undoped and doped Ppy.

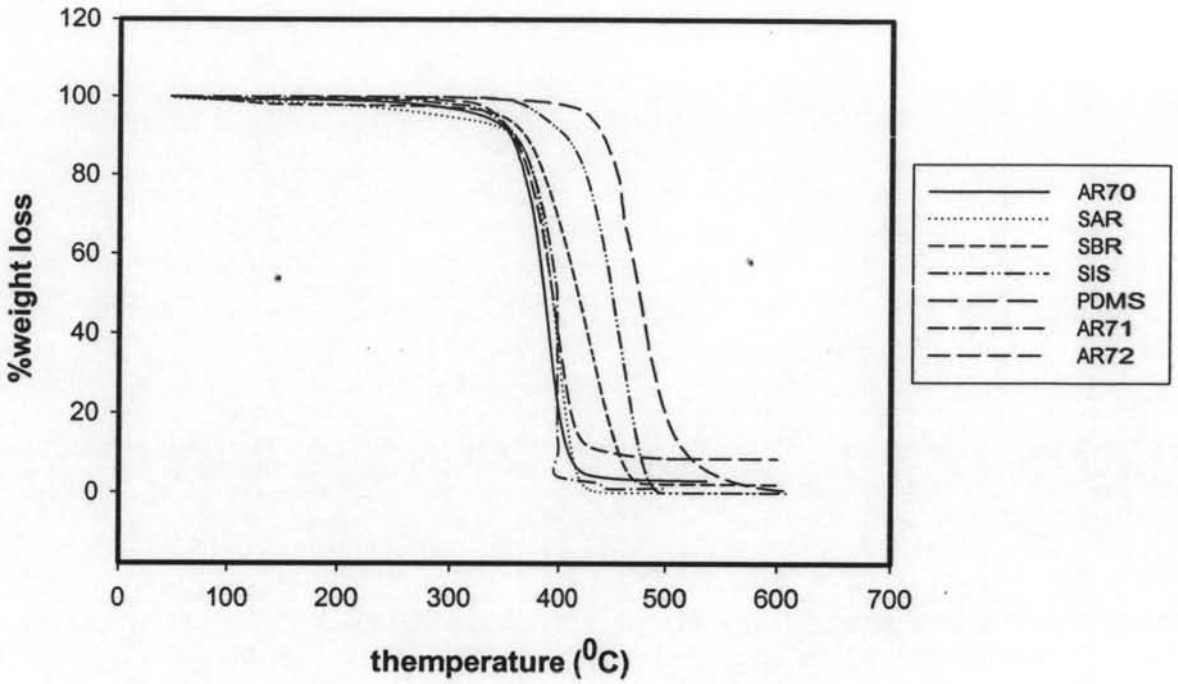

Figure E2 The TGA thermograms of various elastomer matrices.

Appendix F Specification of the elastomer matrices

F.1 Poly(dimethylsiloxane), hydroxy terminated (PDMS, Aldrich 432997)

Table F1 Properties of poly(dimethylsiloxane)

Properties	Typical value
Boiling point	93 ^{0}C
Density	0.97 g/ml at 25 °C
Viscosity	18,000-22,000 cSt

F.2 Styrene acrylate copolymer rubber latex (SAR, Dow chemical Latex T – 3356 F)

Table F2 Physical and chemical properties of styrene acrylate copolymer

Properties	Typical value
Physical state	Fluids
Color	White
Odour	Mild
Molecular weight	Mixture
Boiling Point	100 ^{0}C
Freezing Point	0 ^{0}C
Melting point	Not applicable
Flash point	Not applicable (aqueous system)
Flammable limits	Lower: not applicable(aqueous system)
In air (% by volume)	Upper: not applicable(aqueous system)
Specific gravity (H_2O=1)	1.1
Vapour pressure	same as water
Vapour density (air = 1)	< 1
Evapouration rate (butyl acetate = 1)	is slower than butyl acetate

F.3 Styrene butadiene copolymer rubber latex (SBR, Dow Chemical DL 849)

Table F3 Physical and chemical properties of styrene butadiene latex

Properties	Typical value
Solubility in water	as emulsion is misible with water
Boiling point	100 ^{0}C
Appearance	milky white liquid emulsion
Odour	practically odourless
Freezing point/	0 ^{0}C (relates to water component)
Specific gravity (H_2O=1)	0.98-1.040
pH value	5.0-8.0
Vapour pressure	17.5 mmHg @ 20 ^{0}C (relates to water component)
Vapour density	0.624 at 27^{0}C (relates to water component)
Solids content	52 %
pH	7.7
RVT Brookfield viscosity (#2, 50 rpm.)	<700 m.Pa.S
Particle size	140 nm
Stabilizer	anionic
Glass transition temperature (T_g)	-7 ^{0}C
Antioxidant	Present
200 mesh residue	<0.5 g/l
Mechanical stability	Excellent
Hand	Medium soft
Adhesion (on fabric)	43 N/50 mm

F.4 Acrylate copolymer rubber latex (AR, Dow chemical Latex R 7018)

Table F4 Physical and chemical properties of acrylate copolymer

Properties	Typical value
Physical state	Fluids
Color	White
Odour	Mild
Molecular weight	Mixture
Boiling Point	100 ^{0}C
Freezing Point	0 ^{0}C
Melting point	Not applicable
Flash point	Not applicable (aqueous system)
Flammable limits	Lower: not applicable(aqueous system)
In air (% by volume)	Upper: not applicable(aqueous system)
Specific gravity (H_2O=1)	1.1
Vapour pressure	Same as water
Vapour density (air = 1)	< 1
Solubility in water	Dilutable
Evapouration rate (butyl acetate = 1)	Is slower than butyl acetate
Percent volatiles	51 wt%(water)

F5 Acrylate copolymer (Nipol AR71 and Nipol AR72HF, Nipon Zeon Advance Polymix Co,.LTD)

Table F5 Physical and chemical properties of Acrylate copolymer (AR71 and AR72)

Property	AR71	AR72 HF
Elongation(%)	400	230
Volatile matter (%)	0.32	0.56
Tensile Strength (MPa)	11.8	11.2
100% Modulus (MPa)	4.1	6
Ash (%)	0.22	0.16
Moony Viscosity at 100 ^{0}C	50	48
Glass Transition C	-15	-28
Specific Gravity	1.11	1.11
Type	Heat resistance	Low Temperature resistance

F.6 Styrene isoprene styrene copolymer rubber latex (SIS, Shell Chemicals D113P)

Table F6 Physical and chemical properties of Styrene isoprene styrene copolymer

Property	Value	Unit	Method
Tensile strength	600	psi	ASTM D412 tensile tester jaw separation speed 10in/min
300 % Modulus	50	%	ASTM D412 tensile tester jaw separation speed 10in/min
Elongation	1,500	%	ASTM D412 tensile tester jaw separation speed 10in/min
Set at break	20	%	-
Hardness, Shore A (10 sec)[3]	23	-	-
Brookfield Viscosity (Toluene Solution), cps at 77 ^{0}F	600	-	-
Specific Gravity	0.92	-	Neat polymer concentration, 25%w.
Melt Index	24	gms/10 min	200 ^{0}C, 5 kg
Plasticizer Oil Content	0	%w.	-
Styrene/Rubber Ratio	16/84	-	-
Plastic Form	Pellet	-	-
Diblock	55	%	-

Appendix G Determination of the Correction Factor (K)

The electrical conductivity of undoped and doped Ppy was measured by a two-point probe meter. The meter consists of two probes, making contact on the surface of film sample. These probes were connected to a source meter (Keithley, Model 6517A) for a constant voltage source and for reading the resultant current.

The geometrical correction factor was taken into account of geometric effects, depending on the configuration and probe tip spacing.

$$K = \frac{w}{l}$$

(E.1)

K is geometrical correction factor, w is the width of probe tip spacing (cm), l is the length between probes (cm).

In this measurement, the constant K value was determined by using standard materials where specific resistivity values were known; we used silicon wafer chips (SiO_2). In our case, the sheet resistivity was measured by using our custom made two-point probe and then the geometric correction factor was calculated by equation (E.2) as follows:

$$K = \frac{\rho}{R \times t} = \frac{I \times \rho}{V \times t}$$

(E.2)

K is the geometric correction factor, ρ is the resistivity of a standard silicon wafer, calibrated by using a four point probe at King Mongkut's Institute Technology of Lad Krabang (Ω.cm), t is the film thickness (cm), R is the film resistance (Ω), I is the measured current (A), and V is the voltage drop (V).

Standard Si wafer were cleaned to remove organic impurities prior to be used according to the standard RCA method (Kern, 1993).

Materials

Acetones (Scharlau, 99.5%), Methanol (CARLO ERBA, 99.9%), Ammonium hydroxide (Merk, 99.9%), Hydrogen peroxide (CARLO ERBA, 30% in water), and dilute (2%) Hydrofuric acid

Experiment

The cleaning procedures contain 3 steps: the solvent clean, the RCA01 and the HF dip. The first step is the solvent clean step, employed to remove oils and organic residues that appeared on Si wafer surface. The Si wafer was placed into the acetone at 55°C for 10 min, removed and placed in methanol for 2-5 min, subsequently rinsed with deionized water and blown dried with nitrogen gas. Second step is the RCA clean, to remove organic residues from silicon wafers. This process oxidized the silicon wafer and left a thin oxide on the surface of the wafer. RCA solution was prepared with 5 parts of water (H_2O), 1 part of 27% ammonium hydroxide (NH_4OH), and 1 part of 30% hydrogen peroxide (H_2O_2). 65 ml of NH_4OH (27%) was added into 325 ml of deionized water in a beaker and then heated to 70 ± 5°C. The mixture would bubble vigorously after 1-2 min, indicated that it was ready to use. Silicon wafer was soaked in the solution for 15 min, consequently overflowed with deionized water in order to rinse and remove the solution. The third step is the HF dip, which was carried out to remove native silicon dioxide from wafer. 480 ml of deionized water was added to the polypropylene bottle and then added to 20 ml HF. Wafer was soaked in this solution for 2 min, removed and checked for hydrophobicity by performing the wetting test. Deionized water was poured onto the surface wafer; the clean silicon surface would shows that the beads of water would roll off. Clean Si wafer was further blown dried with nitrogen and stored in a clean and dry environment.

Table G1 Determination the geometrical factor of probe A

Probe	K (correction factor)				
	1	2	3	Average	STD
A	4.88E-06	4.92E-06	4.94E-06	4.92E-06	1.62E-07

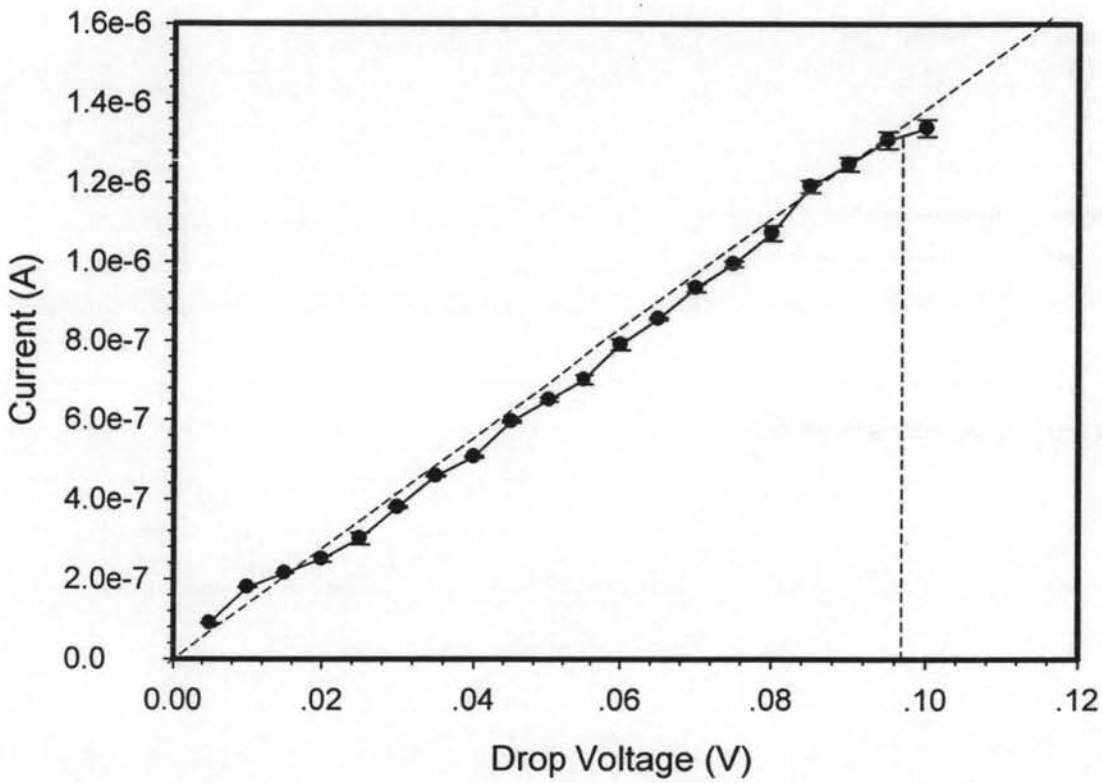

Figure G1 The calibration data of Si-wafer: K tay which specific resistivity (ρ) 0.014265 Ω.cm, thickness 0.0724 cm, 24-25°C, 55-59 %R.H.

Table G2 Determination the geometric correction factor of probe A with standard Si wafer (specific resistivity 0.014265 Ω.cm, thickness 0.0724 cm, 24-25°C, 55-59% R.H)

Applied Voltages (V)	Current (A)		
	1	2	3
0.005	8.95E-08	8.88E-08	9.01E-08
0.01	1.80E-07	1.79E-07	1.79E-07
0.015	2.15E-07	2.16E-07	2.15E-07
0.02	2.57E-07	2.52E-07	2.42E-07
0.025	2.85E-07	3.03E-07	3.15E-07
0.03	3.78E-07	3.83E-07	3.78E-07
0.035	4.59E-07	4.58E-07	4.55E-07
0.04	5.03E-07	5.09E-07	5.06E-07
0.045	5.95E-07	5.92E-07	5.99E-07
0.05	6.45E-07	6.51E-07	6.55E-07
0.055	6.92E-07	6.97E-07	7.15E-07
0.06	7.83E-07	7.81E-07	8.06E-07
0.065	8.53E-07	8.53E-07	8.59E-07
0.07	9.22E-07	9.34E-07	9.43E-07
0.075	9.96E-07	9.99E-07	9.86E-07
0.08	1.06E-06	1.07E-06	1.09E-06
0.085	1.20E-06	1.20E-06	1.17E-06
0.09	1.26E-06	1.23E-06	1.25E-06
0.095	1.29E-06	1.30E-06	1.33E-06
0.1	1.36E-06	1.33E-06	1.32E-06

Appendix H Conductivity Measurement

The specific conductivity, which is the inversion of specific resistivity (ρ) of undoped and doped Ppy pellets was measured by using the two-point probe connected to a source meter (Keithley, Model 6517A) for a constant voltage source and for reading resultant current under the atmospheric pressure, 54-60% relative humidity and 24-25°C. The geometric correction factor (K) of probe A is 1.23×10^{-5}. The thickness of pellets was measured by a thickness gauge. The applied voltage was plotted versus the current change to determine the linear ohmic regime of each sample. The applied voltage and the current change in the linear ohmic regime were converted to the electrical conductivity of the polymer by using equation (H.1) as follows:

$$\sigma = \frac{1}{\rho} = \frac{1}{R_s \times t} = \frac{I}{K \times V \times t} \qquad \text{(H.1)}$$

Where σ is the specific conductivity (S/cm), ρ is the specific resistivity (Ω.cm), R_s is the sheet resistivity (Ω), I is the measured current (A), K is the geometric correction factor, V is the applied voltage (voltage drop) (V), t is the pellet thickness (cm).

In addition, the conductivity of matrixes can be measured by using the resistivity testing fixture (Keithley, Model 8009) connected to a source meter (Keithley, Model 6517A) for a constant voltage source and for reading resultant current under the atmospheric pressure, 54-60% relative humidity and 24-25°C. The conductivity of matrixes was calculated by using equation (H.2 – H.3) as follows:

$$K_v = \pi \times \frac{(D + [\beta \times g])}{4}^2 \qquad \text{(H.2)}$$

Where K_v is the effective area of the guarded electrode for the particular electrode arrangement employed (cm^2), D is the diameter of the guarded electrode (cm), β is the effective area coefficient (cm^2) (β is always zero), g is the distance between the guarded electrode and the ring electrode (cm):

$$\sigma = \frac{1}{\rho} = \frac{t \times I}{22.9 \times V} \quad \text{(H.3)}$$

Where σ is the specific conductivity (S/cm), ρ is the specific resistivity (Ω.cm), I is the measured current (A), V is the applied voltage (voltage drop) (V), t is the sheet thickness (cm).

Table H1 Determination the specific conductivity (S/cm) of matrixes, undoped and doped poly(pyrrole) at various mole ratios of acid to monomer

Code	Specific conductivity (S/cm)	STD
AR70	8.13E-13	7.84E-14
AR71	5.16E-12	1.38E-13
AR72	1.03E-12	1.24E-14
PDMS	2.73E-06	4.27E-07
SAR	6.86E-15	2.03E-16
SIS	8.72E-17	3.67E-17
SBR	5.65E-15	5.43E-16
Ppy_U	5.21E-01	4.37E-02
Ppy_1:1	4.07E+00	3.16E-01
AR70:1_un	1.28E-12	2.54E-15
AR70:2_un	1.30E-12	8.89E-15
AR70:3_un	4.18E-12	1.4354E-13
AR70:4_un	4.94E-12	3.21E-14
AR70:5_un	5.33E-12	5.48E-15

Table H2 The raw data of the determination conductivity of AR70 at 24-25°C, 54-60% R.H. was measured by using the resistivity testing fixture (Keithley, Model 8009)

Sample	Thickness	Applied voltage (V)			Measured Current (A)			Conductivity (S/cm)		
	(cm)	1	2	3	1	2	3	1	2	3
AR70	1) 0.133	0.5	0.5	0.5	5.59E-11	5.58E-11	5.61E-11	6.45E-13	6.43E-13	6.46E-13
	2) 0.132	1	1	1	1.31E-10	1.31E-10	1.31E-10	7.55E-13	7.54E-13	7.55E-13
	3) 0.132	1.5	1.5	1.5	2.06E-10	2.07E-10	2.07E-10	7.90E-13	7.97E-13	7.94E-13
		2	2	2	2.84E-10	2.88E-10	2.86E-10	8.17E-13	8.30E-13	8.23E-13
		2.5	2.5	2.5	3.66E-10	3.70E-10	3.68E-10	8.43E-13	8.53E-13	8.48E-13
		3	3	3	4.49E-10	4.51E-10	4.50E-10	8.63E-13	8.67E-13	8.65E-13
		3.5	3.5	3.5	5.33E-10	5.36E-10	5.34E-10	8.77E-13	8.83E-13	8.80E-13
		4	4	4	6.18E-10	6.21E-10	6.20E-10	8.91E-13	8.95E-13	8.94E-13
		4.5	4.5	4.5	7.05E-10	7.08E-10	7.07E-10	9.03E-13	9.07E-13	9.05E-13
		5	5	5	7.93E-10	7.97E-10	7.95E-10	9.15E-13	9.19E-13	9.17E-13
		5.5	5.5	5.5	8.85E-10	8.88E-10	8.86E-10	9.27E-13	9.31E-13	9.29E-13
		6	6	6	9.76E-10	9.80E-10	9.78E-10	9.38E-13	9.42E-13	9.40E-13
		6.5	6.5	6.5	1.07E-09	1.07E-09	1.07E-09	9.47E-13	9.52E-13	9.52E-13
		7	7	7	1.16E-09	1.17E-09	1.16E-09	9.57E-13	9.61E-13	9.59E-13
		7.5	7.5	7.5	1.26E-09	1.26E-09	1.26E-09	9.67E-13	9.70E-13	9.69E-13
		8	8	8	1.35E-09	1.36E-09	1.36E-09	9.76E-13	9.80E-13	9.78E-13
		8.5	8.5	8.5	1.45E-09	1.46E-09	1.45E-09	9.85E-13	9.88E-13	9.87E-13
		9	9	9	1.55E-09	1.56E-09	1.56E-09	9.96E-13	9.99E-13	9.98E-13
		9.5	9.5	9.5	1.66E-09	1.66E-09	1.66E-09	1.01E-12	1.01E-12	1.01E-12
		10	10	10	1.75E-09	1.77E-09	1.76E-09	1.01E-12	1.02E-12	1.01E-12

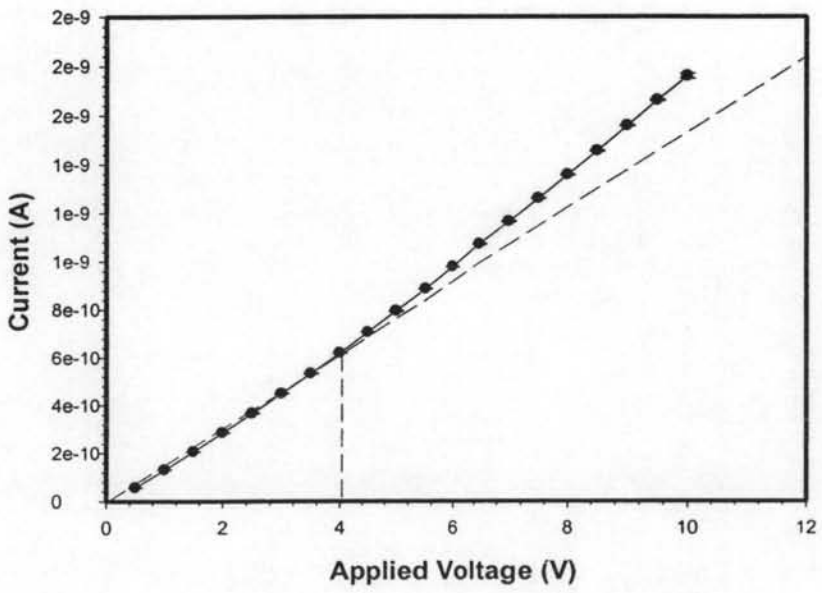

Table H3 The raw data of the determination conductivity of AR71 at 24-25°C, 54-60% R.H. was measured by using the resistivity testing fixture(Keithley, Model 8009)

Sample	Thickness	Applied voltage (V)			Measured Current (A)			Conductivity (S/cm)		
	(cm)	1	2	3	1	2	3	1	2	3
AR71	1) 0.0235	10	10	10	5.17E-08	5.28E-08	5.39E-08	5.26E-12	5.37E-12	5.48E-12
	2) 0.0222	20	20	20	1.06E-07	1.05E-07	1.06E-07	5.39E-12	5.34E-12	5.39E-12
	3) 0.0241	30	30	30	1.56E-07	1.52E-07	1.59E-07	5.29E-12	5.16E-12	5.39E-12
		40	40	40	2.02E-07	2.01E-07	2.00E-07	5.14E-12	5.11E-12	5.09E-12
		50	50	50	2.46E-07	2.49E-07	2.48E-07	5.01E-12	5.07E-12	5.05E-12
		60	60	60	3.04E-07	3.06E-07	3.10E-07	5.16E-12	5.19E-12	5.26E-12
		70	70	70	3.51E-07	3.50E-07	3.48E-07	5.10E-12	5.09E-12	5.06E-12
		80	80	80	3.98E-07	3.99E-07	3.97E-07	5.06E-12	5.07E-12	5.05E-12
		90	90	90	4.43E-07	4.49E-07	4.45E-07	5.01E-12	5.08E-12	5.03E-12
		100	100	100	4.97E-07	4.92E-07	4.94E-07	5.06E-12	5.01E-12	5.03E-12

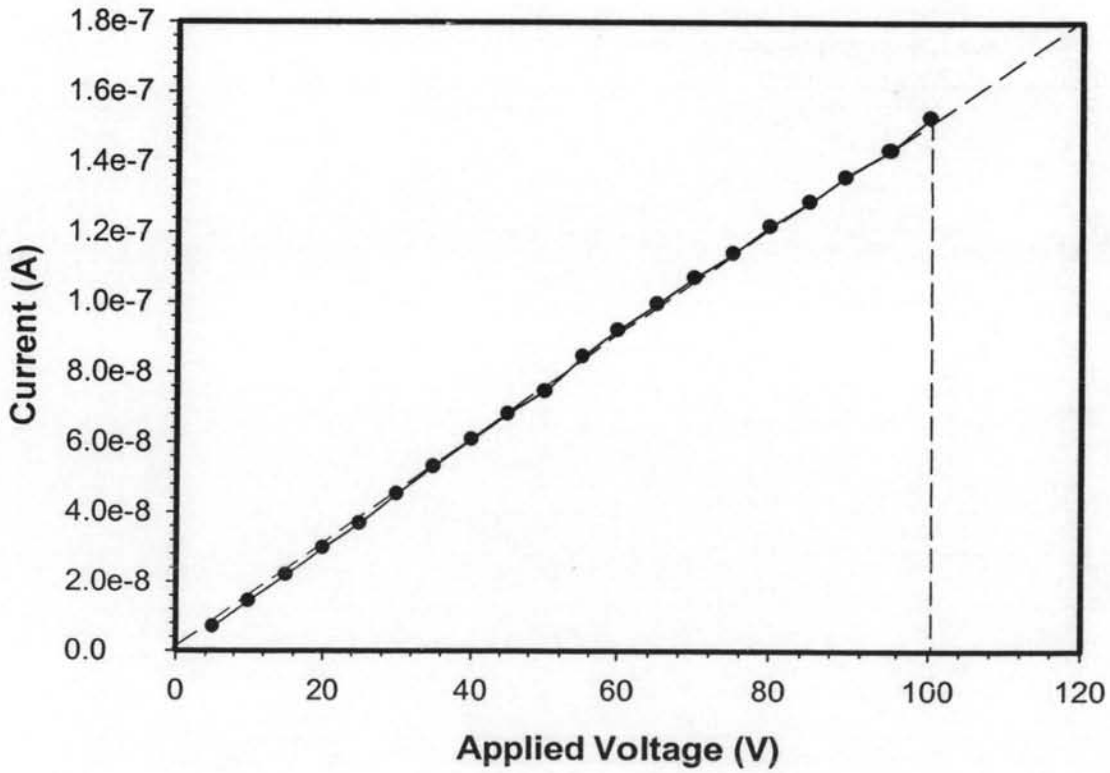

Table H4 The raw data of the determination conductivity of AR72 at 24-25°C, 54-60% R.H. was measured by using the resistivity testing fixture (Keithley, Model 8009

Sample	Thickness	Applied voltage (V)			Measured Current (A)			Conductivity (S/cm)		
	(cm)	1	2	3	1	2	3	1	2	3
AR72	1) 0.0157	5	5	5	6.88E-09	6.91E-09	6.89E-09	9.43E-13	9.47E-13	9.45E-13
	2) 0.0155	10	10	10	1.44E-08	1.44E-08	1.43E-08	9.87E-13	9.87E-13	9.80E-13
	3) 0.0158	15	15	15	2.19E-08	2.18E-08	2.20E-08	1.00E-12	9.96E-13	1.01E-12
		20	20	20	2.96E-08	2.96E-08	2.97E-08	1.01E-12	1.01E-12	1.02E-12
		25	25	25	3.68E-08	3.67E-08	3.66E-08	1.01E-12	1.01E-12	1.00E-12
		30	30	30	4.51E-08	4.50E-08	4.55E-08	1.03E-12	1.03E-12	1.04E-12
		35	35	35	5.30E-8	5.30E-8	5.31E-08	1.04E-12	1.04E-12	1.04E-12
		40	40	40	6.08E-8	6.08E-08	6.08E-08	1.04E-12	1.04E-12	1.04E-12
		45	45	45	6.87E-08	6.87E-08	6.68E-08	1.05E-12	1.05E-12	1.02E-12
		50	50	50	7.48E-08	7.44E-08	7.45E-08	1.03E-12	1.02E-12	1.02E-12
		55	55	55	8.46E-08	8.46E-08	8.44E-08	1.05E-12	1.05E-12	1.05E-12
		60	60	60	9.19E-08	9.20E-08	9.22E-08	1.05E-12	1.05E-12	1.05E-12
		65	65	65	9.94E-08	9.95E-08	9.98E-08	1.05E-12	1.05E-12	1.05E-12
		70	70	70	1.07E-07	1.07E-07	1.07E-07	1.05E-12	1.05E-12	1.05E-12
		75	75	75	1.14E-07	1.14E-07	1.14E-07	1.04E-12	1.04E-12	1.04E-12
		80	80	80	1.21E-07	1.22E-07	1.22E-07	1.04E-12	1.05E-12	1.05E-12
		85	85	85	1.29E-07	1.29E-07	1.28E-07	1.04E-12	1.04E-12	1.03E-12
		90	90	90	1.35E-07	1.36E-07	1.36E-07	1.03E-12	1.04E-12	1.04E-12
		95	95	95	1.43E-07	1.43E-07	1.44E-07	1.03E-12	1.03E-12	1.04E-12
		100	100	100	1.51E-07	1.52E-07	1.55E-07	1.04E-12	1.04E-12	1.06E-12

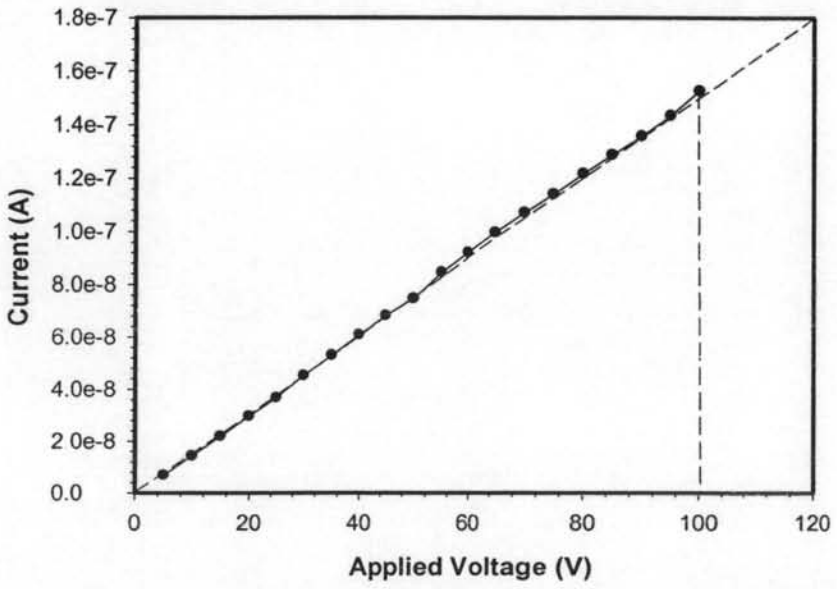

Table H5 The raw data of the determination of linear regime of PDMS at 24-25°C, 54-60% R.H. was measured by using the two-point probe meter

Sample	Thickness	Applied voltage (V)			Measured Current (A)			Conductivity (S/cm)		
	(cm)	1	2	3	1	2	3	1	2	3
PDMS	1) 1.00	0.1	0.1	0.1	1.13E-11	1.17E-11	1.15E-11	3.97E-06	4.11E-06	4.04E-06
	2) 1.02	0.2	0.2	0.2	1.55E-11	1.58E-11	1.56E-11	2.72E-06	2.78E-06	2.74E-06
	3) 1.03	0.3	0.3	0.3	1.91E-11	1.89E-11	1.87E-11	2.24E-06	2.21E-06	2.19E-06
		0.4	0.4	0.4	3.32E-11	3.33E-11	3.34E-11	2.92E-06	2.92E-06	2.93E-06
		0.5	0.5	0.5	4.04E-11	4.08E-11	4.07E-11	2.84E-06	2.87E-06	2.86E-06
		0.6	0.6	0.6	4.62E-11	4.66E-11	4.60E-11	2.70E-06	2.73E-06	2.69E-06
		0.7	0.7	0.7	5.50E-11	5.60E-11	5.59E-11	2.76E-06	2.81E-06	2.81E-06
		0.8	0.8	0.8	6.21E-11	5.97E-11	6.11E-11	2.73E-06	2.62E-06	2.68E-06
		0.9	0.9	0.9	6.73E-11	6.70E-11	6.72E-11	2.63E-06	2.62E-06	2.62E-06
		1	1	1	7.28E-11	7.39E-11	7.35E-11	2.56E-06	2.60E-06	2.58E-06
		1.1	1.1	1.1	7.71E-11	7.87E-11	7.87E-11	2.46E-06	2.51E-06	2.51E-06
		1.2	1.2	1.2	8.49E-11	8.50E-11	8.54E-11	2.49E-06	2.49E-06	2.50E-06
		1.3	1.3	1.3	8.86E-11	8.90E-11	8.81E-11	2.39E-06	2.40E-06	2.38E-06
		1.4	1.4	1.4	9.23E-11	9.24E-11	9.26E-11	2.32E-06	2.32E-06	2.32E-06
		1.5	1.5	1.5	1.02E-10	1.02E-10	1.02E-10	2.39E-06	2.39E-06	2.39E-06
		1.6	1.6	1.6	1.05E-10	1.04E-10	1.03E-10	2.31E-06	2.28E-06	2.26E-06
		1.7	1.7	1.7	1.10E-10	1.11E-10	1.09E-10	2.27E-06	2.29E-06	2.25E-06
		1.8	1.8	1.8	1.18E-10	1.17E-10	1.17E-10	2.30E-06	2.28E-06	2.28E-06
		1.9	1.9	1.9	1.25E-10	1.25E-10	1.24E-10	2.31E-06	2.31E-06	2.29E-06
		2	2	2	1.36E-10	1.37E-10	1.39E-10	2.39E-06	2.41E-06	2.44E-06
		2.2	2.2	2.2	1.48E-10	1.48E-10	1.49E-10	2.36E-06	2.36E-06	2.38E-06

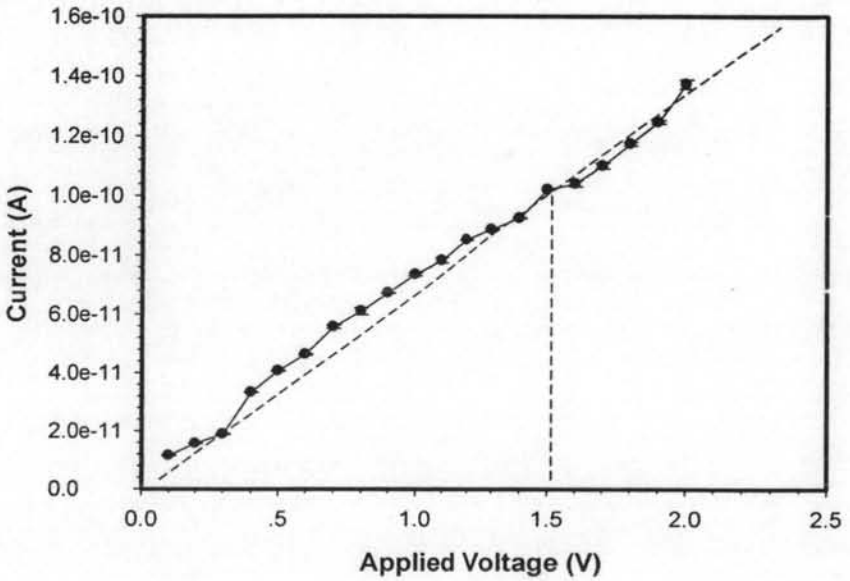

Table H6 The raw data of the determination conductivity of SAR at 24-25°C, 54-60% R.H. was measured by using the resistivity testing fixture (Keithley,Model 8009)

Sample	Thickness	Applied voltage (V)			Measured Current (A)			Conductivity (S/cm)		
	(cm)	1	2	3	1	2	3	1	2	3
SAR	1) 0.090	2	2	2	3.41E-12	3.40E-12	3.42E-12	6.48E-15	6.46E-15	6.50E-15
	2) 0.086	3	3	3	5.30E-12	5.32E-12	5.28E-12	6.71E-15	6.74E-15	6.69E-15
	3) 0.084	4	4	4	7.10E-12	7.13E-12	7.08E-12	6.75E-15	6.77E-15	6.72E-15
		5	5	5	8.63E-12	8.61E-12	8.65E-12	6.55E-15	6.54E-15	6.57E-15
		6	6	6	1.06E-11	1.08E-11	1.07E-11	6.73E-15	6.84E-15	6.75E-15
		7	7	7	1.25E-11	1.26E-11	1.25E-11	6.81E-15	6.83E-15	6.79E-15
		8	8	8	1.45E-11	1.47E-11	1.45E-11	6.89E-15	7.00E-15	6.87E-15
		9	9	9	1.64E-11	1.64E-11	1.63E-11	6.91E-15	6.92E-15	6.89E-15
		10	10	10	1.73E-11	1.79E-11	1.82E-11	6.56E-15	6.80E-15	6.93E-15
		11	11	11	2.02E-11	2.03E-11	2.02E-11	6.98E-15	7.00E-15	6.97E-15
		12	12	12	2.22E-11	2.23E-11	2.22E-11	7.04E-15	7.06E-15	7.03E-15
		13	13	13	2.42E-11	2.42E-11	2.42E-11	7.07E-15	7.08E-15	7.06E-15
		14	14	14	2.62E-11	2.63E-11	2.62E-11	7.11E-15	7.12E-15	7.10E-15
		15	15	15	2.82E-11	2.83E-11	2.82E-11	7.15E-15	7.16E-15	7.13E-15
		16	16	16	3.03E-11	3.03E-11	3.02E-11	7.19E-15	7.20E-15	7.17E-15
		17	17	17	3.24E-11	3.25E-11	3.24E-11	7.25E-15	7.26E-15	7.24E-15
		18	18	18	3.45E-11	3.46E-11	3.45E-11	7.29E-15	7.30E-15	7.27E-15
		19	19	19	3.67E-11	3.68E-11	3.66E-11	7.34E-15	7.35E-15	7.33E-15
		20	20	20	3.94E-11	3.95E-11	3.93E-11	7.48E-15	7.50E-15	7.47E-15
		21	21	21	4.12E-11	4.13E-11	4.12E-11	7.46E-15	7.47E-15	7.45E-15
		22	22	22	4.33E-11	4.34E-11	4.32E-11	7.48E-15	7.49E-15	7.47E-15

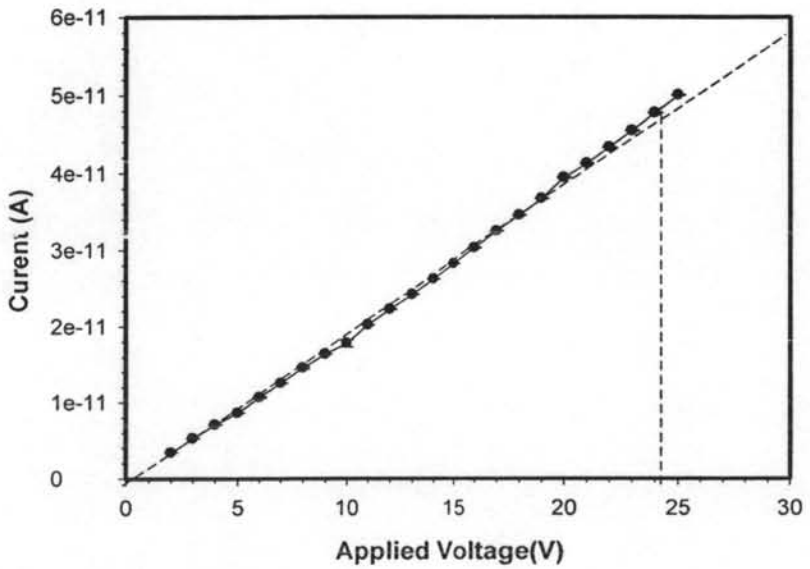

Table H7 The raw data of the determination conductivity of SBR at 24-25°C, 54-60% R.H. was measured by using the resistivity testing fixture (Keithley, Model 8009)

Sample	Thickness	Applied voltage (V)			Measured Current (A)			Conductivity (S/cm)		
	(cm)	1	2	3	1	2	3	1	2	3
SBR	1) 0.188	1	1	1	1.00E-12	7.49E-13	8.86E-13	8.11E-15	6.05E-15	7.16E-15
	2) 0.186	2	2	2	1.48E-12	1.49E-12	1.47E-12	5.98E-15	6.01E-15	5.95E-15
	3) 0.181	3	3	3	2.17E-12	2.15E-12	2.20E-12	5.86E-15	5.79E-15	5.91E-15
		4	4	4	2.85E-12	2.83E-12	2.83E-12	5.76E-15	5.71E-15	5.71E-15
		5	5	5	3.43E-12	3.44E-12	3.42E-12	5.55E-15	5.55E-15	5.52E-15
		6	6	6	4.03E-12	4.06E-12	4.01E-12	5.43E-15	5.47E-15	5.40E-15
		7	7	7	4.90E-12	4.86E-12	4.88E-12	5.65E-15	5.61E-15	5.63E-15
		8	8	8	5.47E-12	5.44E-12	5.49E-12	5.52E-15	5.49E-15	5.55E-15
		9	9	9	5.83E-12	5.92E-12	5.90E-12	5.24E-15	5.31E-15	5.30E-15
		10	10	10	6.42E-12	6.39E-12	6.45E-12	5.19E-15	5.17E-15	5.21E-15
		11	11	11	7.05E-12	7.07E-12	7.02E-12	5.18E-15	5.19E-15	5.16E-15
		12	12	12	7.91E-12	7.89E-12	7.93E-12	5.33E-15	5.31E-15	5.34E-15
		13	13	13	9.10E-12	9.14E-12	9.12E-12	5.66E-15	5.68E-15	5.67E-15
		14	14	14	9.73E-12	9.72E-12	9.73E-12	5.61E-15	5.61E-15	5.62E-15
		15	15	15	1.07E-11	1.06E-11	1.07E-11	5.74E-15	5.71E-15	5.78E-15

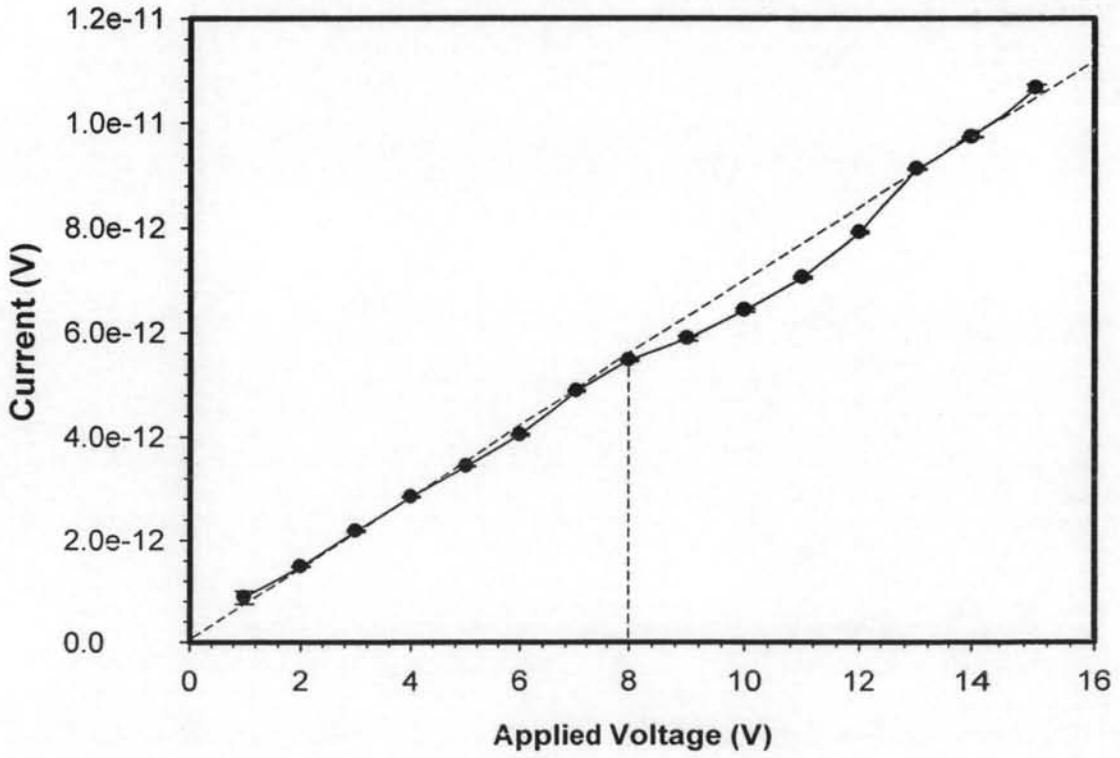

Table H8 The raw data of the determination conductivity of SIS at 24-25°C, 54-60% R.H. was measured by using the resistivity testing fixture (Keithley, Model 8009)

Sample	Thickness	Applied voltage (V)			Measured Current (A)			Conductivity (S/cm)		
	(cm)	1	2	3	1	2	3	1	2	3
SIS	1) 0.77	50	50	50	2.97E-13	2.93E-13	2.96E-13	1.95E-16	1.92E-16	1.94E-16
	2) 0.73	100	100	100	3.86E-13	3.94E-13	4.13E-13	1.26E-16	1.29E-16	1.35E-16
	3) 0.75	150	150	150	4.96E-13	4.90E-13	4.49E-13	1.08E-16	1.07E-16	9.80E-17
		200	200	200	5.22E-13	5.24E-13	5.30E-13	8.55E-17	8.58E-17	8.68E-17
		250	250	250	6.21E-13	6.19E-13	6.25E-13	8.14E-17	8.11E-17	8.19E-17
		300	300	300	7.20E-13	7.22E-13	7.25E-13	7.86E-17	7.88E-17	7.91E-17
		350	350	350	8.28E-13	8.25E-13	8.19E-13	7.75E-17	7.72E-17	7.66E-17
		400	400	400	8.39E-13	8.40E-13	8.53E-13	6.87E-17	6.88E-17	6.98E-17
		450	450	450	9.08E-13	9.00E-13	8.98E-13	6.61E-17	6.55E-17	6.54E-17
		500	500	500	9.23E-13	9.28E-13	9.54E-13	6.05E-17	6.08E-17	6.25E-17
		550	550	550	1.04E-12	1.05E-12	1.05E-12	6.19E-17	6.25E-17	6.25E-17
		600	600	600	1.13E-12	1.12E-12	1.14E-12	6.17E-17	6.11E-17	6.22E-17
		650	650	650	1.22E-12	1.23E-12	1.24E-12	6.15E-17	6.20E-17	6.25E-17
		700	700	700	1.38E-12	1.39E-12	1.38E-12	6.46E-17	6.50E-17	6.46E-17
		750	750	750	1.51E-12	1.52E-12	1.53E-12	6.59E-17	6.64E-17	6.68E-17
		800	800	800	1.65E-12	1.65E-12	1.65E-12	6.75E-17	6.75E-17	6.75E-17
		850	850	850	1.85E-12	1.82E-12	1.79E-12	7.13E-17	7.01E-17	6.90E-17
		900	900	900	1.98E-12	1.99E-12	2.01E-12	7.21E-17	7.24E-17	7.31E-17
		950	950	950	2.29E-12	2.31E-12	2.25E-12	7.89E-17	7.96E-17	7.76E-17
		1000	1000	1000	2.51E-12	2.53E-12	2.51E-12	8.22E-17	8.29E-17	8.22E-17

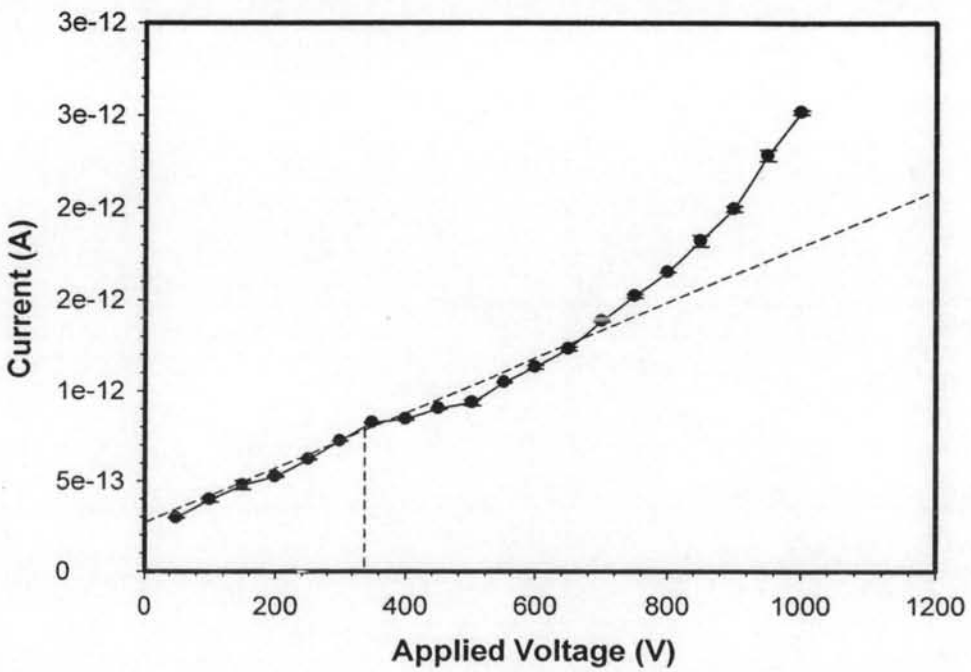

Table H9 The raw data of the determination conductivity of N_{acid}:$N_{monomer}$ (Ppy_U) at 24-25°C, 54-60% R.H. by using the two-point probe meter

Sample	Thickness	Applied voltage (V)			Measured Current (A)			Conductivity (S/cm)		
	(cm)	1	2	3	1	2	3	1	2	3
Ppy_U	1) 0.0353	0.005	0.005	0.005	4.40E-10	4.45E-10	4.54E-10	5.28E-01	5.34E-01	5.44E-01
	2) 0.0341	0.01	0.01	0.01	1.02E-09	1.03E-09	1.03E-09	6.13E-01	6.18E-01	6.19E-01
	3) 0.032	0.015	0.015	0.015	1.33E-09	1.33E-09	1.33E-09	5.32E-01	5.32E-01	5.32E-01
		0.02	0.02	0.02	1.63E-09	1.63E-09	1.63E-09	4.89E-01	4.88E-01	4.89E-01
		0.025	0.025	0.025	1.93E-09	1.93E-09	1.94E-09	4.62E-01	4.63E-01	4.64E-01
		0.03	0.03	0.03	2.49E-09	2.50E-09	2.50E-09	4.98E-01	5.00E-01	5.00E-01
		0.035	0.035	0.035	3.09E-09	3.09E-09	3.09E-09	5.30E-01	5.30E-01	5.30E-01
		0.04	0.04	0.04	3.38E-09	3.37E-09	3.37E-09	5.06E-01	5.06E-01	5.05E-01
		0.045	0.045	0.045	3.95E-09	3.97E-09	3.97E-09	5.26E-01	5.29E-01	5.29E-01
		0.05	0.05	0.05	4.26E-09	4.25E-09	4.25E-09	5.11E-01	5.10E-01	5.10E-01
		0.055	0.055	0.055	4.84E-09	4.84E-09	4.85E-09	5.28E-01	5.28E-01	5.28E-01
		0.06	0.06	0.06	5.44E-09	5.44E-09	5.44E-09	5.44E-01	5.44E-01	5.44E-01
		0.065	0.065	0.065	5.71E-09	5.68E-09	5.67E-09	5.27E-01	5.24E-01	5.23E-01
		0.07	0.07	0.07	6.26E-09	6.27E-09	6.28E-09	5.36E-01	5.37E-01	5.38E-01
		0.075	0.075	0.075	6.59E-09	6.60E-09	6.61E-09	5.27E-01	5.27E-01	5.28E-01
		0.08	0.08	0.08	7.19E-09	7.19E-09	7.19E-09	5.39E-01	5.39E-01	5.39E-01
		0.085	0.085	0.085	7.79E-09	7.80E-09	7.80E-09	5.49E-01	5.50E-01	5.50E-01
		0.09	0.09	0.09	8.08E-09	8.09E-09	8.09E-09	5.38E-01	5.39E-01	5.39E-01
		0.095	0.095	0.095	8.69E-09	8.70E-09	8.70E-09	5.49E-01	5.49E-01	5.49E-01
		0.1	0.1	0.1	9.00E-09	9.01E-09	9.02E-09	5.40E-01	5.40E-01	5.41E-01

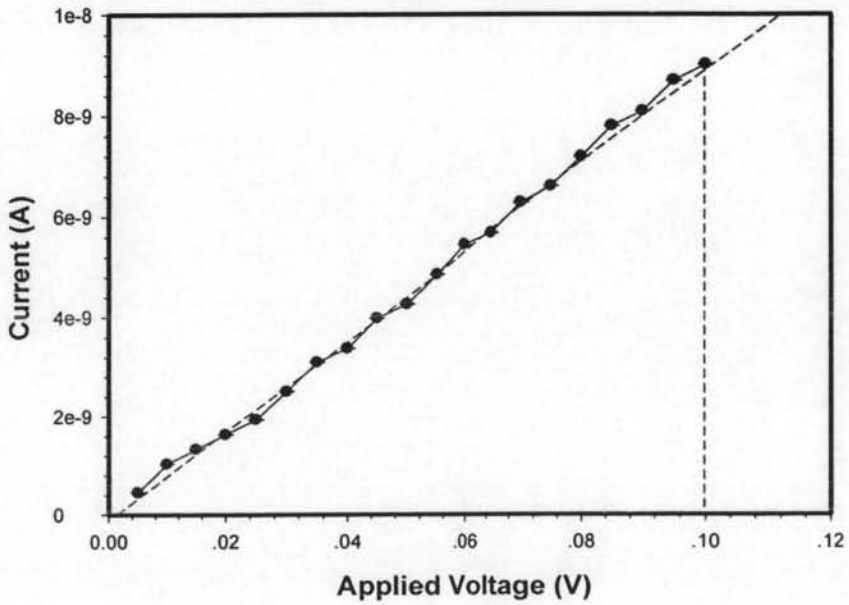

Table H12 The raw data of the determination conductivity of N_{acid}:$N_{monomer}$ (Ppy_1:1) at 24-25°C, 54-60% R.H. was measured by using the two-point probe meter

Sample	Thickness	Applied voltage (V)			Measured Current (A)			Conductivity (S/cm)		
	(cm)	1	2	3	1	2	3	1	2	3
Ppy_1:1	1) 0.0895	0.005	0.005	4.41E-10	8.84E-09	8.86E-09	8.94E-09	3.93E+00	3.94E+00	3.98E+00
	2) 0.0881	0.01	0.01	1.02E-09	2.12E-08	2.13E-08	2.14E-08	4.72E+00	4.74E+00	4.77E+00
	3) 0.0941	0.015	0.015	1.33E-09	2.77E-08	2.79E-08	2.79E-08	4.11E+00	4.14E+00	4.14E+00
		0.02	0.02	1.63E-09	3.42E-08	3.43E-08	3.44E-08	3.81E+00	3.82E+00	3.83E+00
		0.025	0.025	1.93E-09	4.07E-08	4.08E-08	4.08E-08	3.62E+00	3.63E+00	3.63E+00
		0.03	0.03	2.49E-09	5.34E-08	5.36E-08	5.37E-08	3.96E+00	3.97E+00	3.98E+00
		0.035	0.035	3.09E-09	6.65E-08	6.66E-08	6.67E-08	4.23E+00	4.23E+00	4.24E+00
		0.04	0.04	3.38E-09	7.33E-08	7.35E-08	7.35E-08	4.08E+00	4.09E+00	4.09E+00
		0.045	0.045	3.95E-09	8.64E-08	8.66E-08	8.63E-08	4.27E+00	4.28E+00	4.27E+00
		0.05	0.05	4.26E-09	9.31E-08	9.34E-08	9.32E-08	4.14E+00	4.16E+00	4.15E+00
		0.055	0.055	4.84E-09	1.06E-07	1.06E-07	1.06E-07	4.29E+00	4.29E+00	4.29E+00
		0.06	0.06	5.44E-09	1.19E-07	1.19E-07	1.19E-07	4.42E+00	4.41E+00	4.41E+00
		0.065	0.065	5.71E-09	1.26E-07	1.26E-07	1.26E-07	4.30E+00	4.32E+00	4.32E+00
		0.07	0.07	6.26E-09	1.39E-07	1.39E-07	1.38E-07	4.41E+00	4.41E+00	4.40E+00
		0.075	0.075	6.59E-09	1.45E-07	1.45E-07	1.45E-07	4.30E+00	4.30E+00	4.31E+00
		0.08	0.08	7.19E-09	1.58E-07	1.58E-07	1.59E-07	4.40E+00	4.41E+00	4.41E+00
		0.085	0.085	7.79E-09	1.72E-07	1.72E-07	1.72E-07	4.50E+00	4.49E+00	4.49E+00
		0.09	0.09	8.08E-09	1.78E-07	1.79E-07	1.79E-07	4.41E+00	4.42E+00	4.43E+00
		0.095	0.095	8.69E-09	1.92E-07	1.91E-07	1.91E-07	4.50E+00	4.47E+00	4.47E+00
		0.1	0.1	9.00E-09	1.97E-07	1.97E-07	1.97E-07	4.39E+00	4.38E+00	4.38E+00

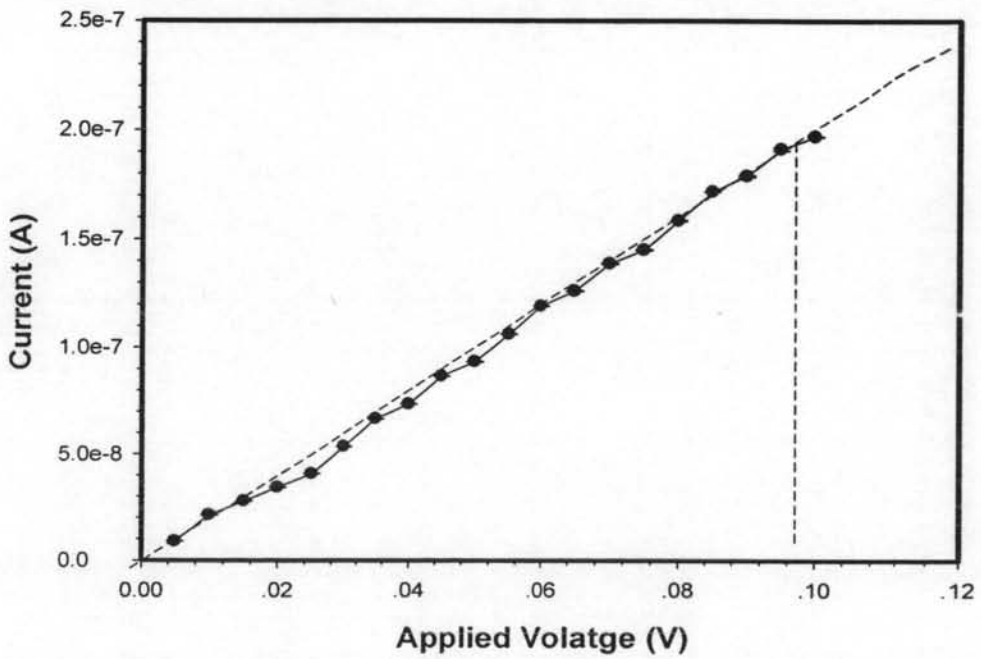

Table H13 The raw data of the determination conductivity of AR70 with 1% undoped Ppy (AR70:1_un) at 24-25°C, 54-60% R.H.

Sample	Thickness	Applied voltage (V)			Measured Current (A)			Conductivity (S/cm)		
	(cm)	1	2	3	1	2	3	1	2	3
AR70:1_un	1) 0.085	10	10	10	3.15E-09	3.21E-09	3.24E-09	1.16E-12	1.18E-12	1.19E-12
	2) 0.083	20	20	20	6.99E-09	6.97E-09	6.96E-09	1.28E-12	1.28E-12	1.28E-12
	3) 0.083	30	30	30	1.08E-08	1.08E-08	1.08E-08	1.32E-12	1.32E-12	1.32E-12
		40	40	40	1.48E-08	1.48E-08	1.48E-08	1.35E-12	1.36E-12	1.35E-12
		50	50	50	1.89E-08	1.91E-08	1.92E-08	1.39E-12	1.40E-12	1.41E-12
		60	60	60	2.34E-08	2.35E-08	2.35E-08	1.43E-12	1.44E-12	1.44E-12
		70	70	70	2.81E-08	2.80E-08	2.79E-08	1.47E-12	1.47E-12	1.46E-12
		80	80	80	3.26E-08	3.25E-08	3.25E-08	1.49E-12	1.49E-12	1.49E-12
		90	90	90	3.71E-08	3.69E-08	3.69E-08	1.51E-12	1.50E-12	1.50E-12
		100	100	100	4.16E-08	4.13E-08	4.12E-08	1.53E-12	1.52E-12	1.51E-12

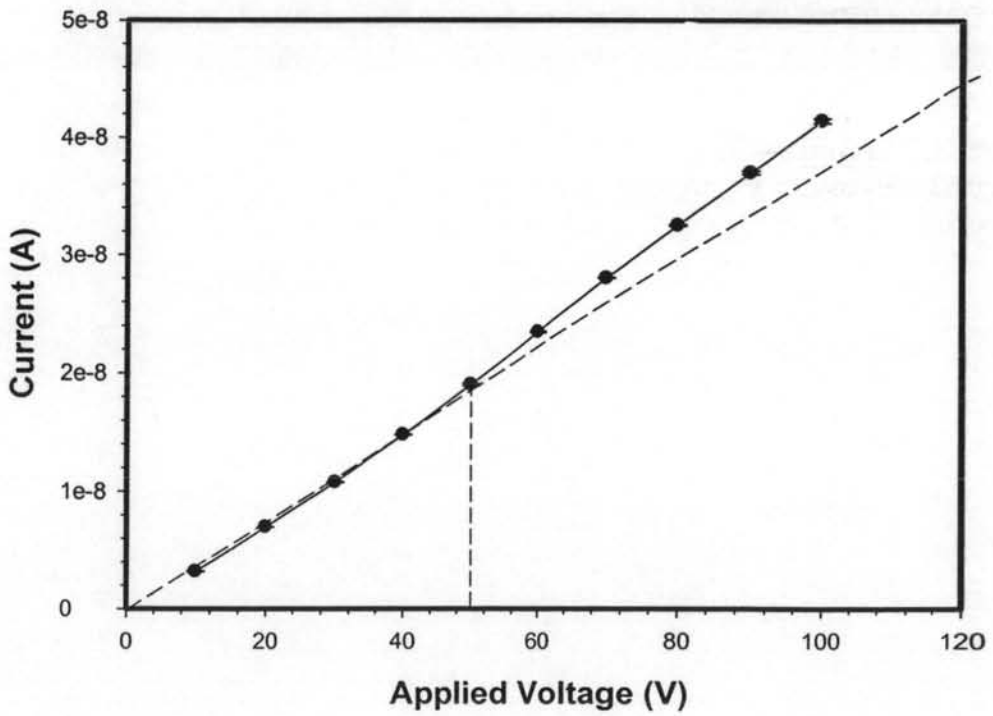

Table H14 The raw data of the determination conductivity of AR70 with 2% undoped Ppy (AR70:2_un) at 24-25°C, 54-60% R.H.

Sample	Thickness	Applied voltage (V)			Measured Current (A)			Conductivity (S/cm)		
	(cm)	1	2	3	1	2	3	1	2	3
AR70:2_un	1) 0.068	5	5	5	2.01E-09	1.99E-09	1.97E-09	1.21E-12	1.20E-12	1.19E-12
	2) 0.071	10	10	10	4.33E-09	4.30E-09	4.28E-09	1.31E-12	1.30E-12	1.29E-12
	3) 0.067	15	15	15	6.80E-09	6.78E-09	6.78E-09	1.37E-12	1.36E-12	1.36E-12
		20	20	20	9.50E-09	9.53E-09	9.59E-09	1.43E-12	1.44E-12	1.44E-12
		25	25	25	1.24E-08	1.26E-08	1.25E-08	1.50E-12	1.52E-12	1.50E-12
		30	30	30	1.53E-08	1.53E-08	1.53E-08	1.54E-12	1.53E-12	1.53E-12
		35	35	35	1.84E-08	1.84E-08	1.84E-08	1.58E-12	1.59E-12	1.58E-12
		40	40	40	2.24E-08	2.21E-08	2.24E-08	1.69E-12	1.67E-12	1.69E-12
		45	45	45	2.64E-08	2.60E-08	2.61E-08	1.77E-12	1.74E-12	1.75E-12
		50	50	50	3.01E-08	3.01E-08	3.01E-08	1.82E-12	1.81E-12	1.81E-12

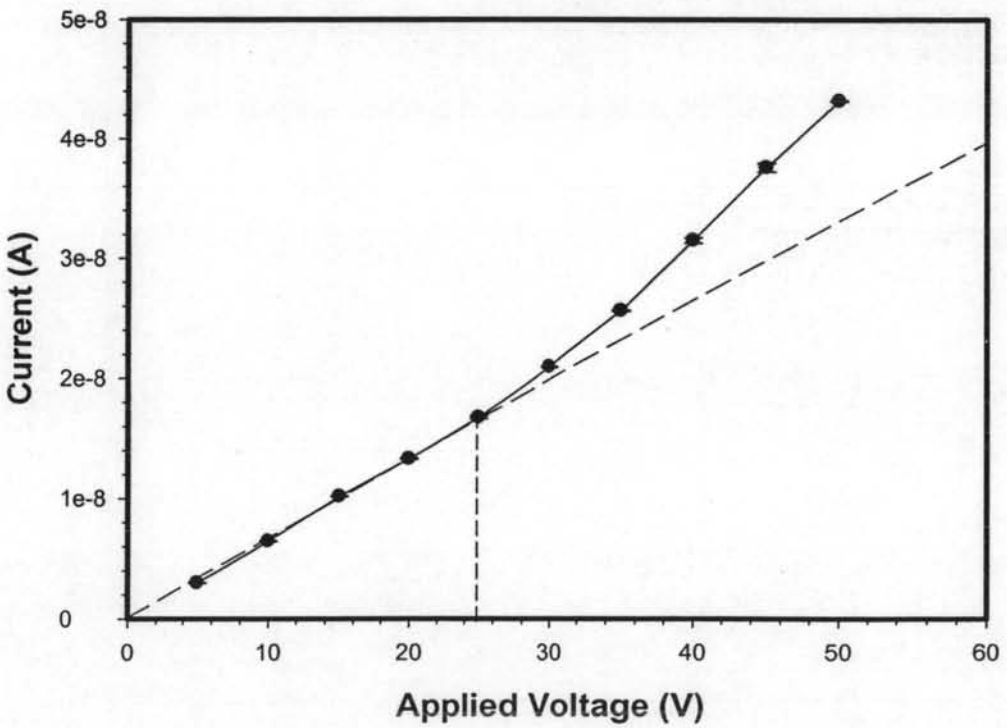

Table H15 The raw data of the determination conductivity of AR70 with 3% undoped Ppy (AR70:3_un) at 24-25°C, 54-60% R.H.

Sample	Thickness	Applied voltage (V)			Measured Current (A)			Conductivity (S/cm)		
	(cm)	1	2	3	1	2	3	1	2	3
AR70:3_un	1) 0.085	5	5	5	6.47E-09	6.84E-09	6.98E-09	3.90E-12	4.12E-12	4.21E-12
	2) 0.090	10	10	10	1.36E-08	1.34E-08	1.31E-08	4.11E-12	4.04E-12	3.95E-12
	3) 0.088	15	15	15	2.18E-08	2.05E-08	2.05E-08	4.38E-12	4.12E-12	4.12E-12
		20	20	20	2.83E-08	2.85E-08	2.90E-08	4.26E-12	4.30E-12	4.37E-12
		25	25	25	3.51E-08	3.58E-08	3.51E-08	4.24E-12	4.31E-12	4.24E-12
		30	30	30	4.46E-08	4.43E-08	4.49E-08	4.48E-12	4.45E-12	4.51E-12
		35	35	35	5.50E-08	5.40E-08	5.48E-08	4.73E-12	4.65E-12	4.72E-12
		40	40	40	6.58E-08	6.56E-08	6.52E-08	4.96E-12	4.94E-12	4.91E-12
		45	45	45	7.66E-08	7.57E-08	7.50E-08	5.13E-12	5.07E-12	5.02E-12
		50	50	50	9.06E-08	9.04E-08	9.02E-08	5.46E-12	5.45E-12	5.44E-12

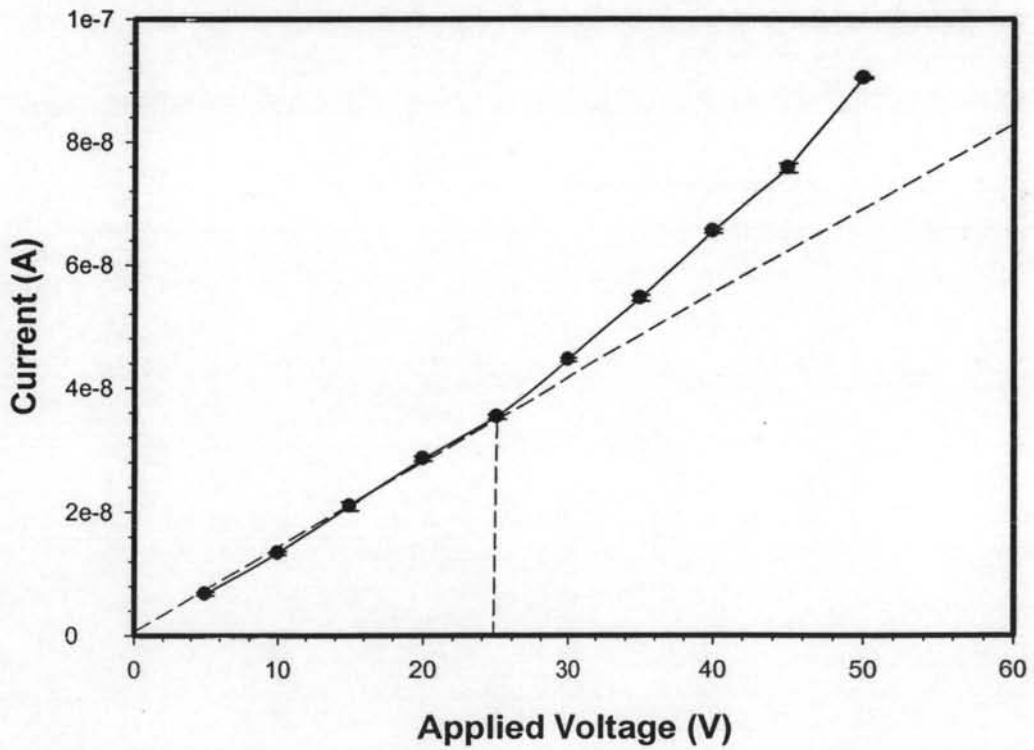

Table H16 The raw data of the determination conductivity of AR70 with 4% undoped Ppy (AR70:4_un) at 24-25°C, 54-60% R.H.

Sample	Thickness	Applied voltage (V)			Measured Current (A)			Conductivity (S/cm)		
	(cm)	1	2	3	1	2	3	1	2	3
AR70:4_un	1) 0.068	2	2	2	3.04E-09	3.24E-09	3.05E-09	4.58E-12	4.87E-12	4.59E-12
	2) 0.069	4	4	4	6.46E-09	6.49E-09	6.46E-09	4.86E-12	4.89E-12	4.86E-12
	3) 0.071	6	6	6	1.09E-08	1.10E-08	1.09E-08	5.48E-12	5.51E-12	5.47E-12
		8	8	8	1.35E-08	1.35E-08	1.35E-08	5.07E-12	5.10E-12	5.10E-12
		10	10	10	1.63E-08	1.64E-08	1.65E-08	4.91E-12	4.95E-12	4.98E-12
		12	12	12	1.94E-08	1.93E-08	1.96E-08	4.88E-12	4.86E-12	4.92E-12
		14	14	14	2.27E-08	2.28E-08	2.28E-08	4.88E-12	4.91E-12	4.91E-12
		16	16	16	2.60E-08	2.61E-08	2.62E-08	4.90E-12	4.91E-12	4.94E-12
		18	18	18	2.99E-08	2.98E-08	2.99E-08	5.01E-12	5.00E-12	5.00E-12
		20	20	20	3.32E-08	3.34E-08	3.37E-08	5.00E-12	5.04E-12	5.07E-12

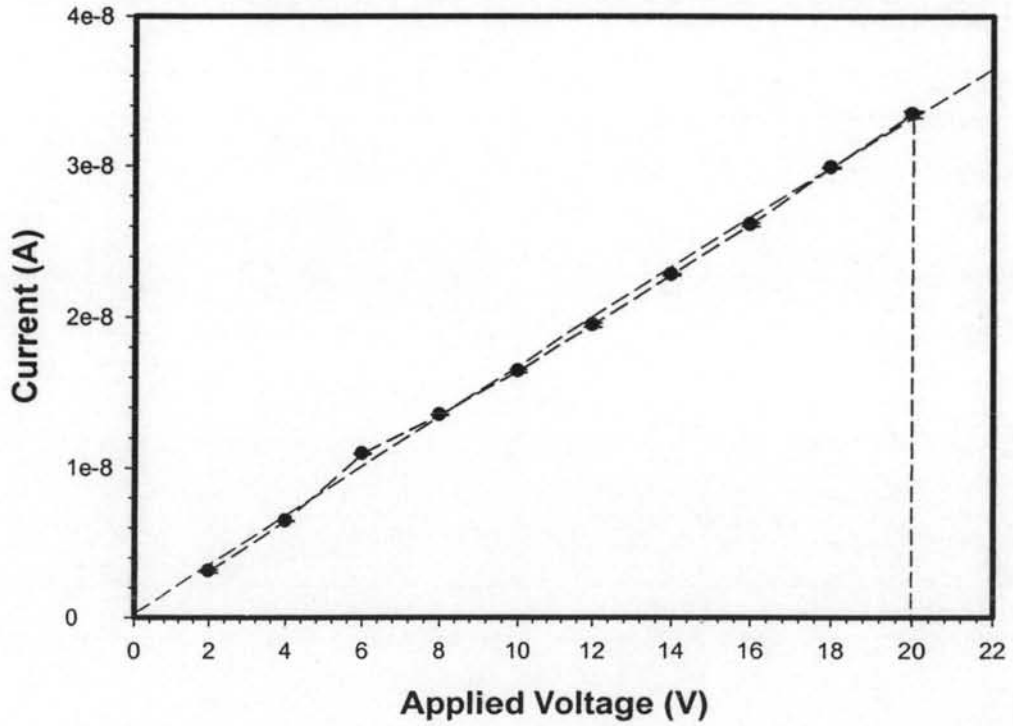

Table H17 The raw data of the determination conductivity of AR70 with 5% undoped Ppy (AR70:5_un) at 24-25°C, 54-60% R.H.

Sample	Thickness	Applied voltage (V)			Measured Current (A)			Conductivity (S/cm)		
	(cm)	1	2	3	1	2	3	1	2	3
AR70:_5un	1) 0.068	2	2	2	2.77E-09	2.76E-09	2.74E-09	6.03E-12	6.00E-12	5.96E-12
	2) 0.069	4	4	4	5.11E-09	5.07E-09	5.07E-09	5.56E-12	5.52E-12	5.52E-12
	3) 0.071	6	6	6	7.47E-09	7.47E-09	7.43E-09	5.42E-12	5.42E-12	5.39E-12
		8	8	8	9.84E-09	9.81E-09	9.78E-09	5.36E-12	5.34E-12	5.32E-12
		10	10	10	1.22E-08	1.22E-08	1.22E-08	5.33E-12	5.32E-12	5.33E-12
		12	12	12	1.46E-08	1.46E-08	1.46E-08	5.32E-12	5.31E-12	5.30E-12
		14	14	14	1.71E-08	1.71E-08	1.71E-08	5.32E-12	5.32E-12	5.31E-12
		16	16	16	1.96E-08	1.95E-08	1.95E-08	5.32E-12	5.31E-12	5.30E-12
		18	18	18	2.19E-08	2.19E-08	2.19E-08	5.30E-12	5.30E-12	5.30E-12
		20	20	20	2.44E-08	2.44E-08	2.44E-08	5.32E-12	5.32E-12	5.31E-12

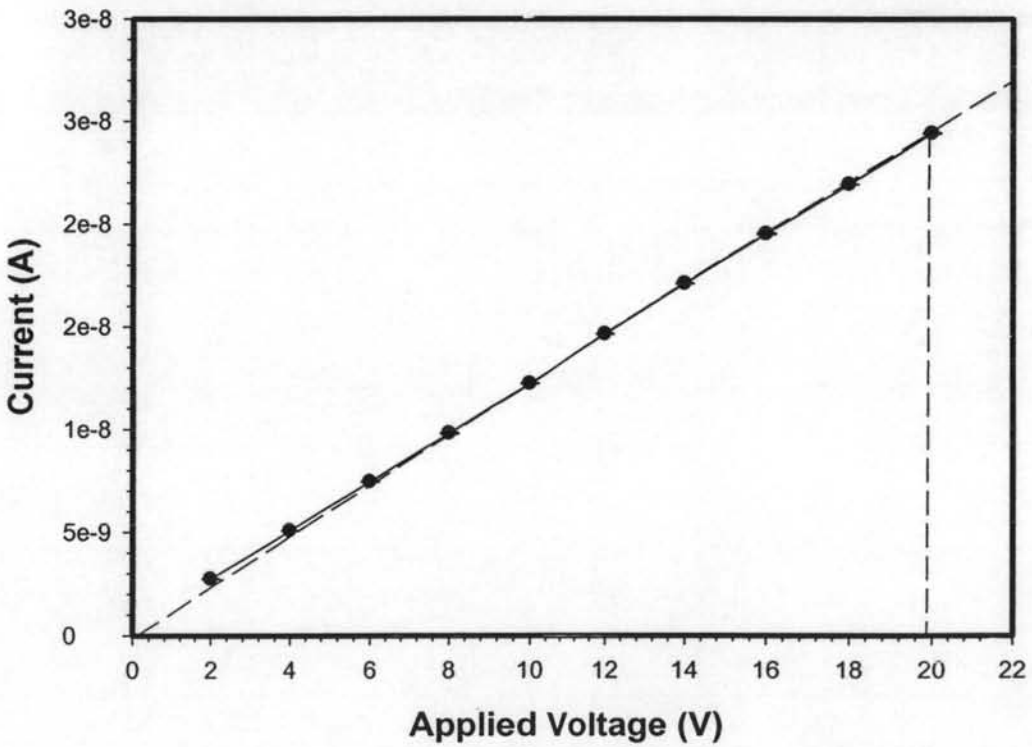

Appendix I Identification of Crystallinity of Undoped and Doped Ppy.

Powder of Ppy was packed on the glass plate and taken into X-ray Rigaku, mode 1860. The data were collected after X-ray passed through the sample. Properties of Ppy can be investigated by the peaks of graph. The characteristic peaks were determined in range 2θ between 5 - 35° as shown in Figure I1. The d-spacing between molecules can be calculated by use this equation.

$$n\lambda = 2d\sin\theta \qquad (I.1)$$

where n is number, λ is wavelength of X-ray source, d is d-spacing, θ is angle that peaks appeared.

Figure I1 XRD Patterns of undoped and doped Ppy

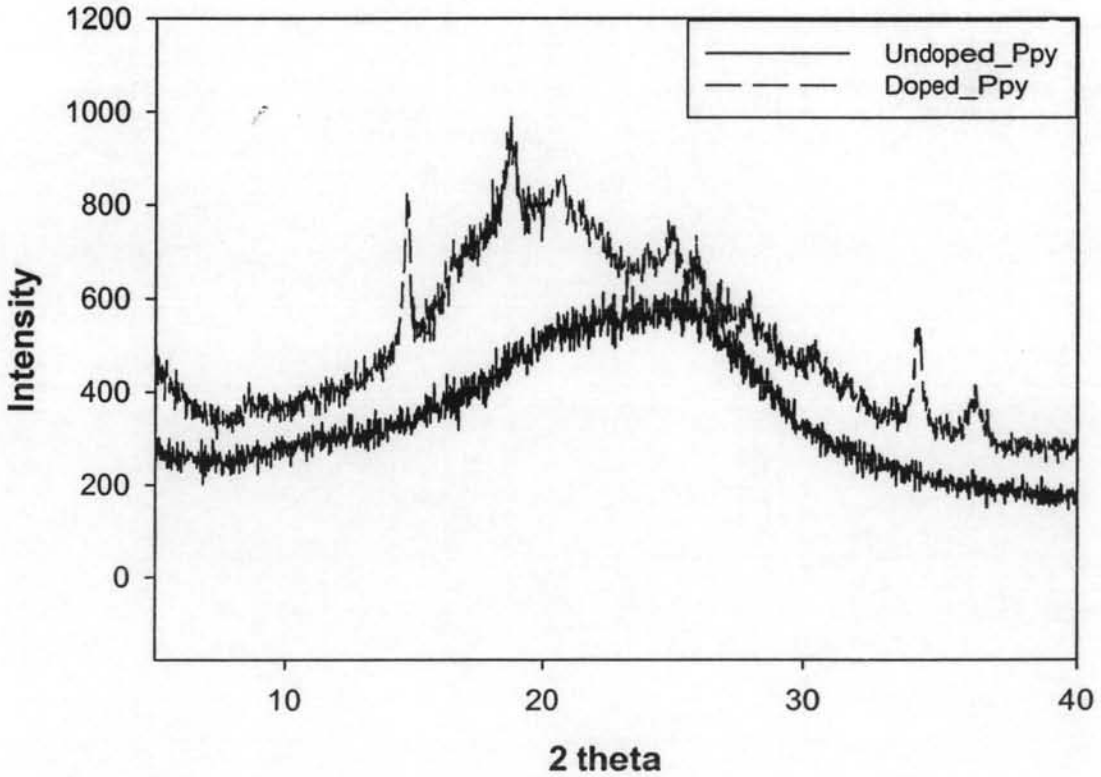

Table I1 shows the raw data of characteristic peaks and d-spacing of Ppy of undoped and doped polypyrrole from $2\theta = 15\text{-}30°$. For doped polypyrrole, the peak at 20^0 can refer to the polypyrrole-counter ion or inter-counter ion interaction scattering (Song, M.K.2006) and The intensity of high angle peak at 26^0 is related to interplanar distance of pyrrole –pyrrole and polypyrrole-counter ion .

Table I1 XRD raw data of undoped and doped Ppy

	2θ (°)	**d-spacing (A°)**	**Intensity**
Undoped			
	26.26, 26*	3.39, 3.42*	2488
Doped Ppy			
	20.32, 20*	4.37, 4.48*	3111
	26.06, 26*	3.42, 3.42*	1774

*Note: Values from Song *et al.*, 2004

Appendix J Scanning Electron Micrograph of Undoped Ppy, Doped Ppy and Polypyrrole/Polyacylate rubber Blends (Ppy_U/AR70)

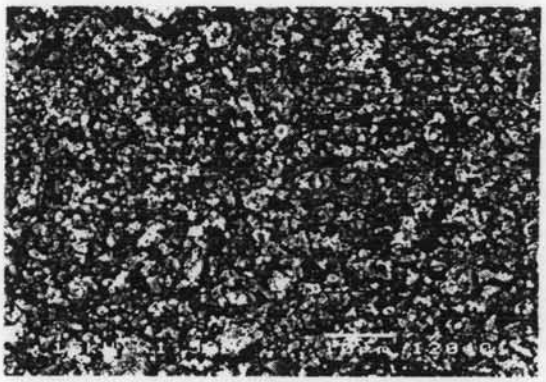

(a)

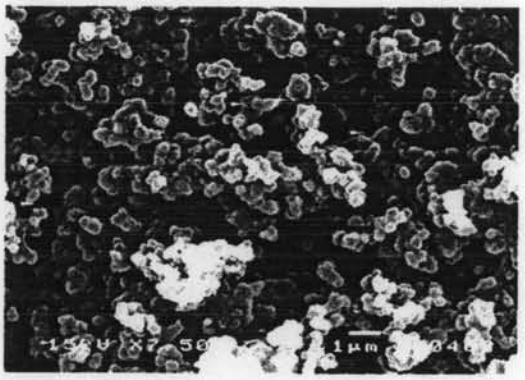

(b)

(c)

Figure J1 The morphology of undoped polypyrrole powder at magnifications of: a) 1500, b) 7,500; and Doped polypyrrole powder at magnifications of c):1500.

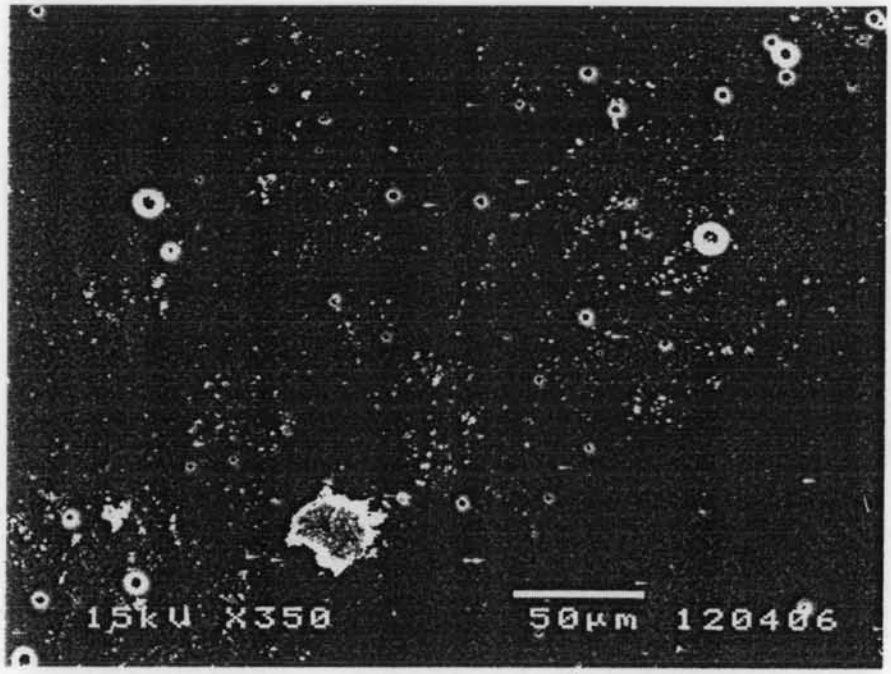

(a)

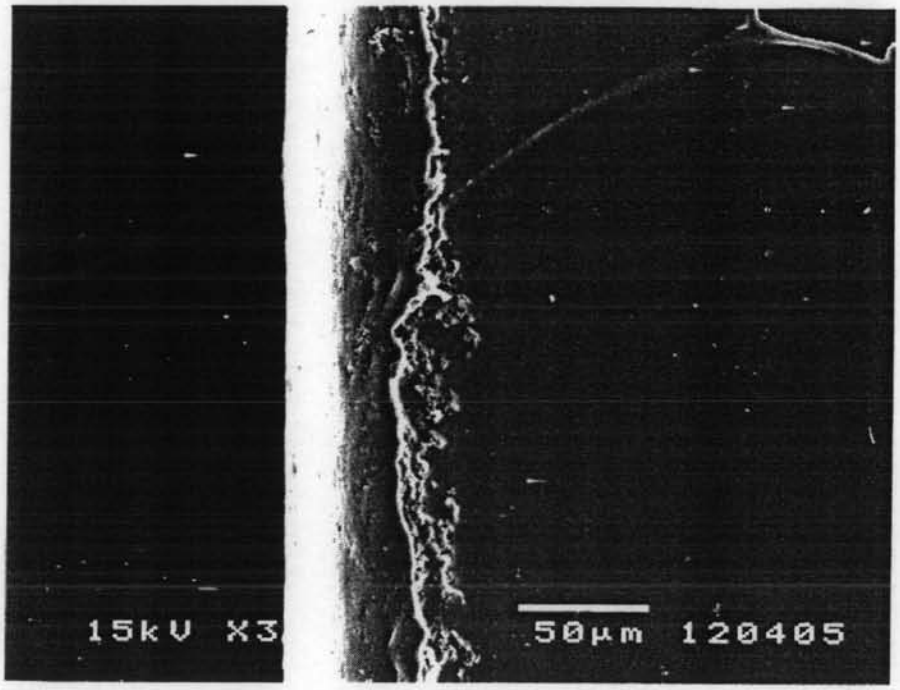

(b)

Figure J2 The morphology of polypyrrole/polyacylate blends at polypyrrole particle concentrations = 1%vol/vol at magnifications of 350: a) surface, and b) cross section pictures.

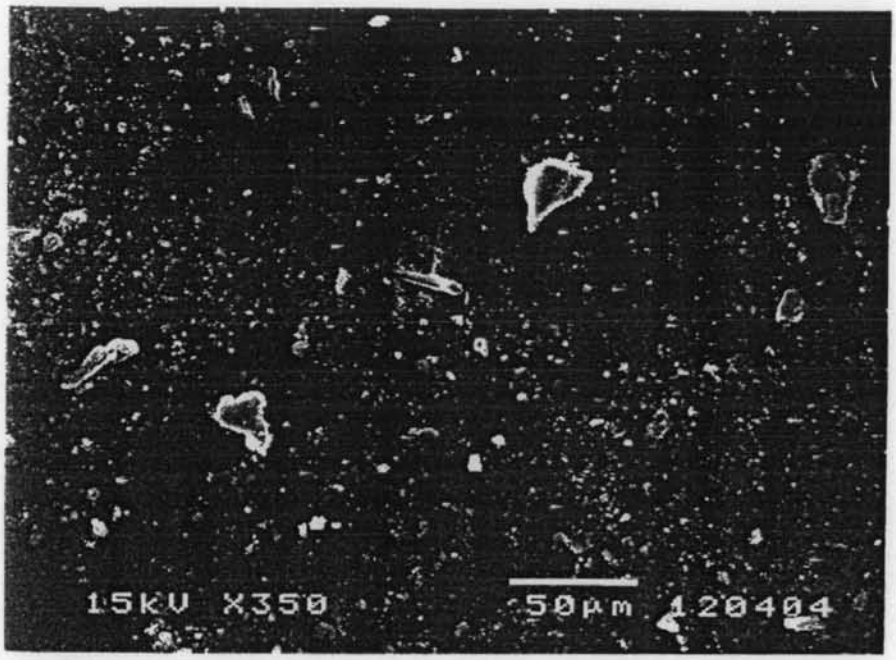

(a)

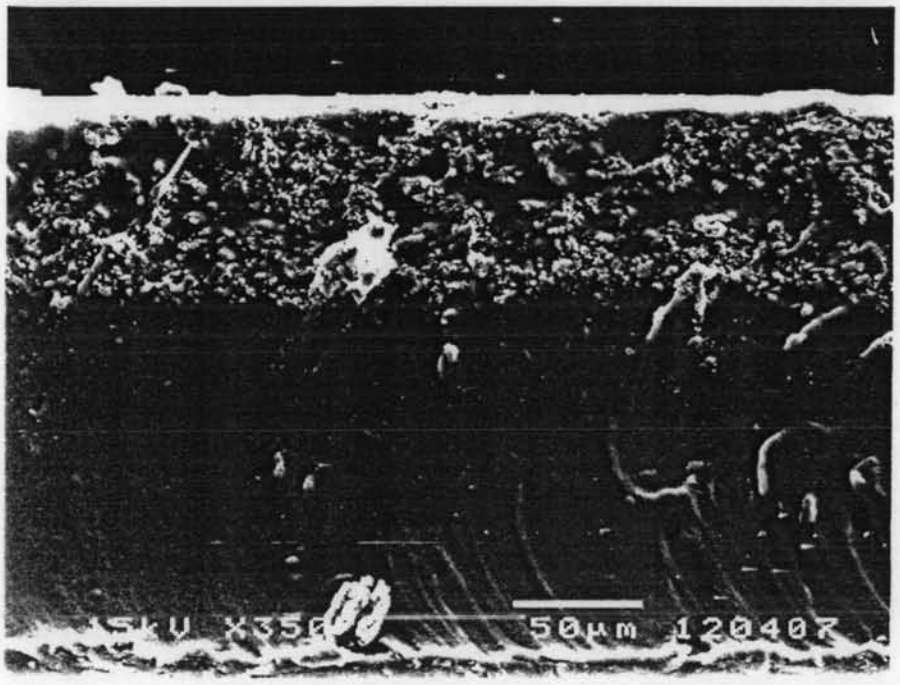

(b)

Figure J3 The morphology of polypyrrole/polyacylate blends as polypyrrole particle concentrations = 3%vol/vol at magnifications of 350: a) surface, and b) cross section pictures.

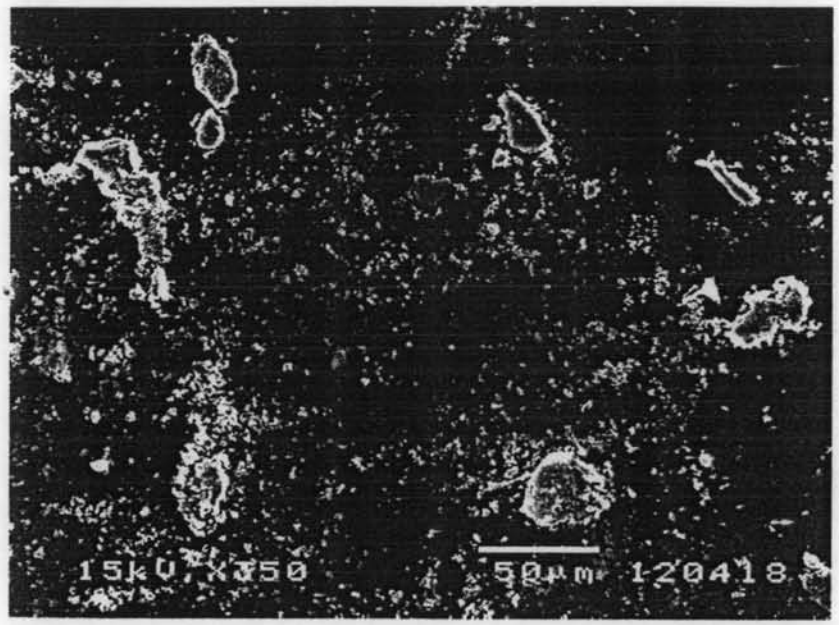

(a)

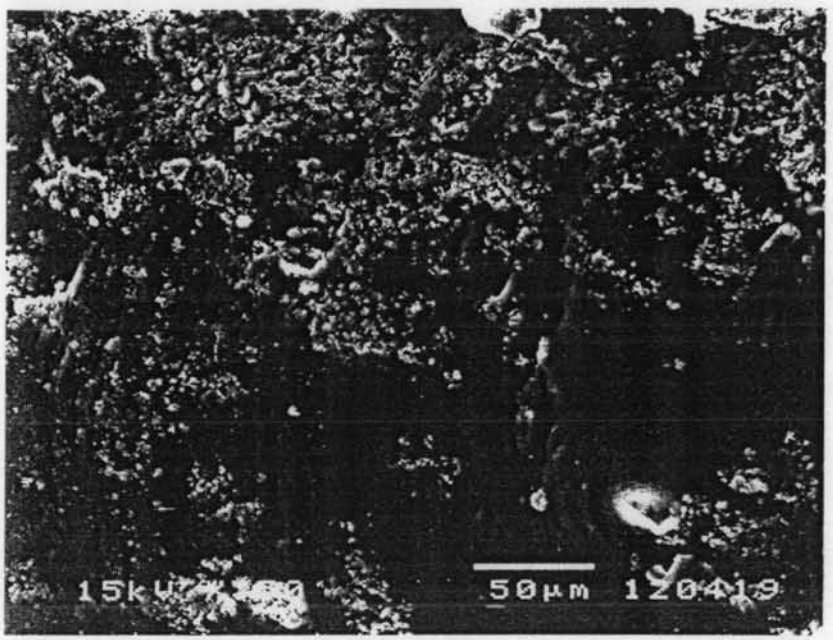

(b)

Figure J4 The morphology of polypyrrole/polyacylate blends as polypyrrole particle concentrations = 5 %vol/vol at magnifications of 350: a) surface, and b) cross section pictures.

Appendix K Electrorheological Properties Measurement of Pure Elastomer Matrix

The electrorheological properties of various pure elastomer matrices were measured by the melt rheometer (Rheometric Scientific, ARES) under oscillatory shear mode and applied electric filed strength varying from 0 to 2 kV/mm. In these experiments, the dynamic moduli (G' and G") were measured as functions of frequency and electric field strength. Strain sweep tests were first carried out to determine the suitable strain to measure G' and G" in the linear viscoelastic regime

K.1) Acrylate copolymer rubber latex (AR 70)

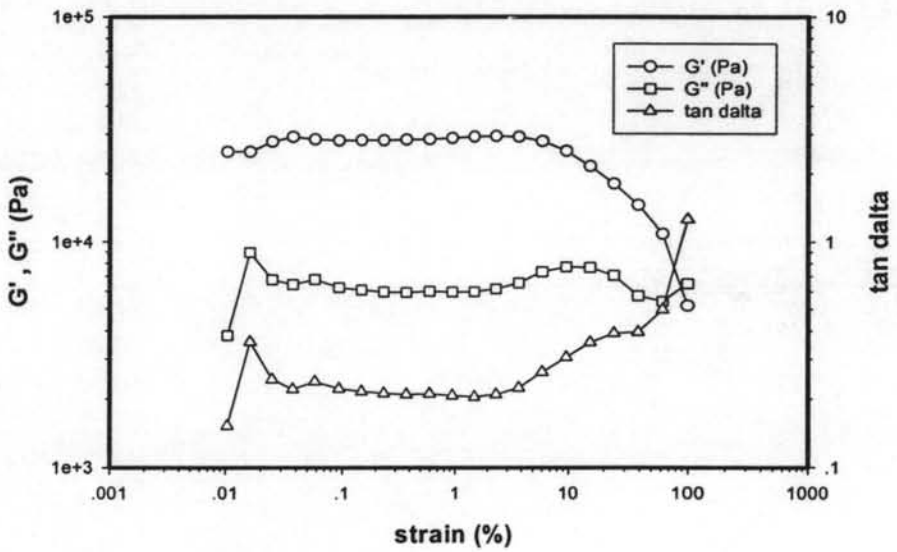

(a)

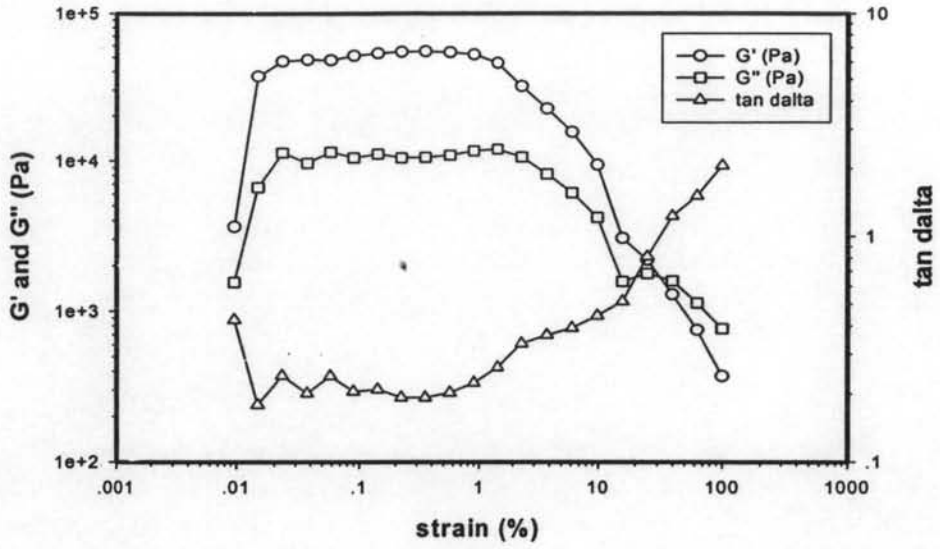

(b)

Figure K4 Strain sweep tests of pure acrylate copolymer rubber latex, frequency 1.0 rad/s, 27°C, gap 0.610 mm: at a) E = 0 V/mm; b) E = 2 kV/mm.

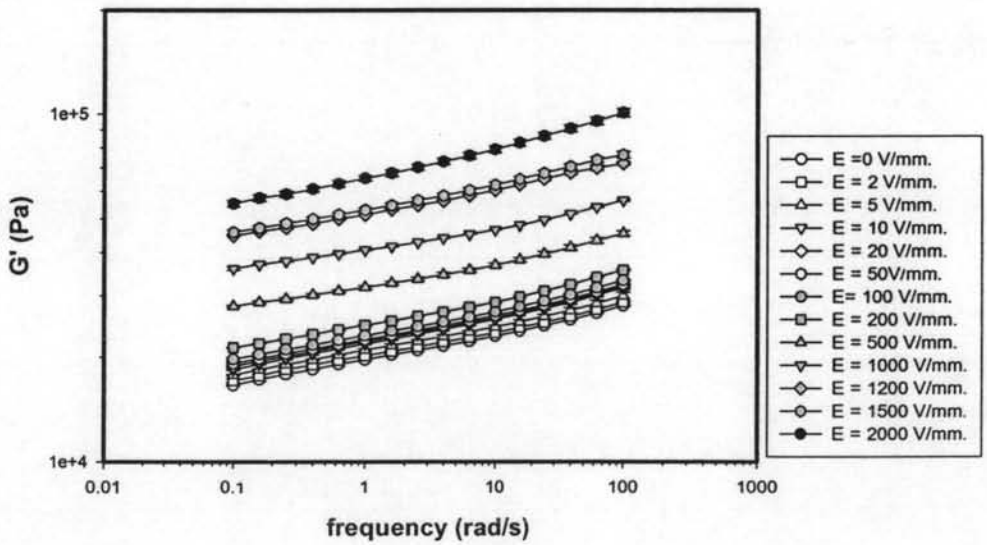

(a)

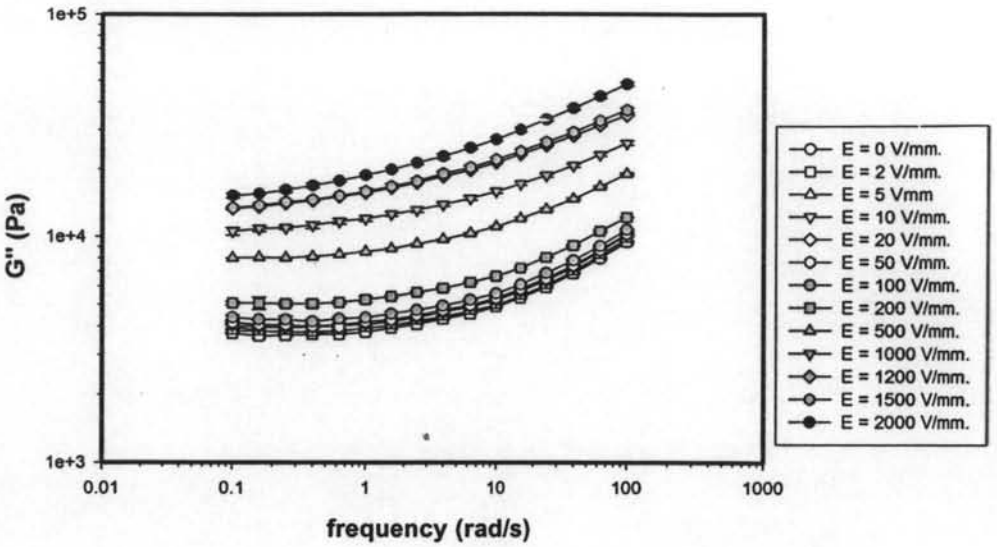

(b)

Figure K5 Frequency sweep tests of pure acrylate copolymer rubber latex, strain 1.0 %, 27°C, gap 0.610 mm with various electric field strengths: a) G'(Pa); b) G"(Pa).

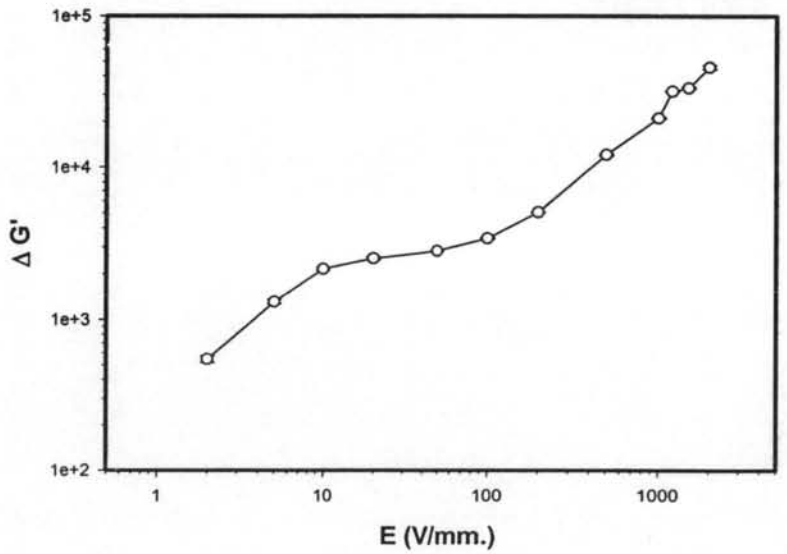

(a)

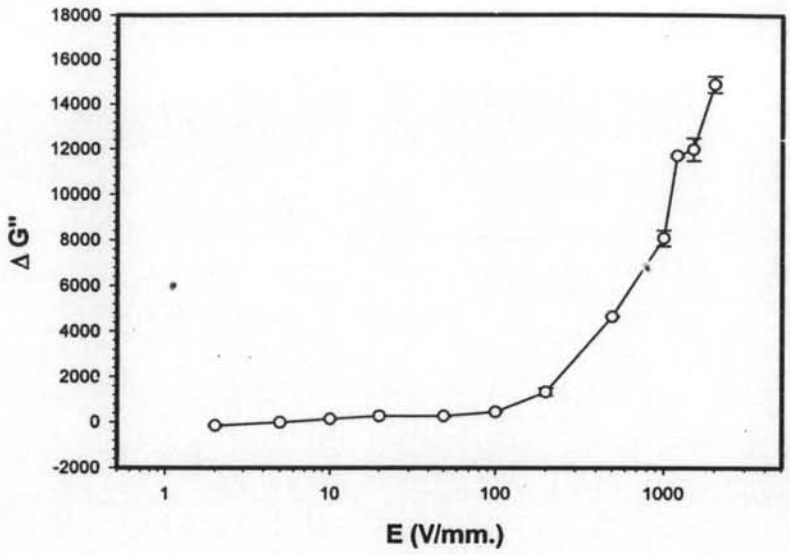

(b)

Figure K6 Responses of the storage and the loss moduli ($\Delta G'(\omega)$ and $\Delta G''(\omega)$)of the acrylate copolymer rubber latex vs. electric field strength, frequency 1.0 rad/s, strain 1% at 27°C: (a) $\Delta G'(\omega)$ when $G'_0 = 19666$ Pa; (b) $\Delta G''(\omega)$ when $G''_0 = 3925$ Pa.

K.2) Acrylate copolymer (AR71)

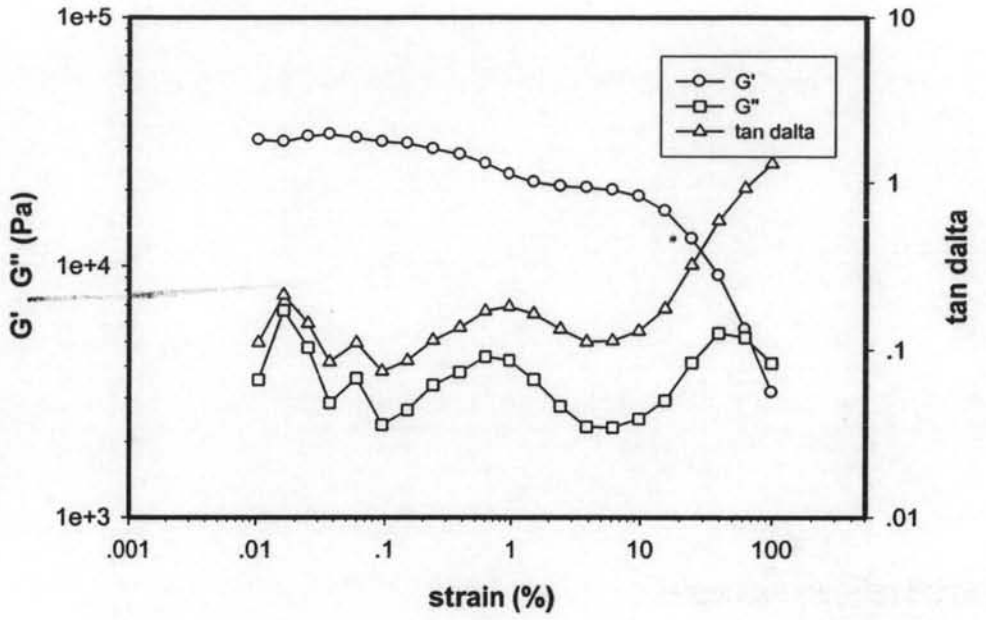

(a)

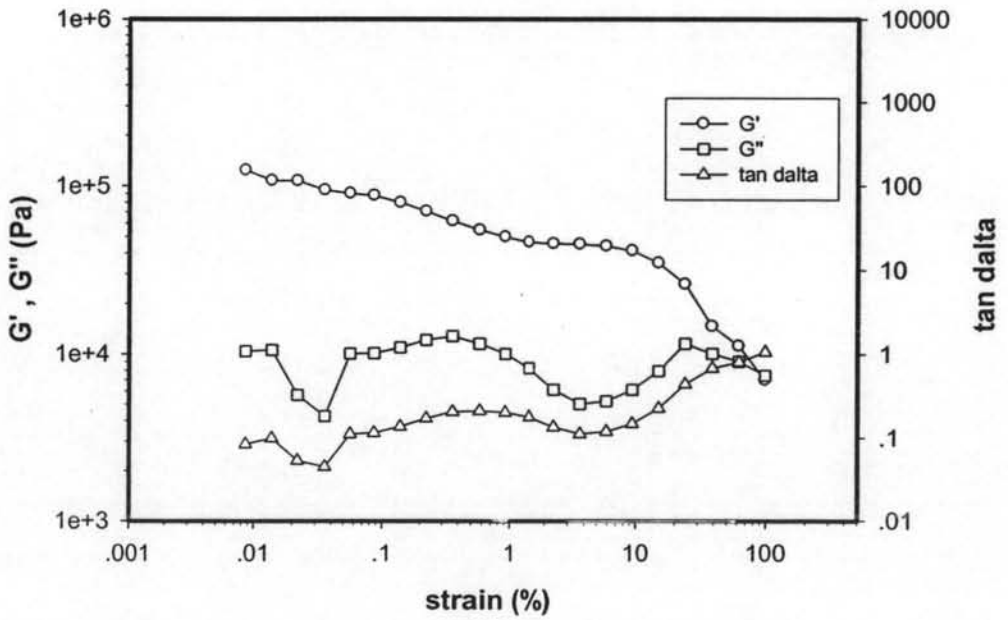

(b)

Figure K16 Strain sweep tests of pure acrylate copolymer(AR71), frequency 1 %, rad/s, 27 °C, and gap 0.600 mm at: a) E = 0 V/mm; b) E = 2 kV/mm.

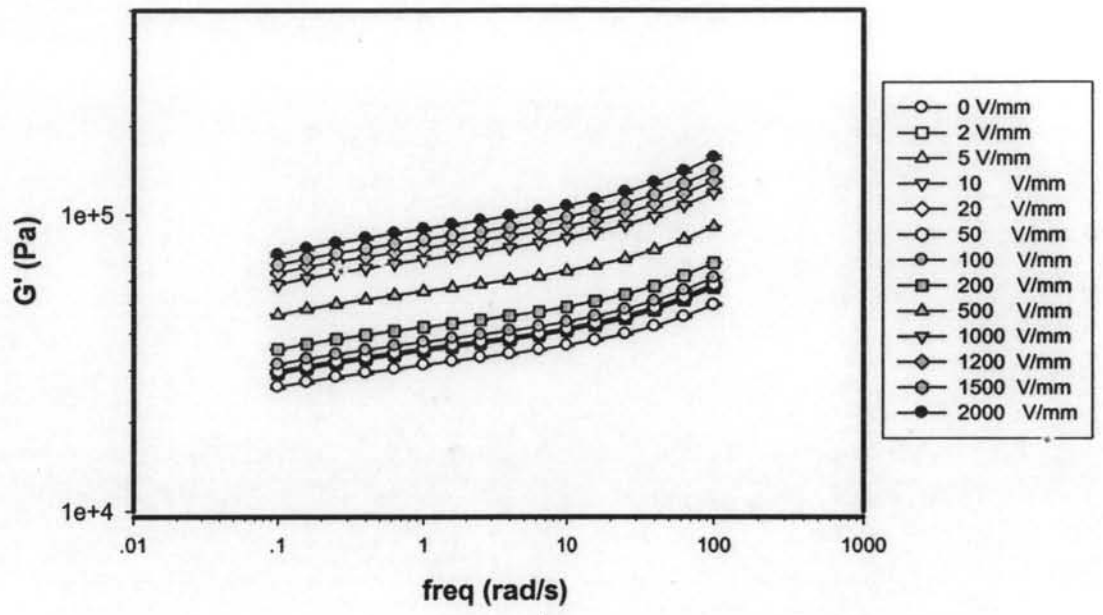

(a)

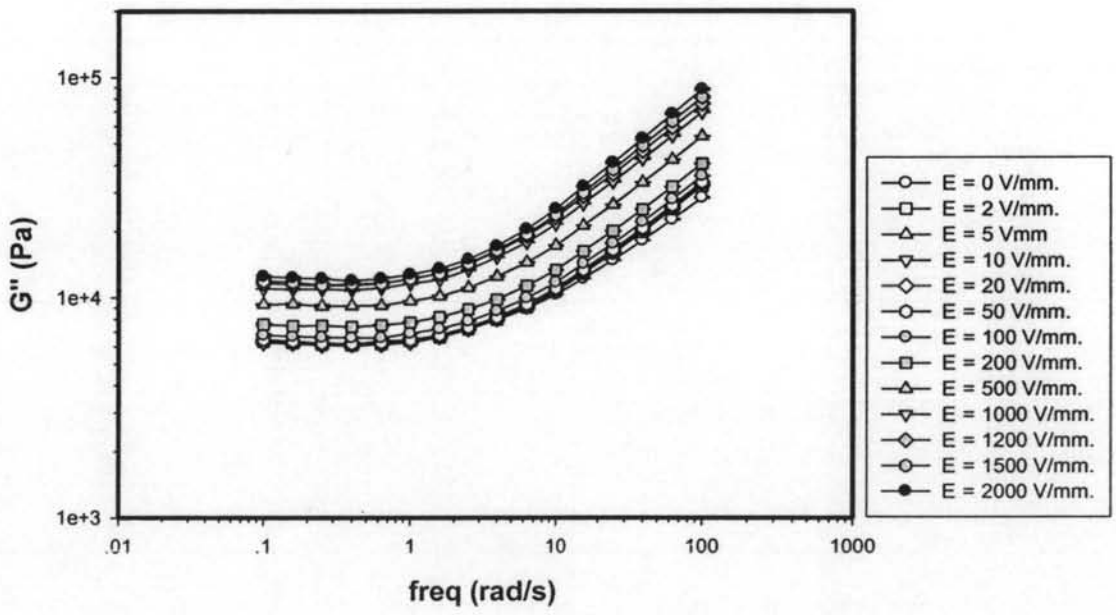

(b)

Figure K17 Frequency sweep tests of pure acrylate copolymer(AR71), strain 1 %, 27 °C, and gap 0.6 mm with various electric field strengths: a) G'(Pa); b) G''(Pa).

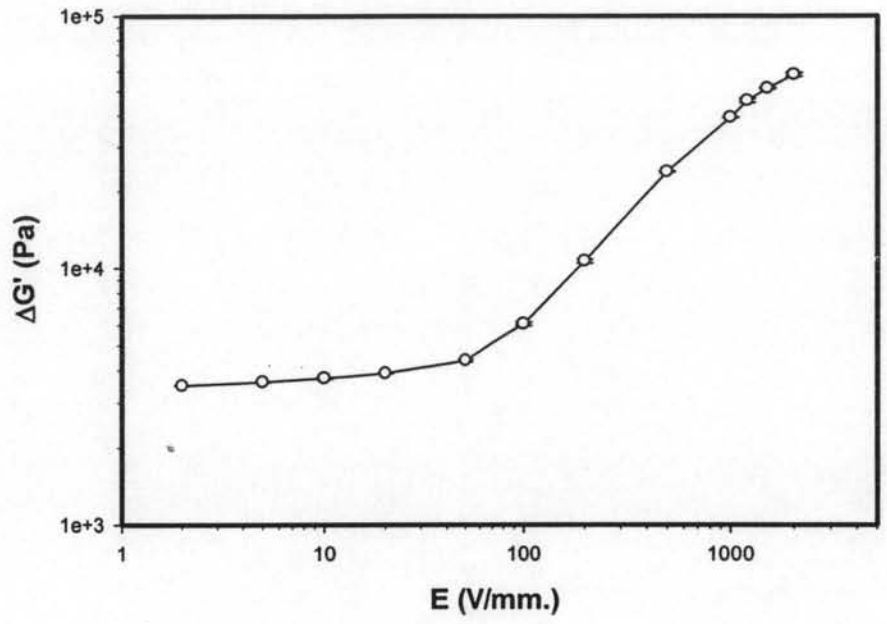

(a)

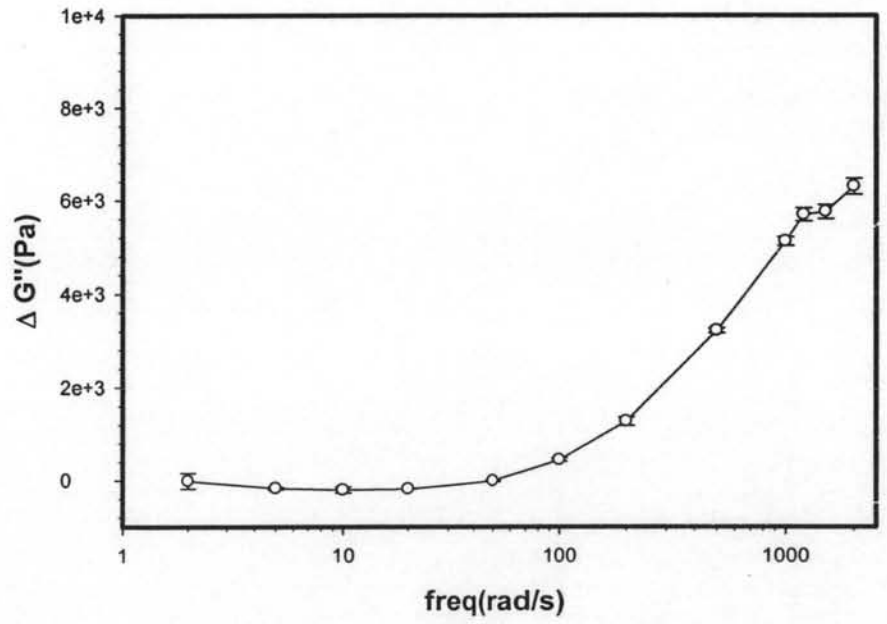

(b)

Figure K18 Responses of the storage and the loss moduli ($\Delta G'(\omega)$ and $\Delta G''(\omega)$)of the acrylate copolymer (AR71) vs. electric field strength, frequency 1 rad/s, strain 1 % at 27 °C: (a) $\Delta G'(\omega)$ when $G'_0 = 31240$ Pa; (b) $\Delta G''(\omega)$ when $G''_0 = 6443.6$ Pa.

K.3) Acrylate copolymer (AR72)

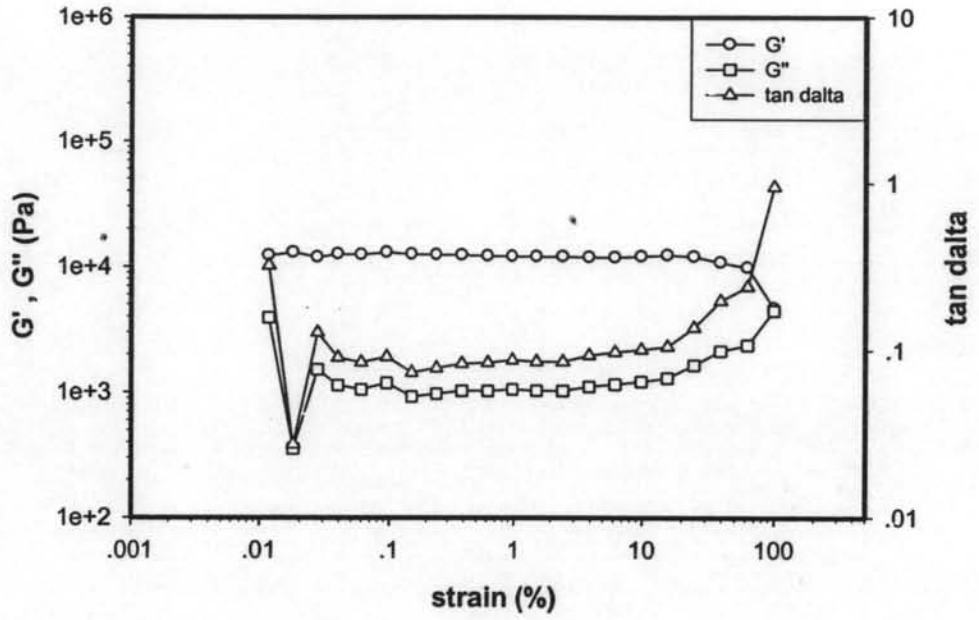

(a)

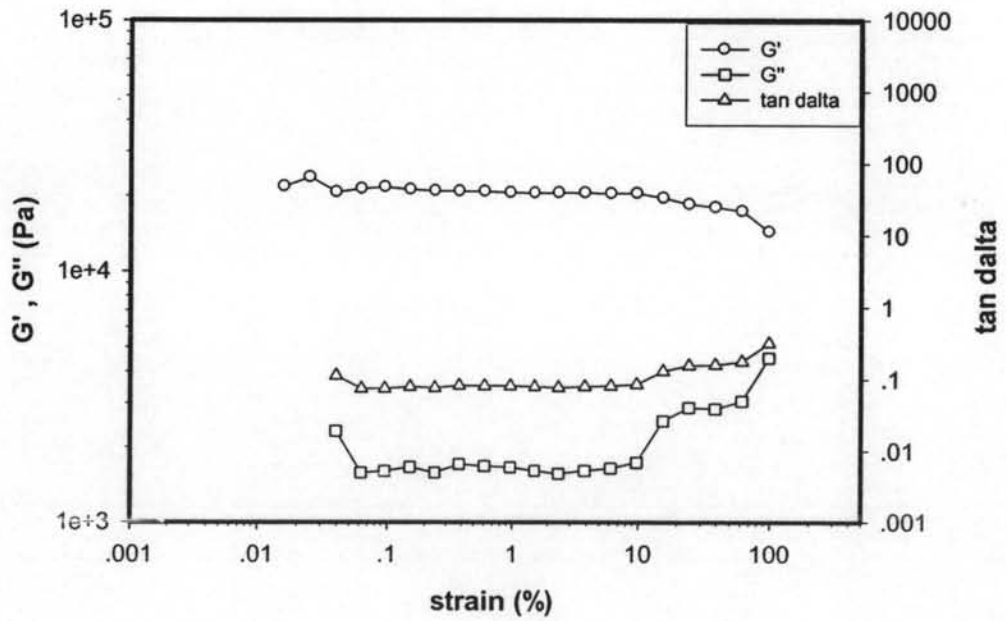

(b)

Figure K16 Strain sweep tests of pure acrylate copolymer(AR72), frequency 1 %, rad/s, 27 °C, and gap 0.600 mm at: a) E = 0 V/mm; b) E = 2 kV/mm.

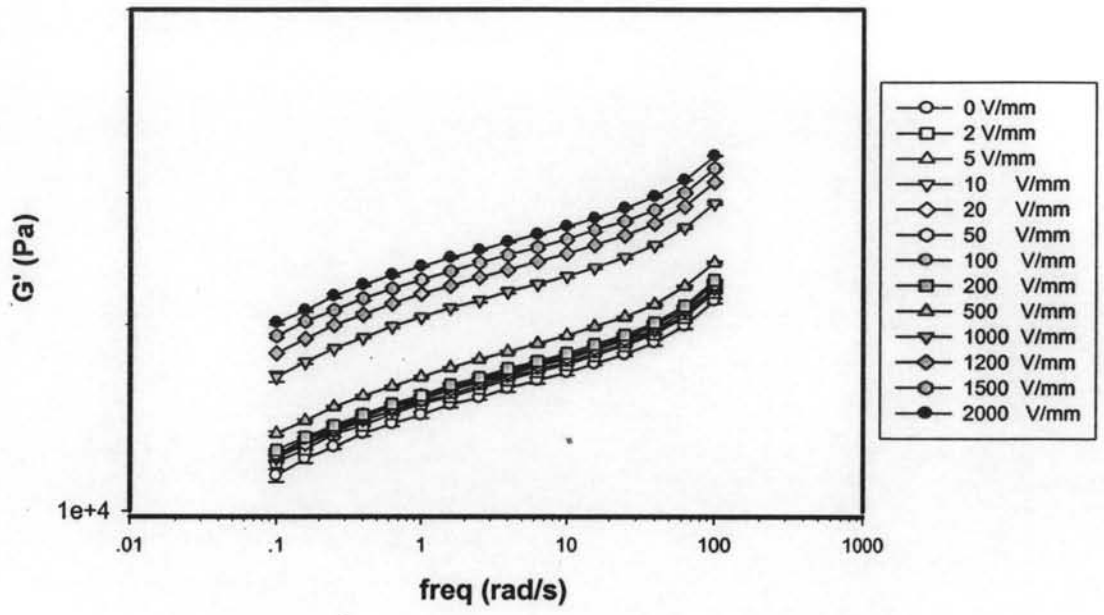

(a)

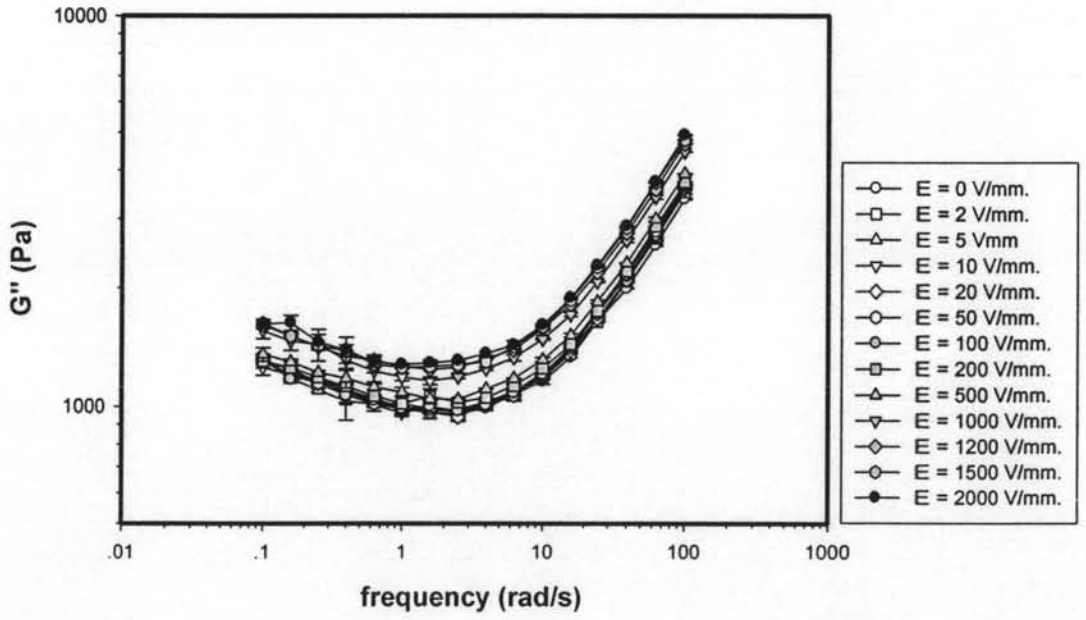

(b)

Figure K17 Frequency sweep tests of pure acrylate copolymer(AR72HF), strain 1 %, 27 °C, and gap 0.600 mm with various electric field strengths: a) G'(Pa); b) G"(Pa).

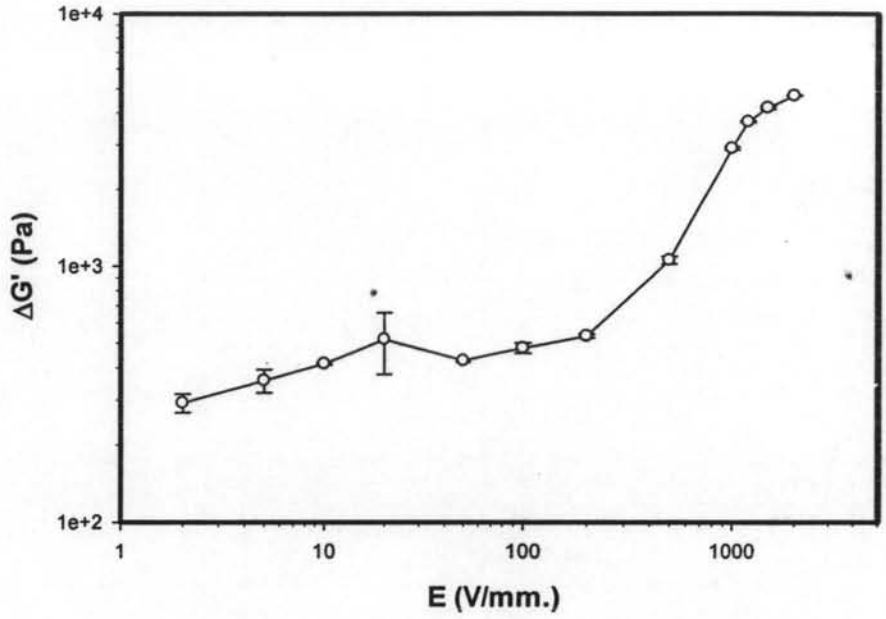

(a)

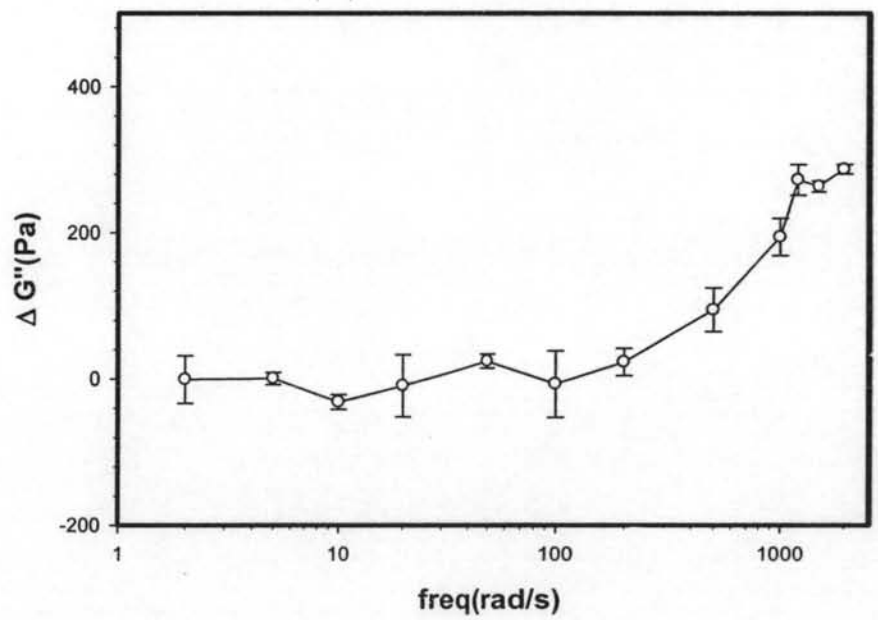

(b)

Figure K18 Responses of the storage and the loss moduli ($\Delta G'(\omega)$ and $\Delta G''(\omega)$)of the acrylate copolymer (AR72) vs. electric field strength, frequency 1 rad/s, strain 1 % at 27 °C: (a) $\Delta G'(\omega)$ when $G'_0 = 12332.7$ Pa; (b) $\Delta G''(\omega)$ when $G''_0 = 993.71$ Pa.

K.4) Poly(dimethyl siloxane) (PDMS)

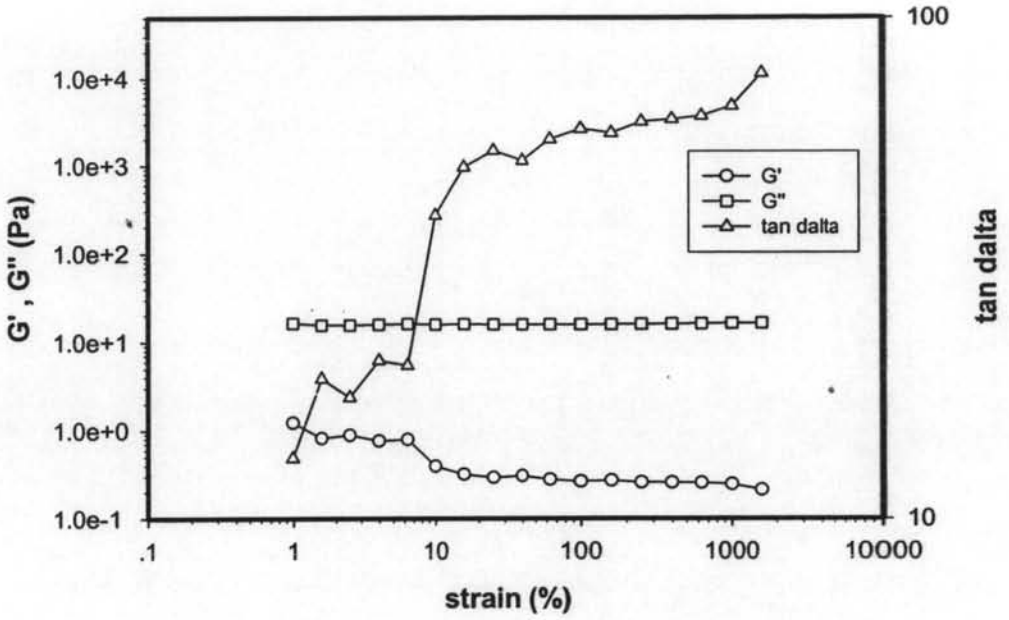

(a)

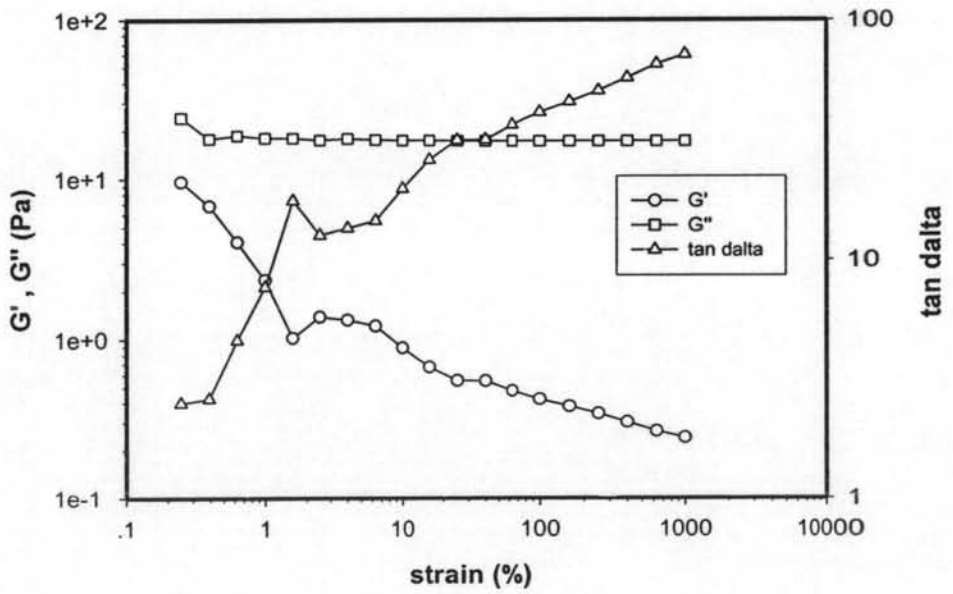

(b)

Figure K10 Strain sweep tests of pure poly(dimethyl siloxane) frequency 1.0 rad/s, 27°C, gap 0.380 mm at: a) E = 0 V/mm; b) E = 2 kV/mm.

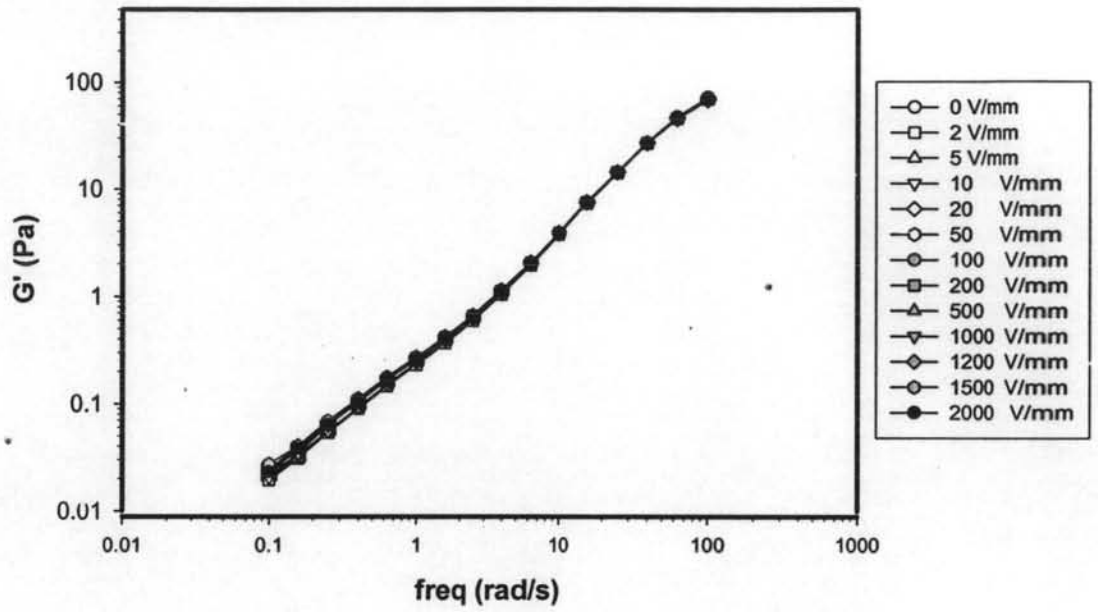

(a)

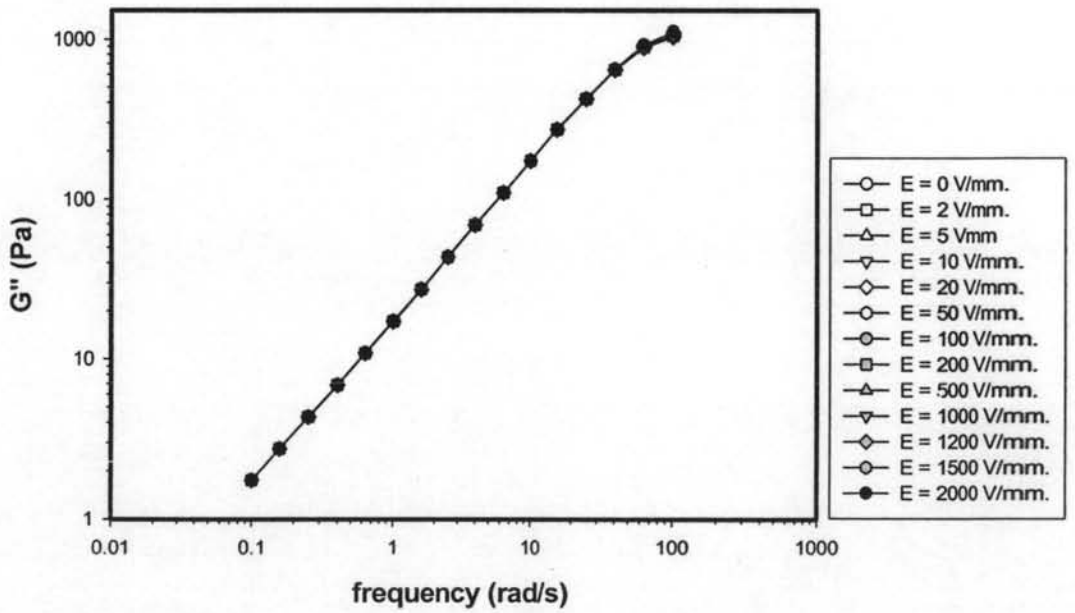

(b)

Figure K11 Frequency sweep tests of pure poly(dimethyl siloxane) strain 700.0 %, 27°C, gap 0.380mm with various electric field strengths: a) G'(Pa); b) G''(Pa).

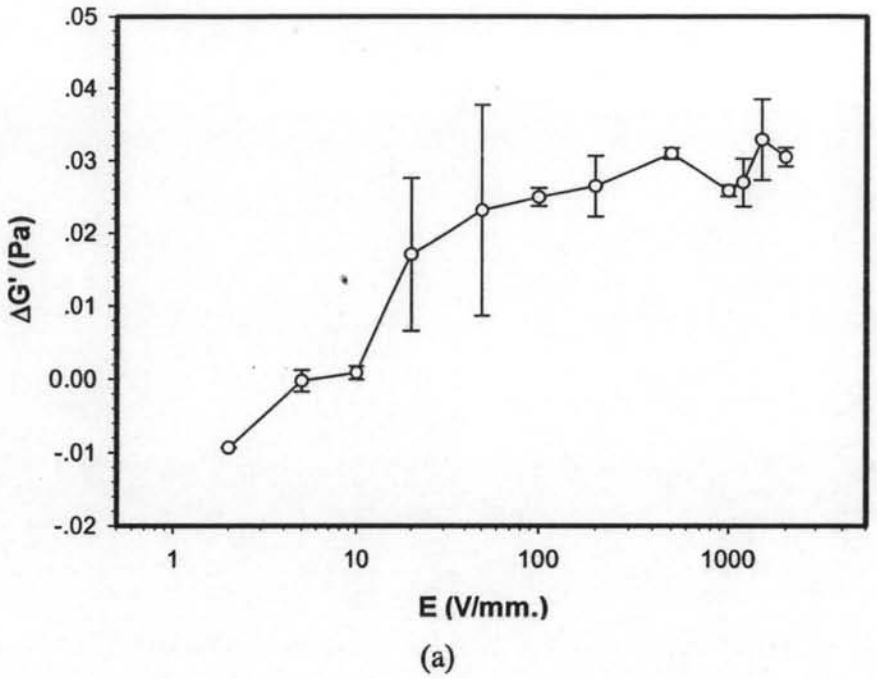

(a)

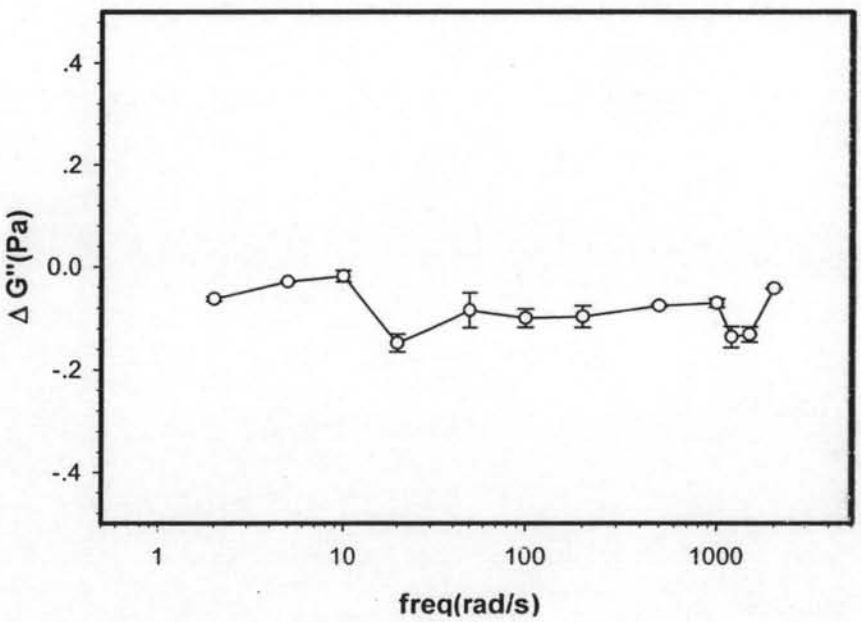

(b)

Figure K12 Responses of the storage and the loss moduli ($\Delta G'(\omega)$ and $\Delta G''(\omega)$)of the poly(dimethyl siloxane) vs. electric field strength, frequency 1.0 rad/s, strain 700% at 27°C: (a) $\Delta G'(\omega)$ when $G'_0 = 0.2391$ Pa; (b) $\Delta G''(\omega)$ when $G''_0 = 17.366$ Pa.

K.5) Styrene acrylate copolymer rubber latex (SAR)

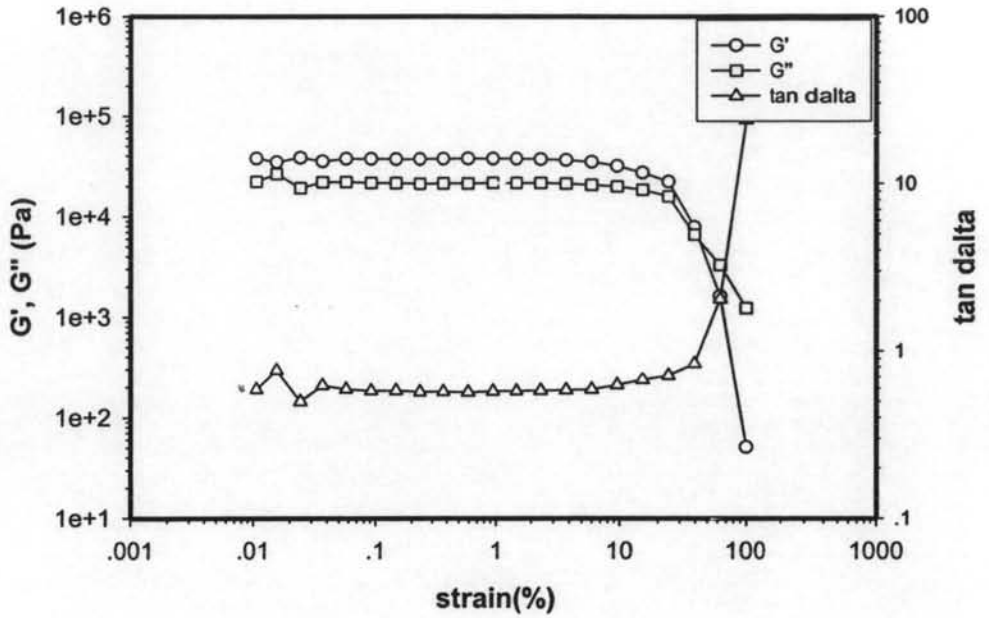

(a)

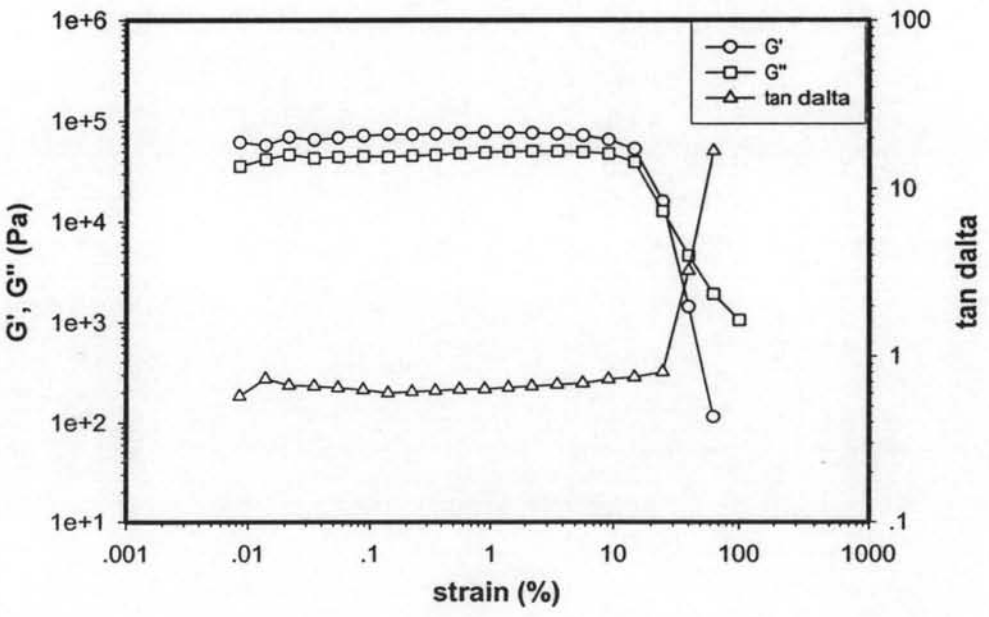

(b)

Figure K1 Strain sweep tests of pure styrene acrylate copolymer rubber latex, frequency 1.0 rad/s, 27°C, gap 0.825 mm at: a) E = 0 V/mm; b) E = 2 kV/mm.

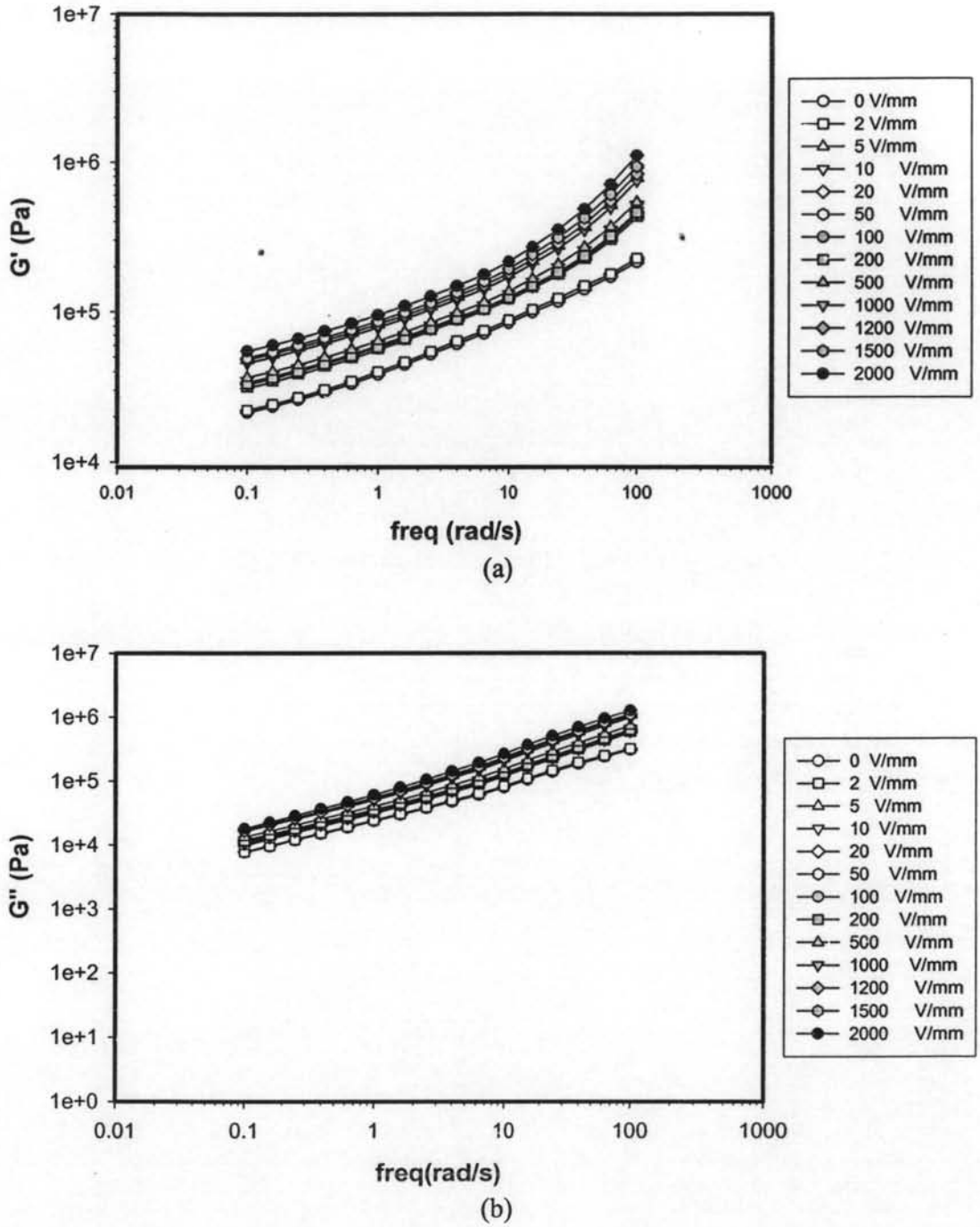

Figure K2 Frequency sweep tests of pure styrene acrylate copolymer, strain 1.0 %, 27°C, gap 0.825 mm with various electric field strengths: a) G'(Pa); b) G"(Pa).

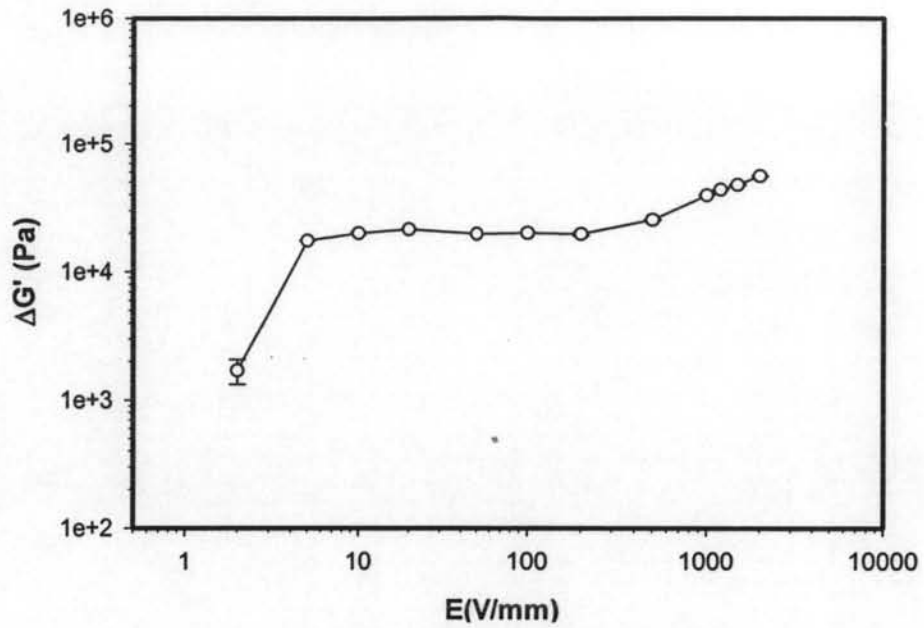

(a)

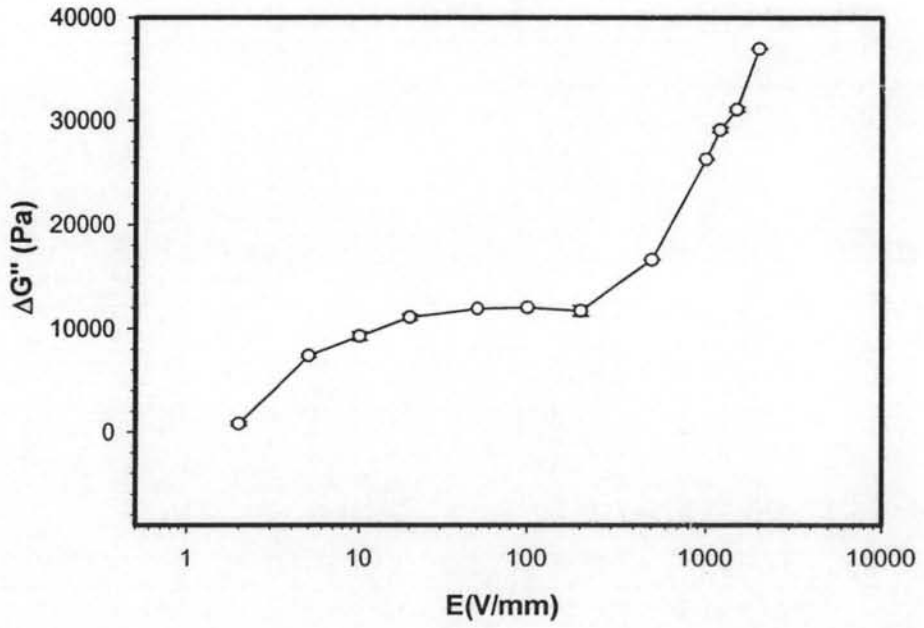

(b)

Figure K3 Responses of the storage and the loss moduli ($\Delta G'(\omega)$ and $\Delta G''(\omega)$)of the styrene acrylate copolymer rubber latex vs. electric field strength, frequency 1.0 rad/s, strain 1% at 27°C: (a) $\Delta G'(\omega)$ when $G'_0 = 38127$ Pa; (b) $\Delta G''(\omega)$ when $G''_0 = 23364$ Pa.

K.6) Styrene butadiene copolymer rubber latex (SBR)

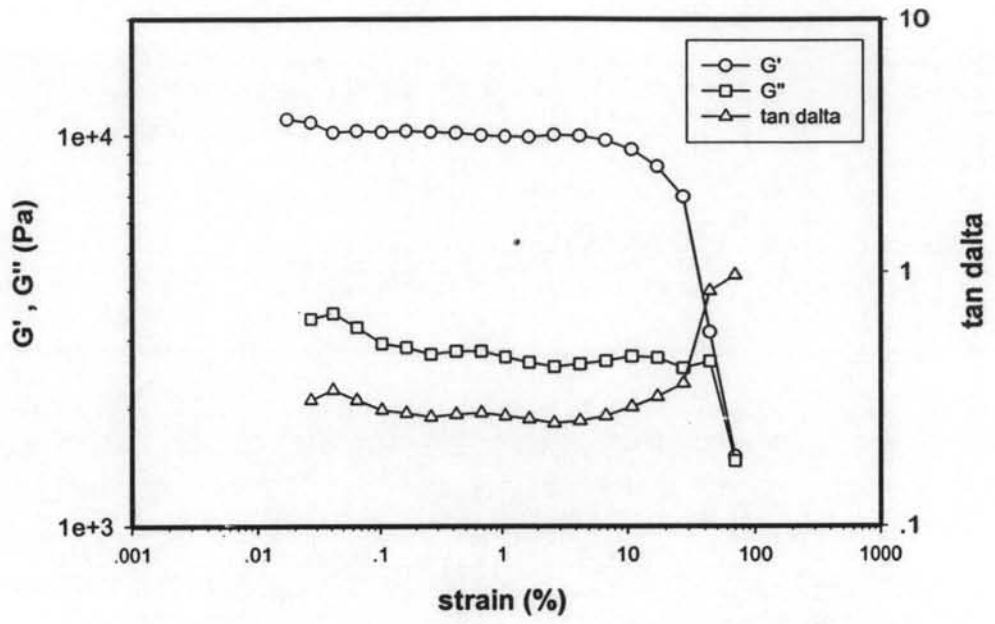

(a)

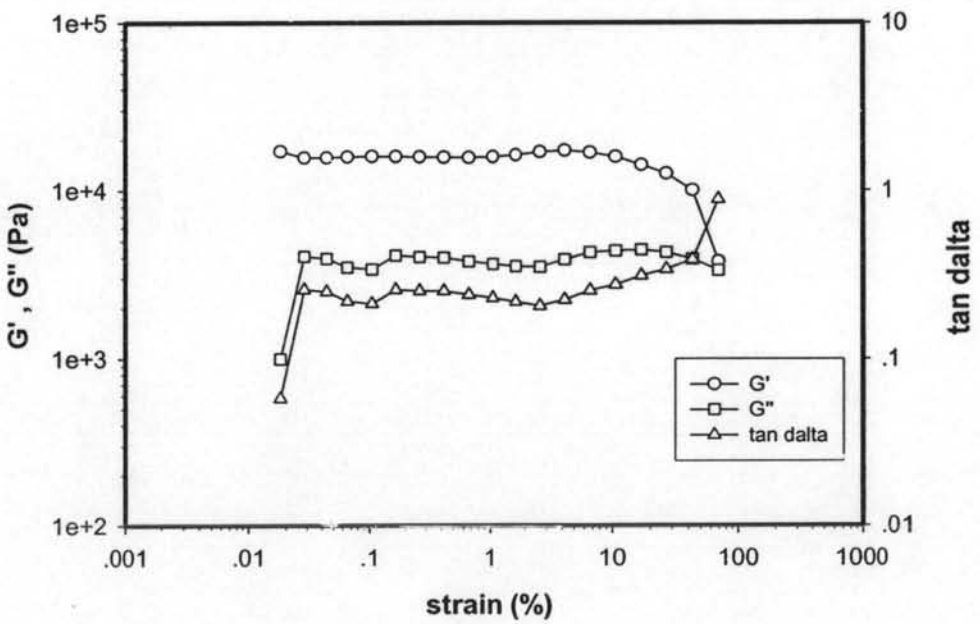

(b)

Figure K7 Strain sweep tests of pure styrene butadiene copolymer rubber latex, frequency 1.0 rad/s, 27°C, gap 0.525 mm at: a) E = 0 V/mm; b) E =2 kV/mm.

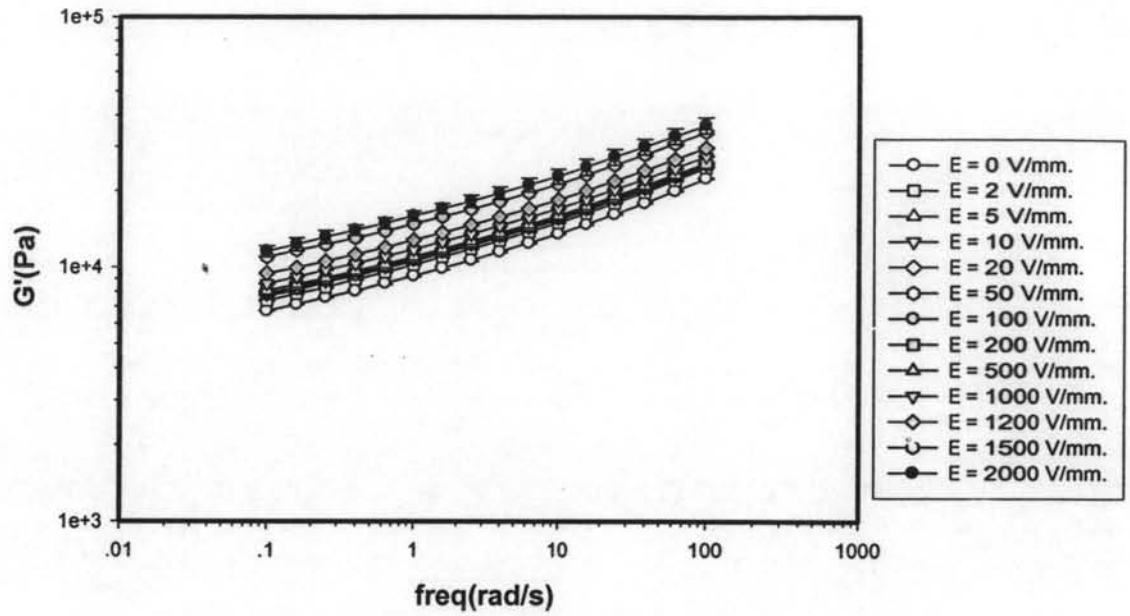

(a)

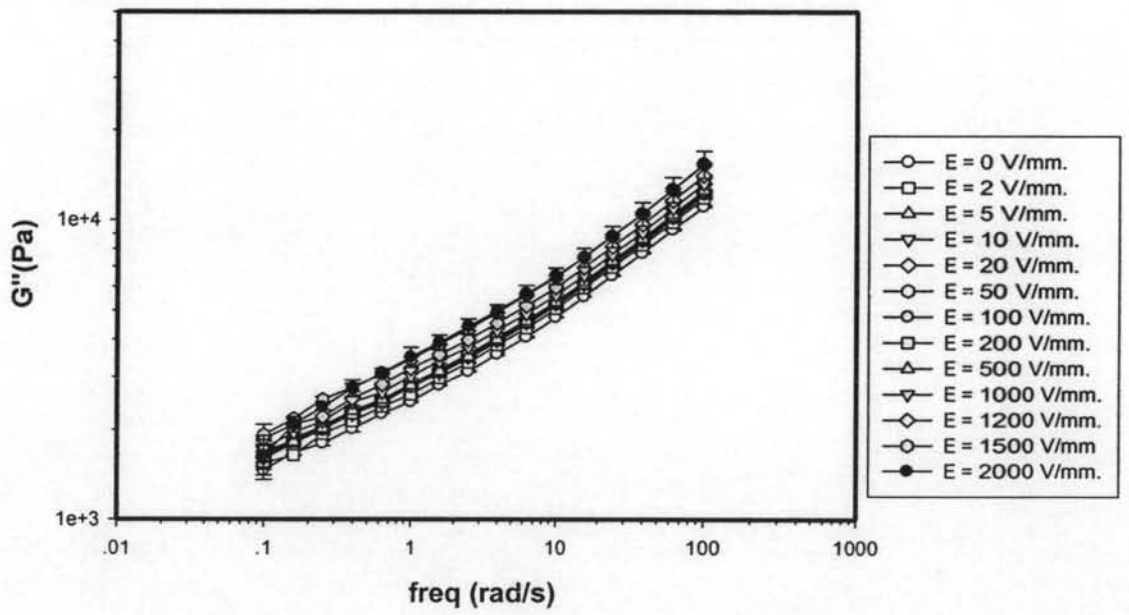

(b)

Figure K8 Frequency sweep tests of pure styrene butadiene copolymer rubber latex, strain 1.0 %, 27°C, gap 0.525 mm with various electric field strengths: a) G'(Pa); b) G"(Pa).

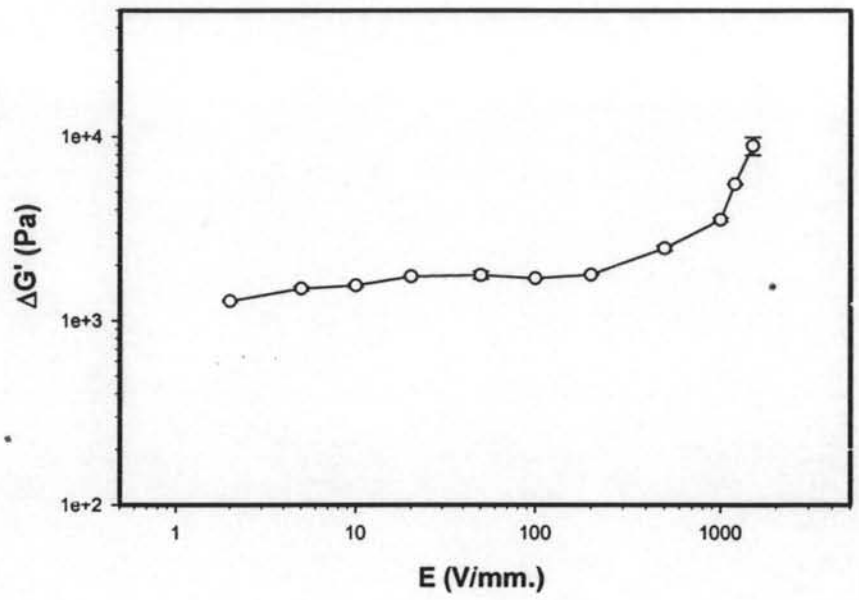

(a)

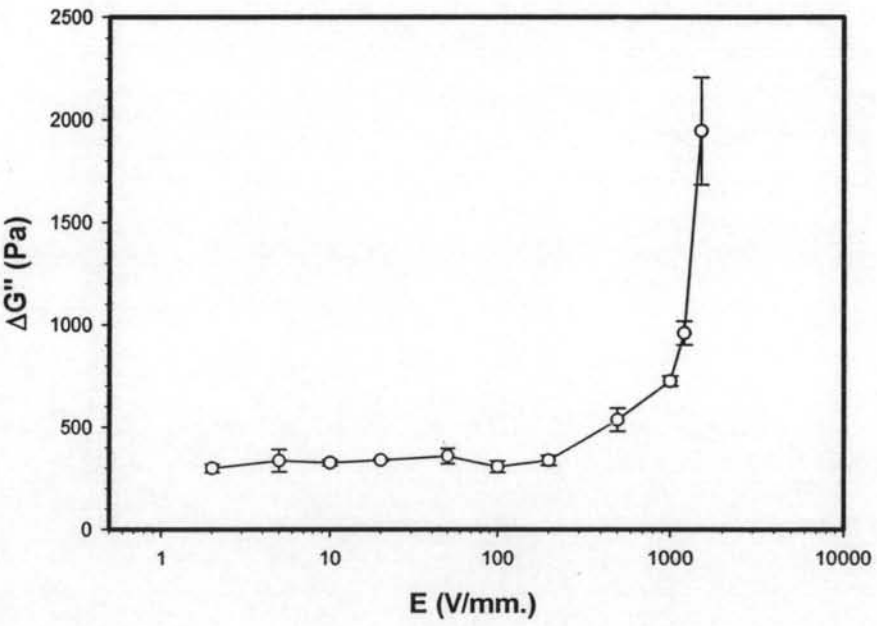

(b)

Figure K9 Responses of the storage and the loss moduli ($\Delta G'(\omega)$ and $\Delta G''(\omega)$)of the styrene butadiene copolymer rubber latex vs. electric field strength, frequency 1.0 rad/s, strain 1% at 27°C: (a) $\Delta G'(\omega)$ when $G'_0 = 9250.5$ Pa; (b) $\Delta G''(\omega)$ when $G''_0 = 2482.5$ Pa

K.7) Styrene isoprene styrene triblock copolymer (SIS)

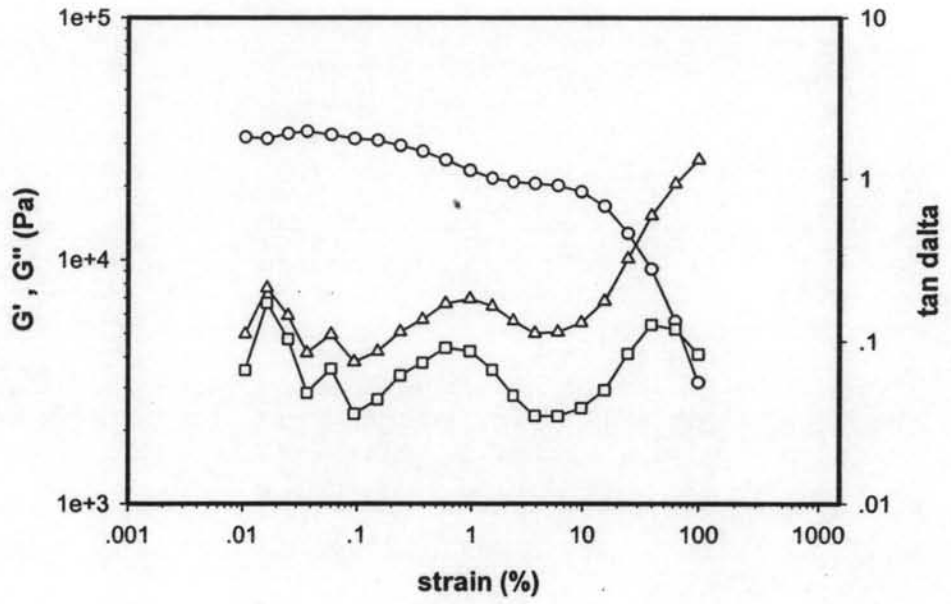

(a)

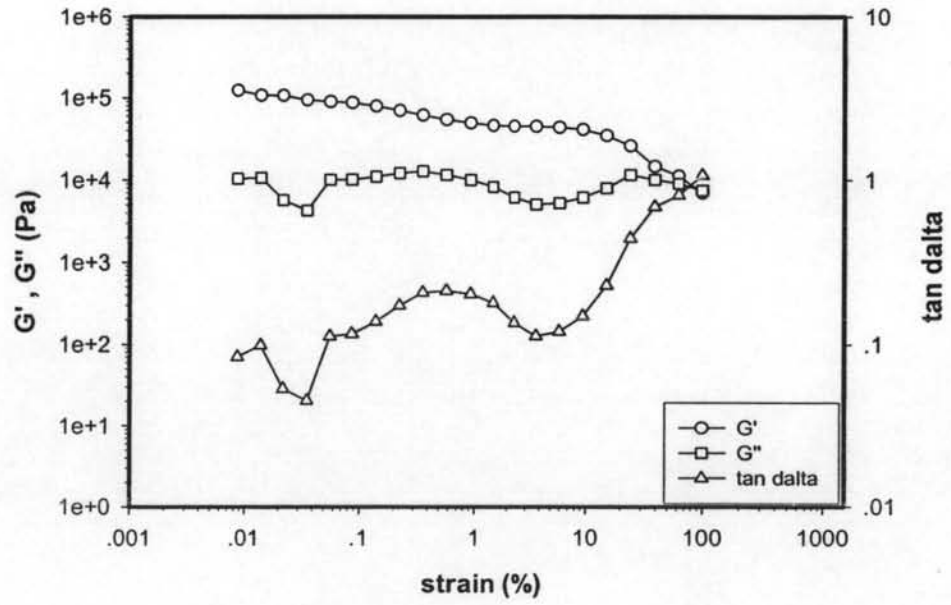

(b)

Figure K13 Strain sweep tests of pure styrene isoprene styrene triblock copolymer, frequency 1.0 rad/s, 27°C, gap 0.560 mm at: a) E = 0 V/mm; b) E =2 kV/mm.

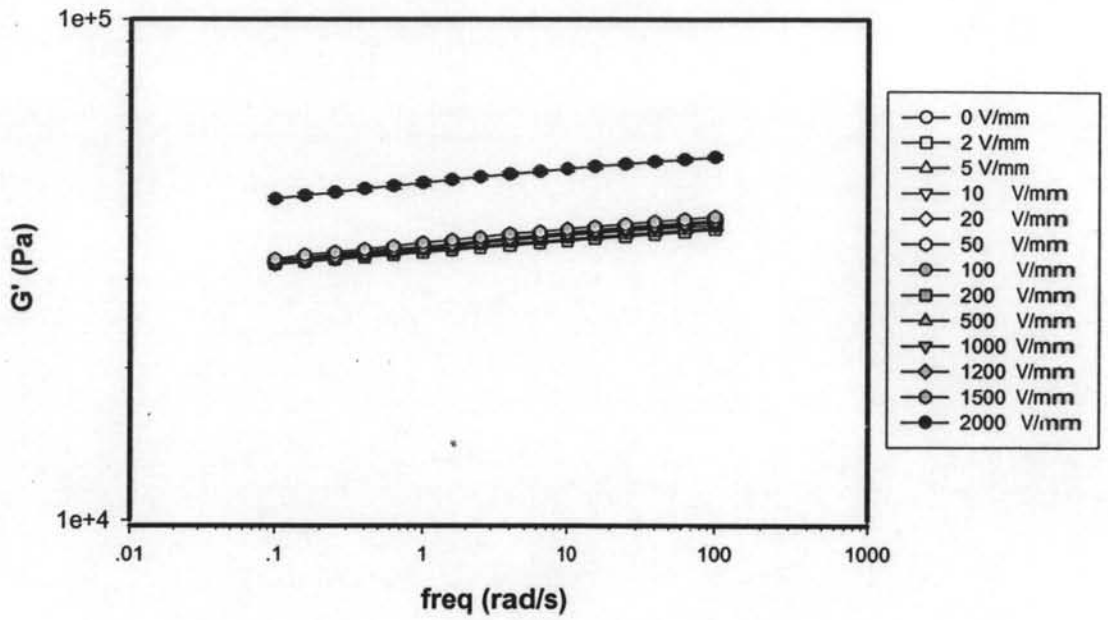

(a)

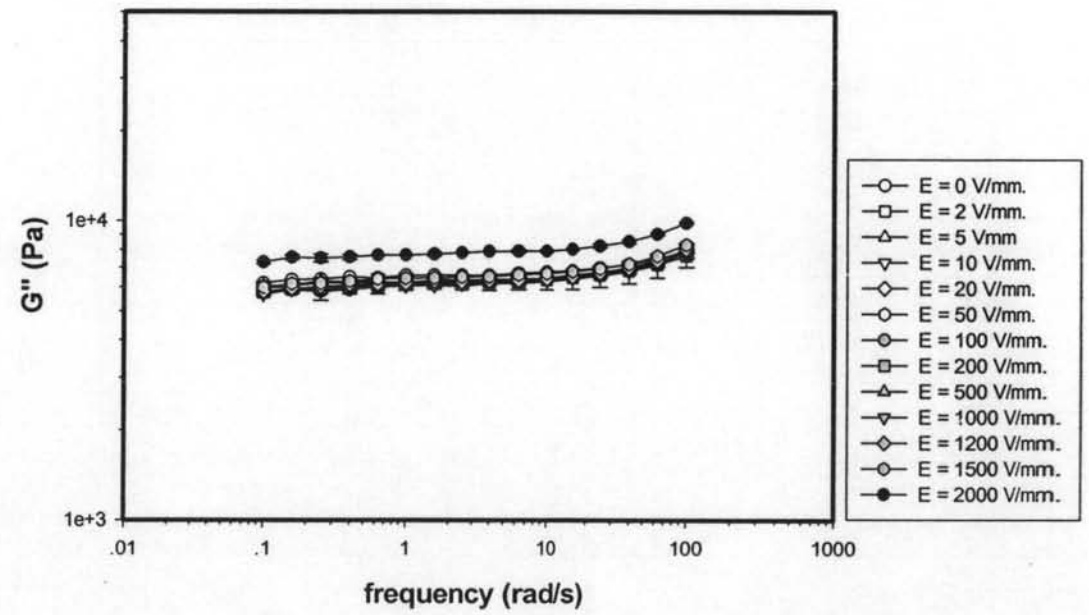

(b)

Figure K14 Frequency sweep tests of pure styrene isoprene styrene triblock copolymer, strain 1.0 %, 27°C, gap 0.56 mm with various electric field strengths: a) G'(Pa); b) G"(Pa).

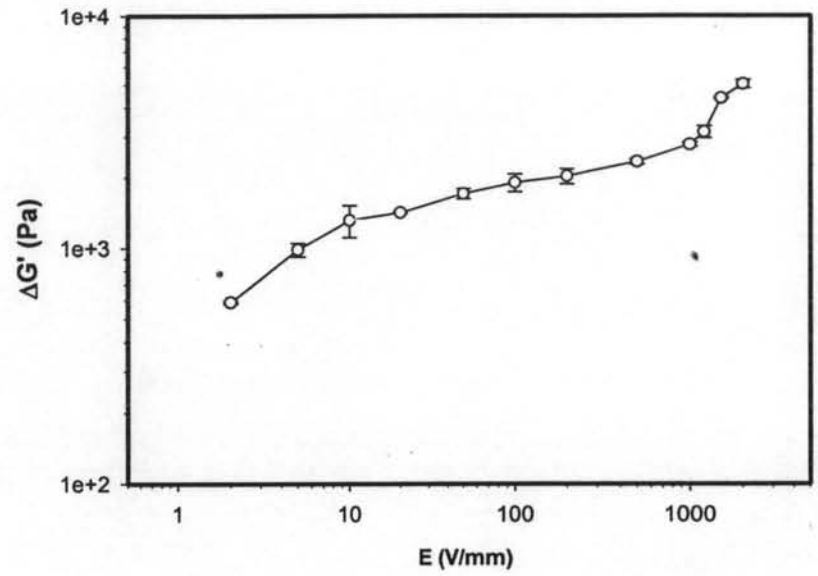

(a)

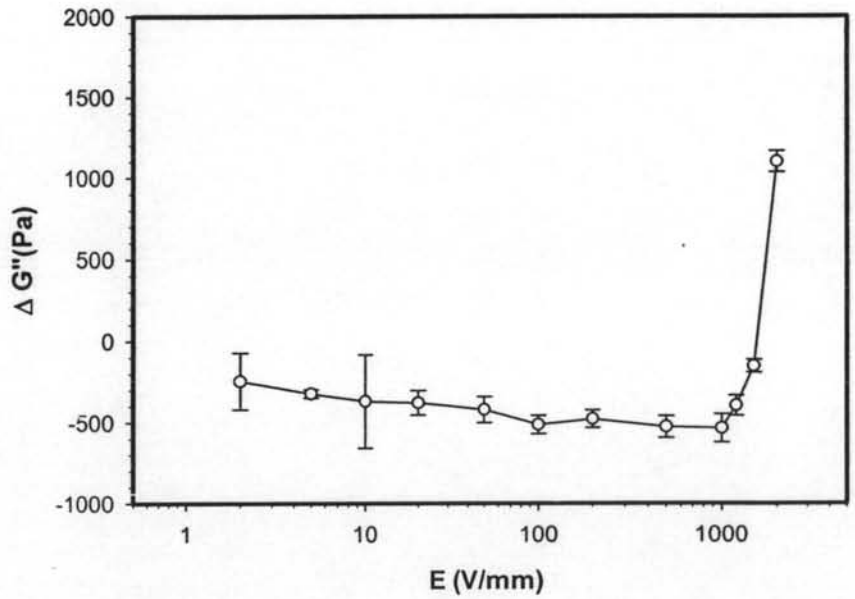

(b)

Figure K15 Responses of the storage and the loss moduli ($\Delta G'(\omega)$ and $\Delta G''(\omega)$)of the styrene isoprene styrene triblock copolymer vs. electric field strength, frequency 1.0 rad/s, strain 1 % at 27°C: (a) $\Delta G'(\omega)$ when $G'_0 = 50606$ Pa; (b) $\Delta G''(\omega)$ when $G''_0 = 5060.0$ Pa

Table K1.Rheology properties of various matrices

Materials	G'_0 (Pa)	G'_{1kV} (Pa)	G'_{2kV} (Pa)	G''_0 (Pa)	G''_{2kV} (Pa)	$\Delta G'_{1kV}$(Pa)	$\Delta G'_{2kV}$ (Pa)	$\Delta G''_{2kV}$ (Pa)	$\Delta G'_{1kV}/G'_0$	$\Delta G'_{2kV}/G'_0$	$\Delta G''_{2kV}/G''_0$	σ_{dc} (S/cm.)
AR 70*	19666	40714	65418	3924.5	18789	21047	45751	14865	1.0702	2.3264	3.7877	9.63E-13
AR 71, 0.1%**	10137	14466	16440	1165.2	1732.1	4328.7	6303.3	566.88	0.4270	0.6218	0.4865	5.16E-12
AR71, 1%***	20140	28306	34130	2460.8	4537.2	8166.6	13990	2076.3	0.4055	0.6947	0.8438	5.16E-12
AR71(2), 1%***	31240	70774	89761	6443.6	12745	39534	58520	6301.1	1.2655	1.8732	0.9779	5.16E-12
AR 72, 0.1%**	11105	14554	14177	1142.4	1351.3	3448.5	3071.3	208.85	0.3105	0.2766	0.1828	1.03E-12
AR72, 1%***	15645	20798	24153	1249.7	2050.7	5153.4	8507.8	801.00	0.3294	0.5438	0.6410	1.03E-12
AR72(2), 1%***	12333	15249	17025	993.70	1280.5	2916.3	4692.6	286.77	0.2365	0.3805	0.2886	1.03E-12
PDMS, 700%	0.2391	0.2650	0.2696	17.366	17.282	0.0259	0.0306	-0.0836	0.1083	0.1278	-0.0048	2.35E-06
SAR*	38127	78141	94869	23364	60350	40014	56742	36986	1.0495	1.4882	1.5830	7.09E-15
SBR*	9250.5	11732	18237	2482.5	4426.8	2481.8	8986.6	1944.4	0.2683	0.9715	0.7832	5.55E-15
SBR(2)*	21557	30657	36429	4277.5	8323.7	9100.2	14872	4046.2	0.4222	0.6899	0.9459	5.55E-15
SIS **	50606	53387	55668	5060.0	5535.5	2780.1	5061.7	475.49	0.0549	0.1000	0.0940	6.51E-17

All of materials was tested at frequency =1 rad/s, strain 1% and, temperature = 27 ^{0}C except AR 71, 0.1%, AR 72, 0.1% were tested at strain 0.1% and PDMS 700% was tested at strain 700%

*films were formed by water solution casting, ** films were formed by acetone solution casting.

*** films were formed by toluene solution casting.

G'_0, and G''_0 is storage and loss modulus without electric field

G'_{1kV} is storage modulus at 1 kV/mm, G'_{2kV} and G''_{2kV} are storage and loss modulus at 2 kV/mm.

$\Delta G'_{1kV}$ is the the storage modulus responses between G'_0 and G'_{1kV}

$\Delta G'_{2kV}$ is the the storage modulus responses between G'_0 and G'_{2kV}

$\Delta G''_{2kV}$ is the the loss modulus responses between G''_0 and G''_{2kV}, $\Delta G'_{1kV}/G'_0$ is sensitivity of the storage modulus at 1 kV, $\Delta G'_{2kV}/G'_0$ is sensitivity of the storage modulus at 2 kV, $\Delta G''_{2kV}/G''_0$ is sensitivity of the loss modulus at 2 kV

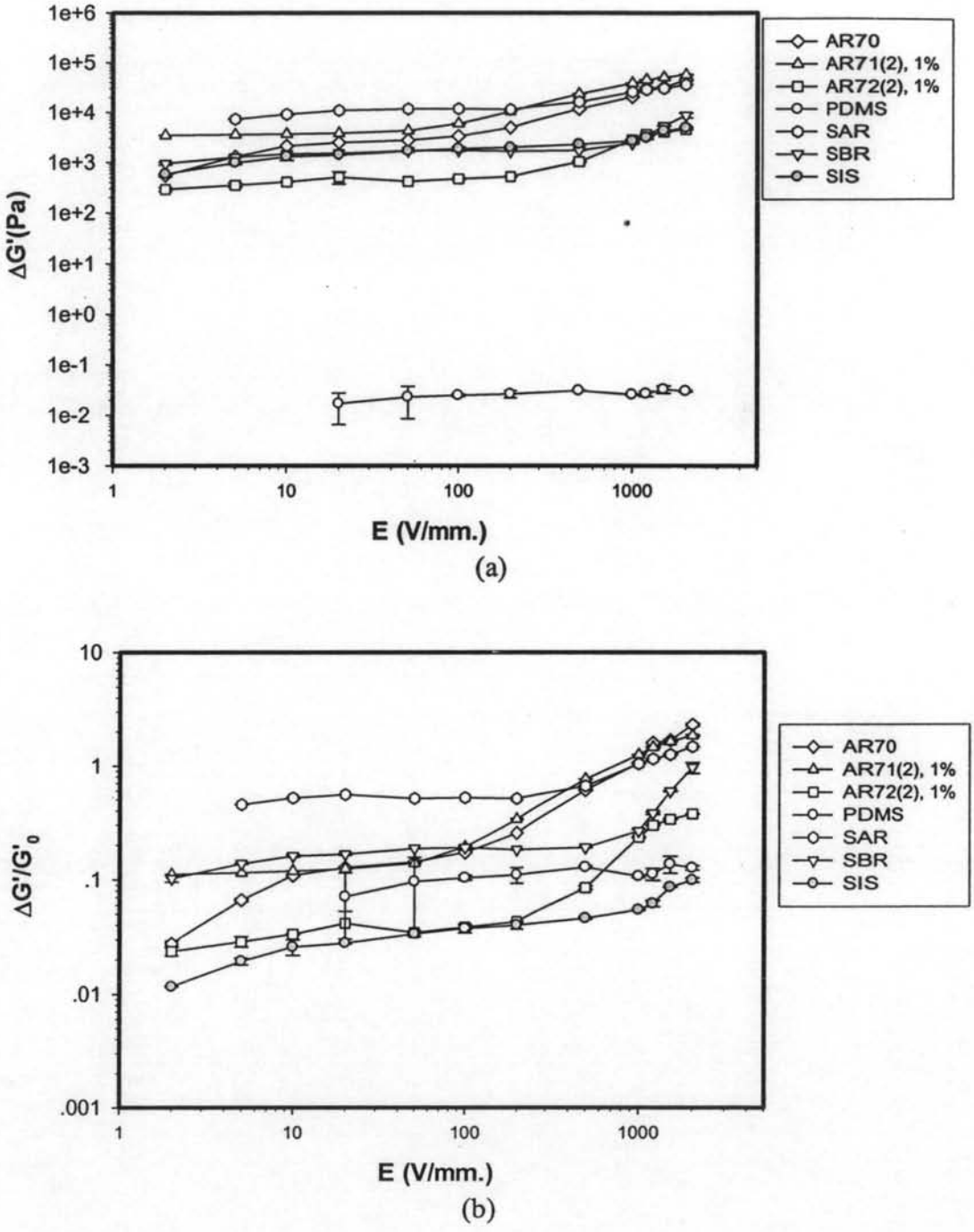

Figure K16 Effect of matrices on: (a) the storage modulus responses (Δ G') and (b) storage modulus sensitivity ($\Delta G'/G'_0$) vs. electric fields strength: 0 to 2 KV/mm at frequency 1 rad/s, strain 1%(except PDMS was tested at 700%), and at 27 ^{0}C.

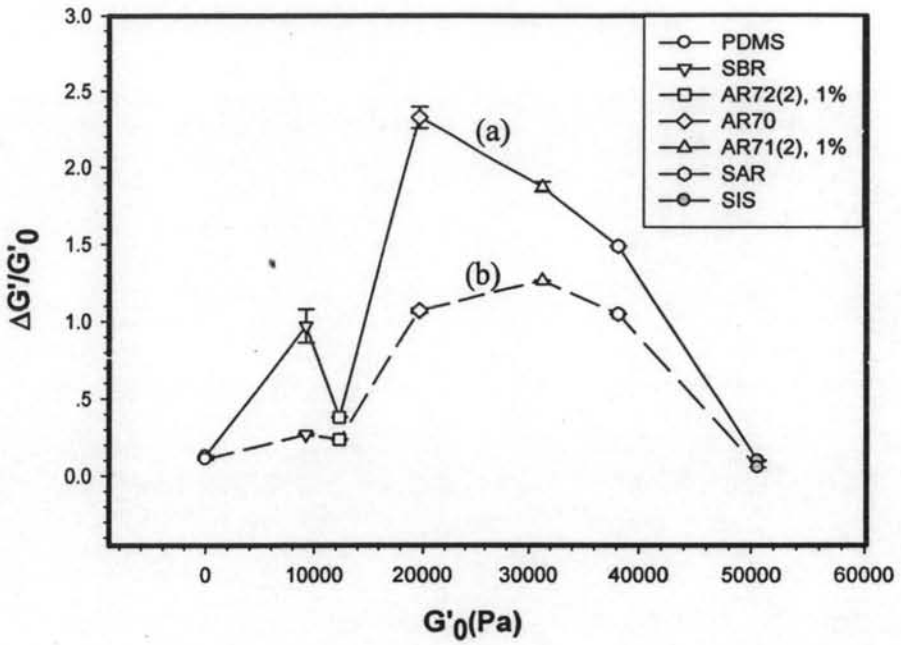

Figure K17 sensitivity vs. G'_0, strain 1.0%(except PDMS was tested at 700%), frequency 1.0 rad/s, and 27 °C at: (a) solid line, 2 kV; (b) dash line, 1 kV.

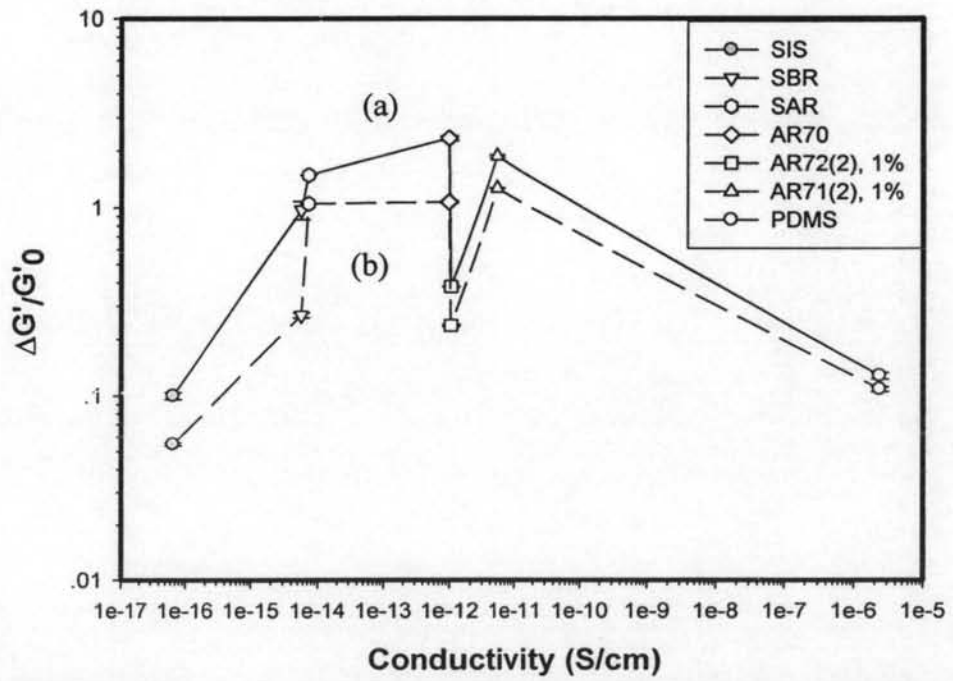

Figure K18 sensitivity vs. conductivity, strain 1.0%(except PDMS was tested at 700%), frequency 1.0 rad/s, and 27°C at: (a) solid line, 2 kV; (b) dash line, 1 kV.

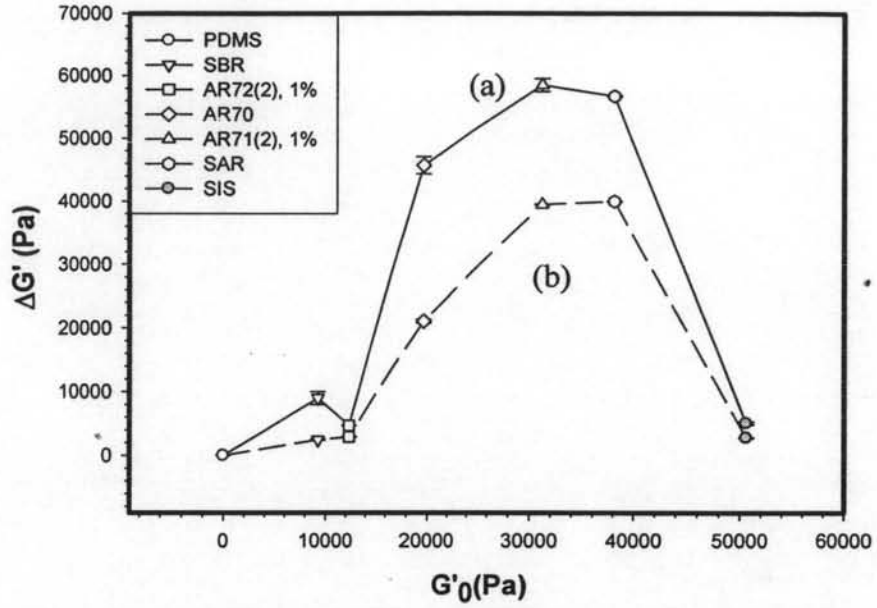

Figure K19 the storage modulus responses (ΔG') vs. G'_0, strain 1.0%(except PDMS was tested at 700%), frequency 1.0 rad/s, and 27 °C at: (a) solid line 2 kV; (b) dash line 1 kV.

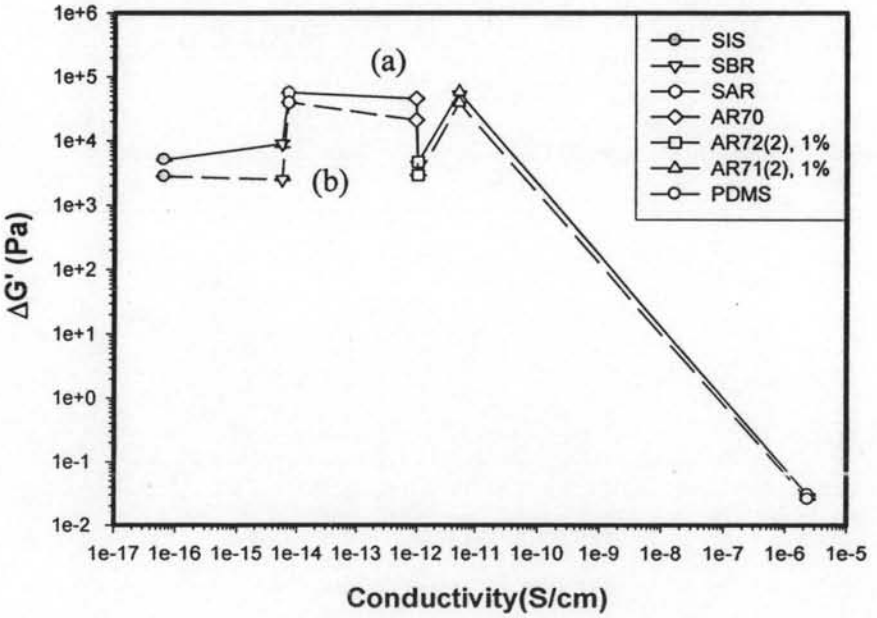

Figure K20 the storage modulus responses (ΔG') vs. G'_0, strain 1.0%(except PDMS was tested at 700%), frequency 1.0 rad/s, and 27 °C at: (a) solid line, 2 kV; (b) dash line, 1 kV.

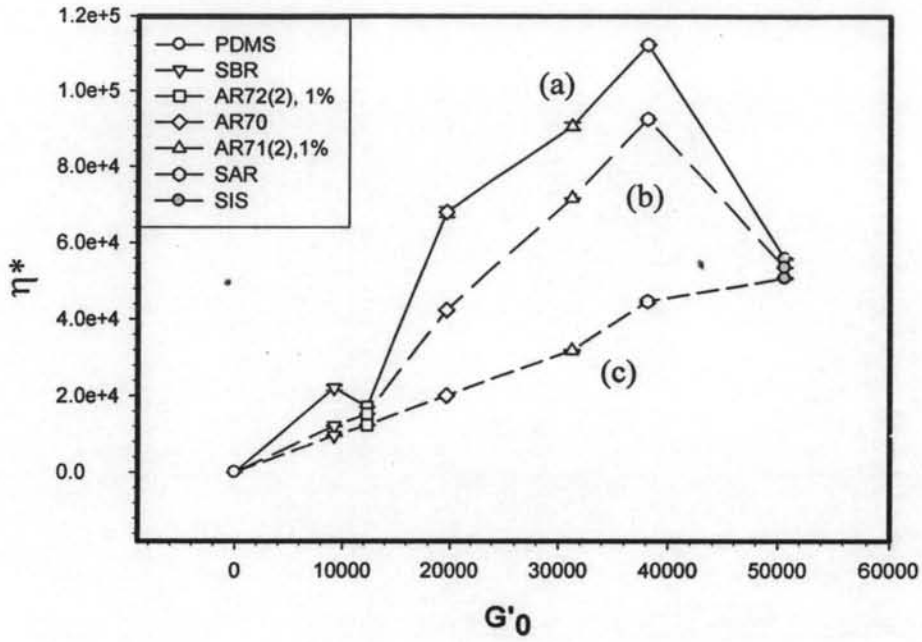

Figure K21 the η*vs. G'_0, strain 1.0%(except PDMS was tested at 700%), frequency 1.0 rad/s, and 27 °C at: (a) solid line, 2 kV; (b)long dash line, 1 kV; (c) medium dash line, 0 kV.

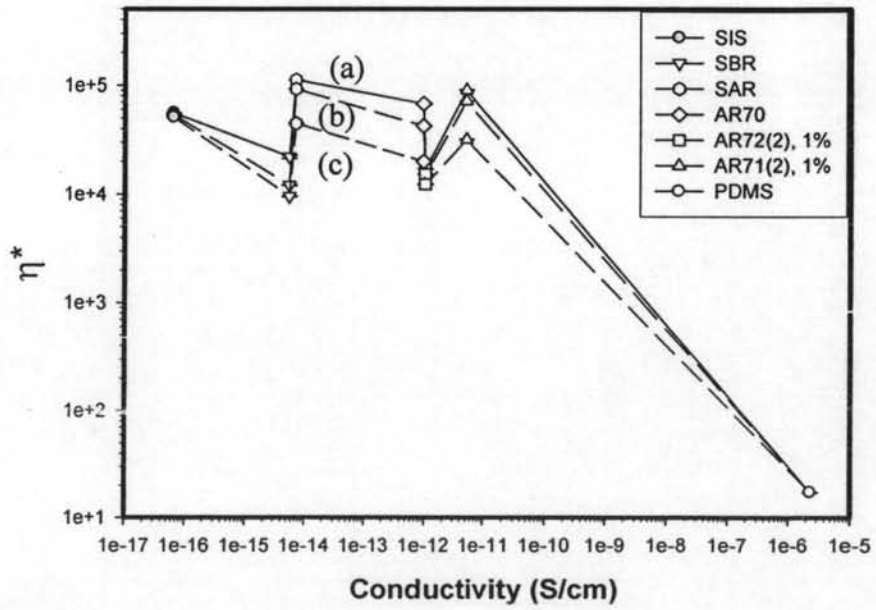

Figure K22 the η*vs. G'_0, strain 1.0%(except PDMS was tested at 700%), frequency 1.0 rad/s, and 27 °C: at (a) solid line, 2 kV; (b) long dash line, 1 kV; (c) medium dash line, 0 kV.

Appendix L Electrorheological Properties Measurement of Polymer Blends between Ppy and AR70 at Various ratio of Ppy.

The electrorheological properties of polymer blends between Ppy and AR70 at various ratio of Ppy were measured by the melt rheometer (Rheometric Scientific, ARES) under oscillatory shear mode and applied electric filed strength varying from 0 to 2 kV/mm. In these experiments, the dynamic moduli (G' and G") were measured as functions of frequency and electric field strength. Strain sweep tests were first carried out to determine the suitable strain to measure G' and G" in the linear viscoelastic regime.

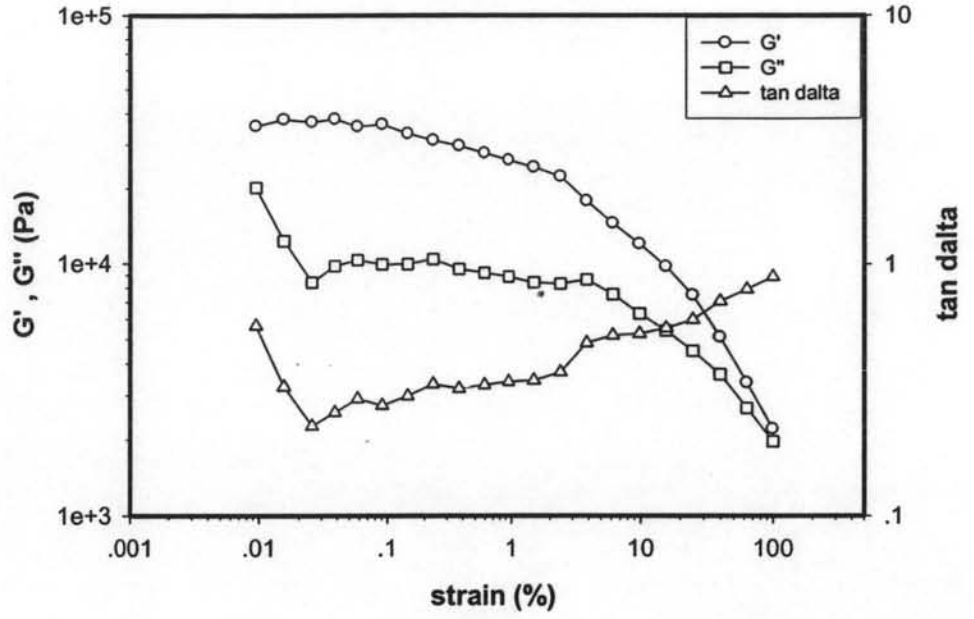

(a)

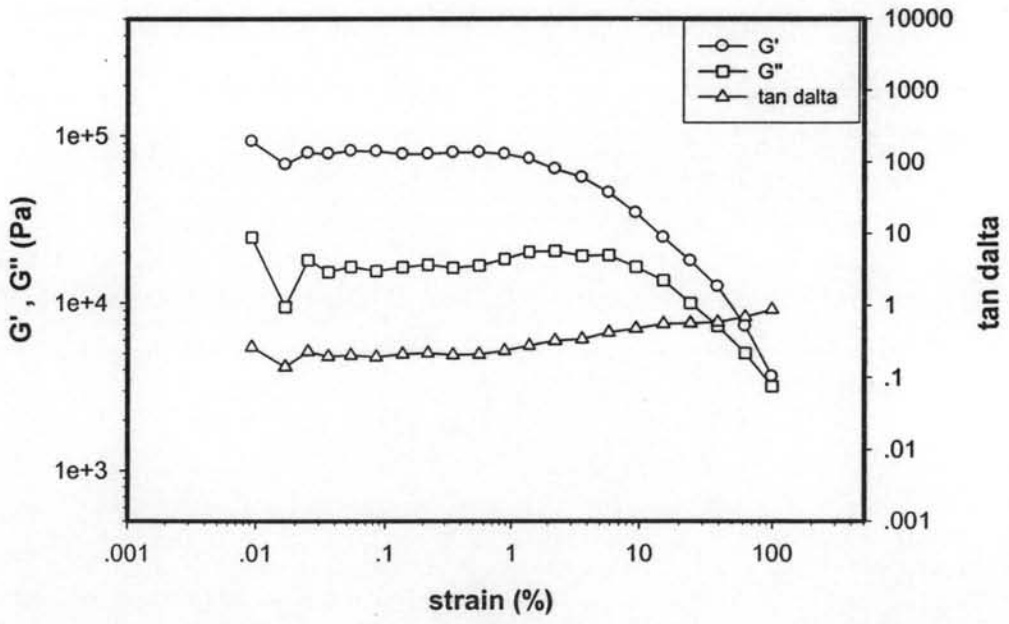

(b)

Figure L1 Strain sweep test of polymer blend between Ppy and AR70 at 1% v/v of Ppy (AR70:1_un), frequency 1.0 rad/s, 27^0 C, gap 0.650 mm at: a) E = 0 V/mm; b) E = 2000 V/mm.

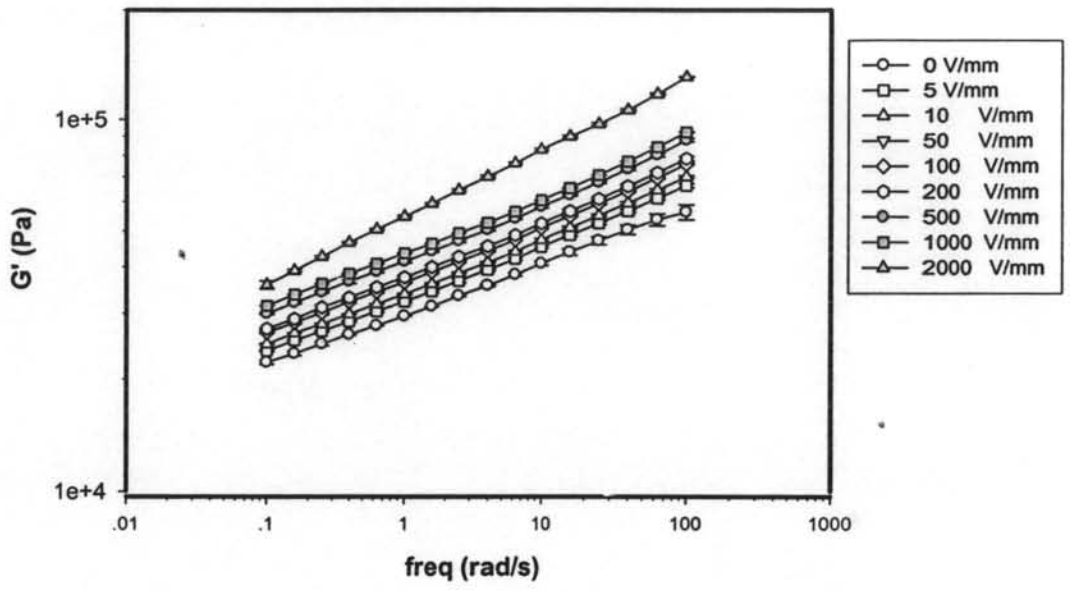

(a)

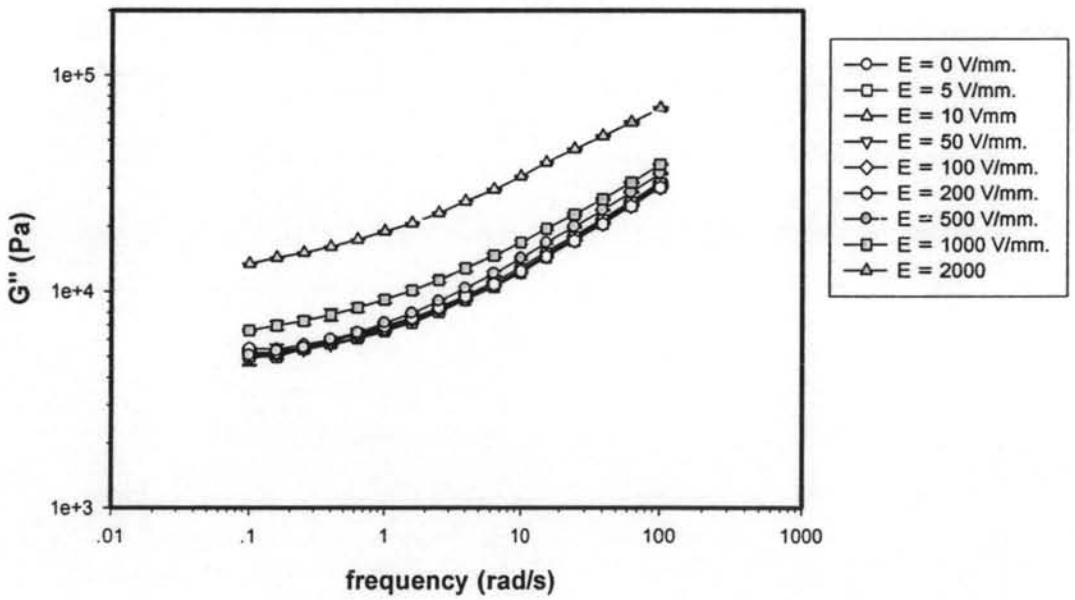

(b)

Figure L2 Frequency sweep test of polymer blend between Ppy and AR70 at 1% v/v of Ppy (AR70:1_un), strain 1%, 27^0 C, gap 0.650 mm at various electric field strengths: a) G'(Pa); b) G" (Pa).

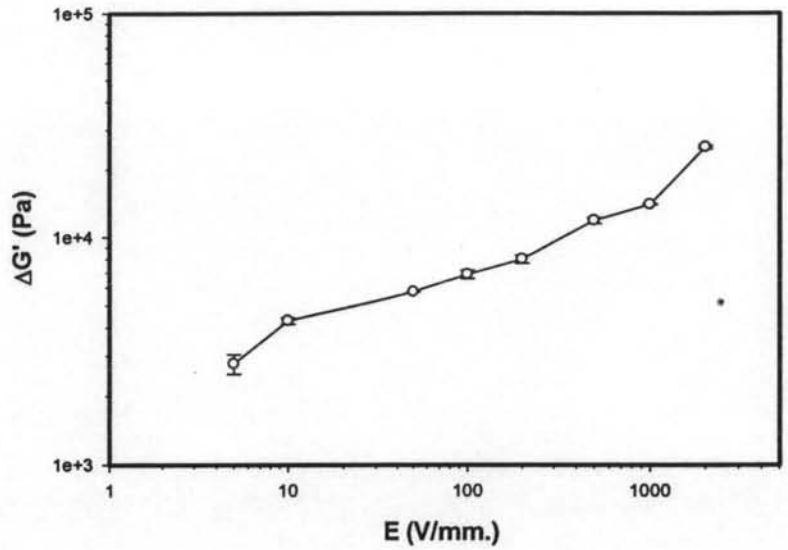

(a)

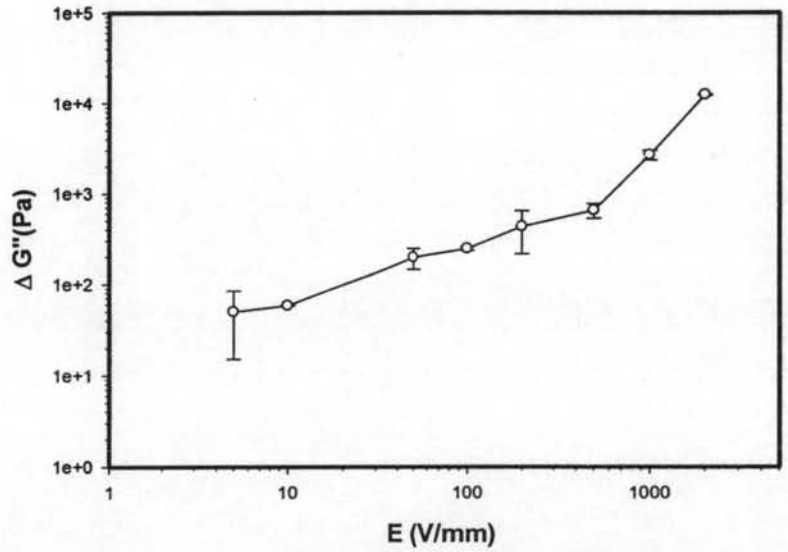

(b)

Figure L3 Responses of the storage and the loss moduli ($\Delta G'(\omega)$ and $\Delta G''(\omega)$) of polymer blend between Ppy and AR70 at 1% v/v of Ppy (AR70:1_un) vs. electric field strength, frequency 1.0 rad/s, strain 1%, gap 0.650 mm at 27^0C: (a) $\Delta G'(\omega)$; (b) $\Delta G''(\omega)$ when $G'_0 = 22{,}545$ Pa and $G''_0 = 7{,}176$ Pa.

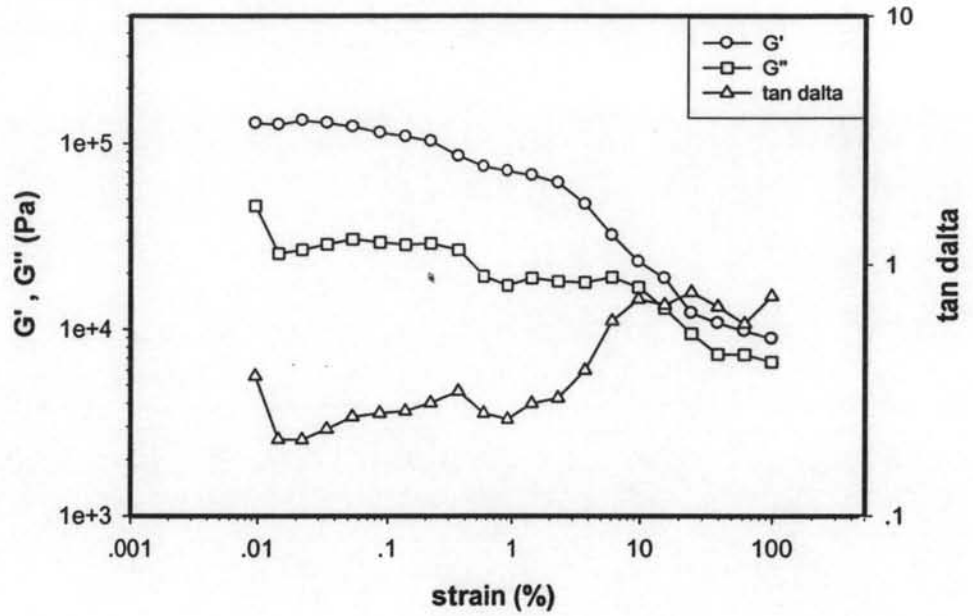

(a)

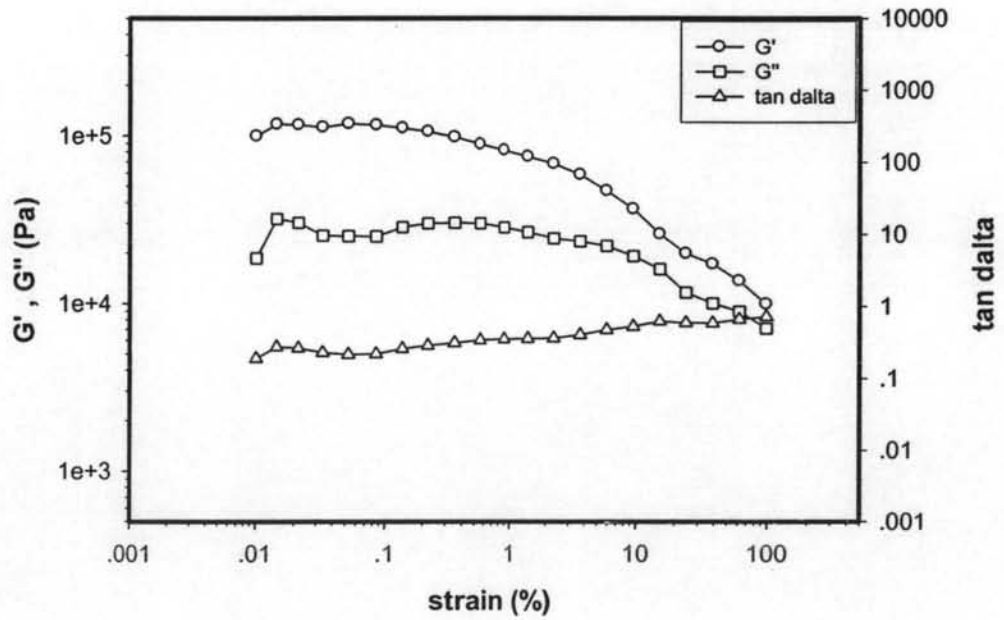

(b)

Figure L4 Strain sweep test of polymer blend between Ppy and AR70 at 2 % v/v of Ppy (AR70:2_un), frequency 1.0 rad/s, 27^0 C, gap 0.720 mm at: a) E = 0 V/mm; b) E = 2000 V/mm.

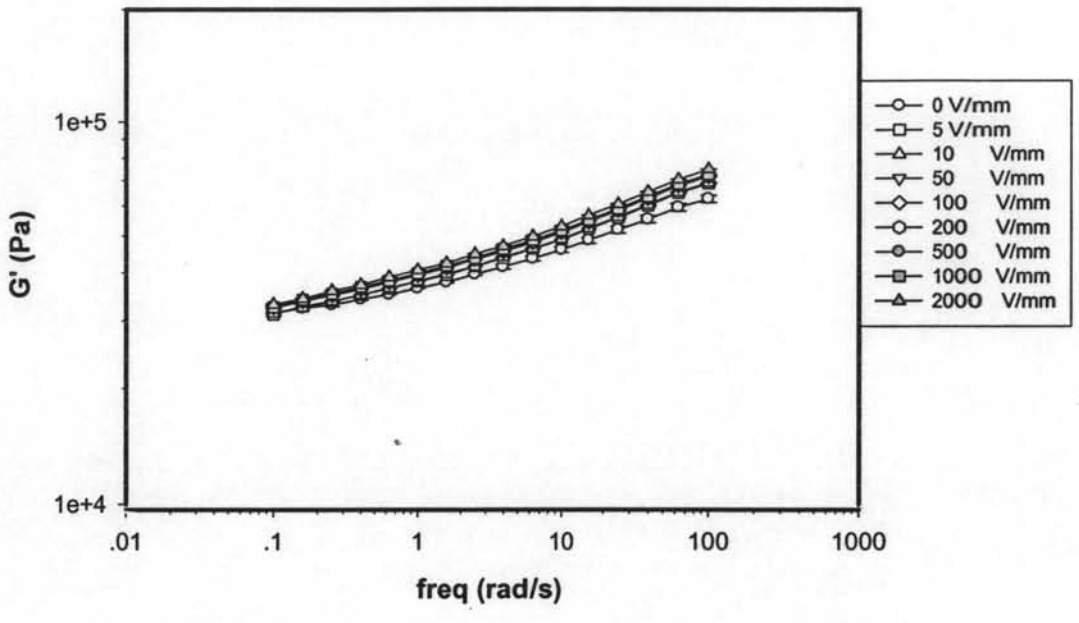

(a)

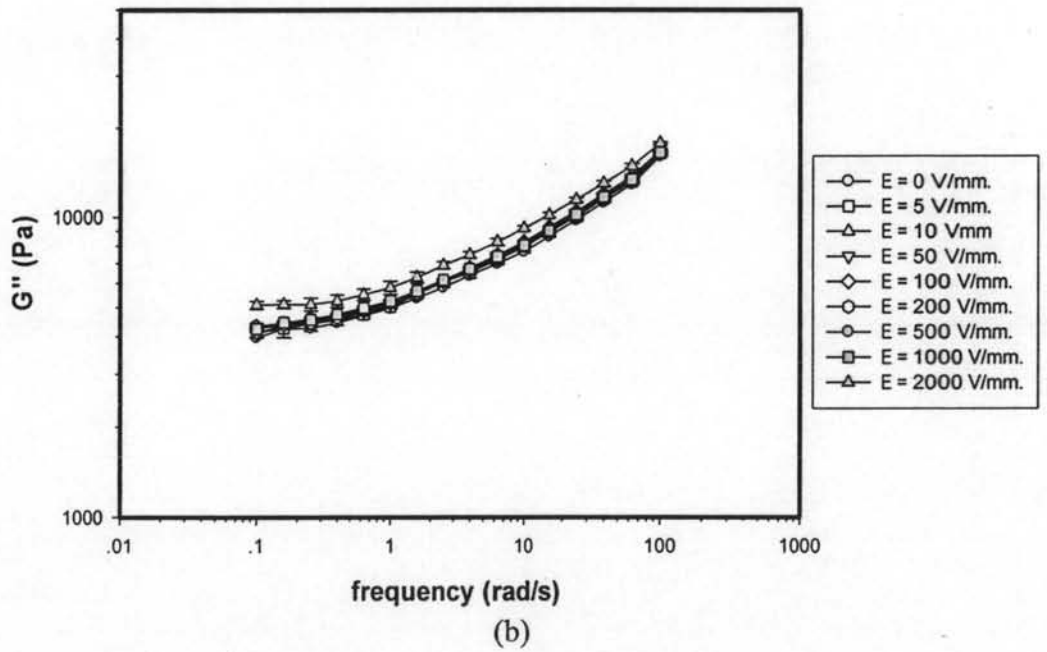

(b)

Figure L5 Frequency sweep test of polymer blend between Ppy and AR70 at 2% v/v of Ppy (AR70:2_un), strain 1%, 27^0 C, gap 0.650 mm at various electric field strengths: a) G'(Pa); b) G" (Pa).

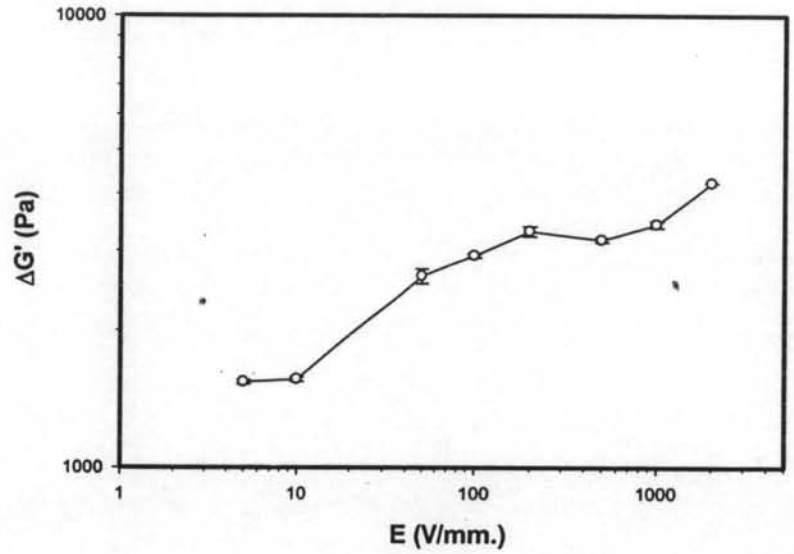

(a)

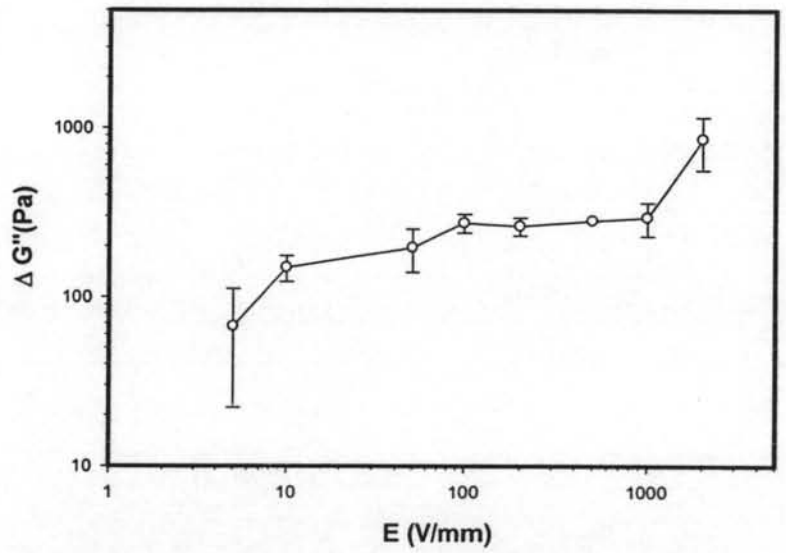

Figure L6 Responses of the storage and the loss moduli ($\Delta G'(\omega)$ and $\Delta G''(\omega)$ of polymer blend between Ppy and AR70 at 2% v/v of Ppy (AR70:2_un) vs. electric field strength, frequency 1.0 rad/s, strain 1%, gap 0.720 mm at 27^0C: (a) $\Delta G'(\omega)$; (b) $\Delta G''(\omega)$ when $G'_0 = 36{,}526$ Pa and $G''_0 = 4{,}963$ Pa.

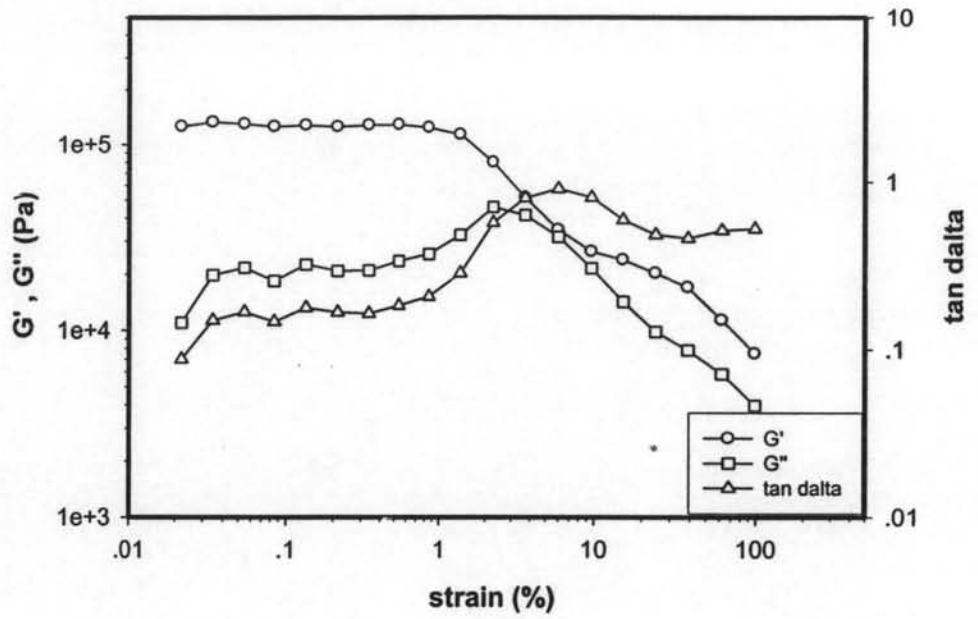

(a)

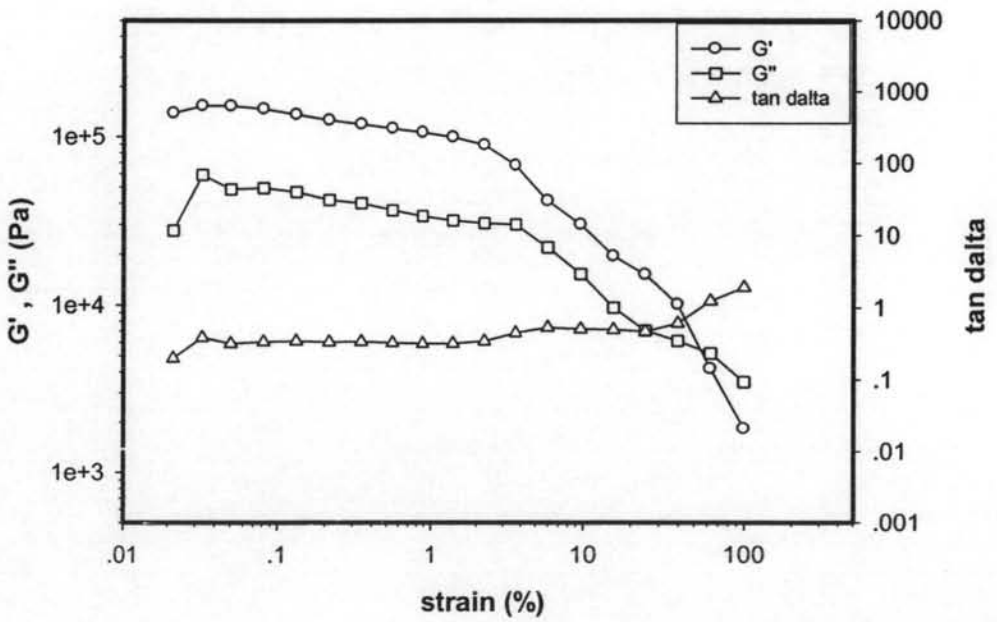

(b)

Figure L7 Strain sweep test of polymer blend between Ppy and AR70 at 3 % v/v of Ppy (AR70:3_un), frequency 1.0 rad/s, 27^0 C, gap 0.643 mm at: a) E = 0 V/mm; b) E = 2000 V/mm.

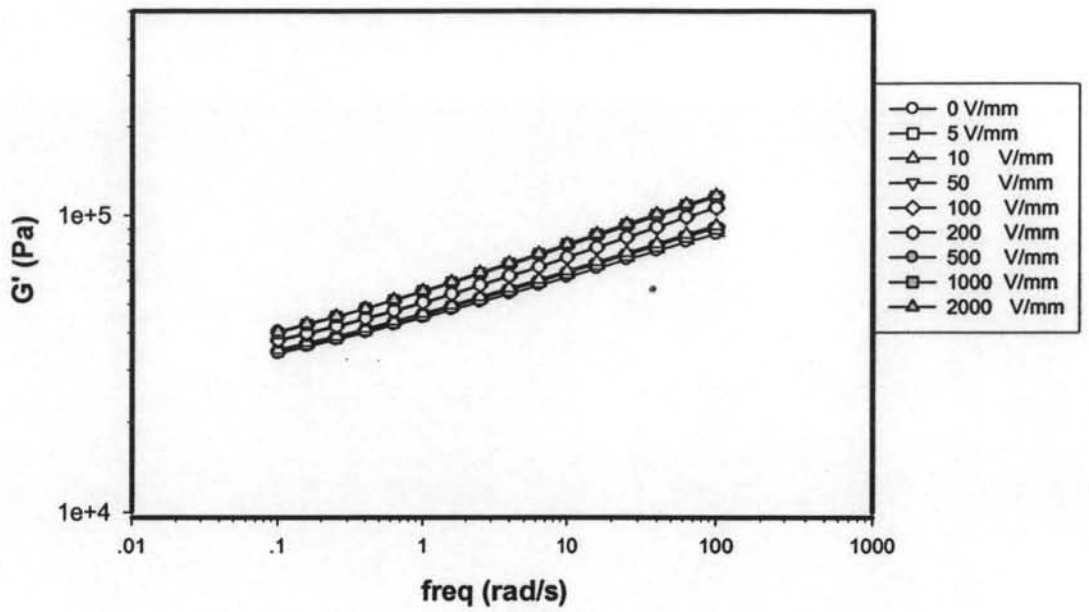

(a)

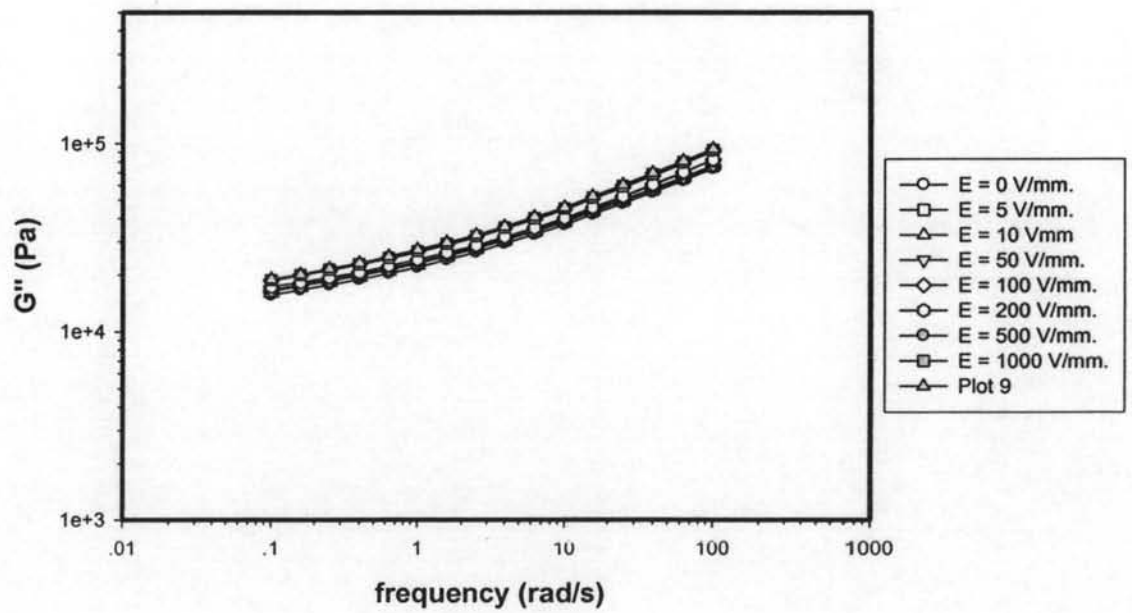

(b)

Figure L8 Frequency sweep test of polymer blend between Ppy and AR70 at 3% v/v of Ppy (AR70:3_un), strain 1%, 27^0 C, gap 0.643 mm at various electric field strengths: a) G'(Pa); b) G" (Pa).

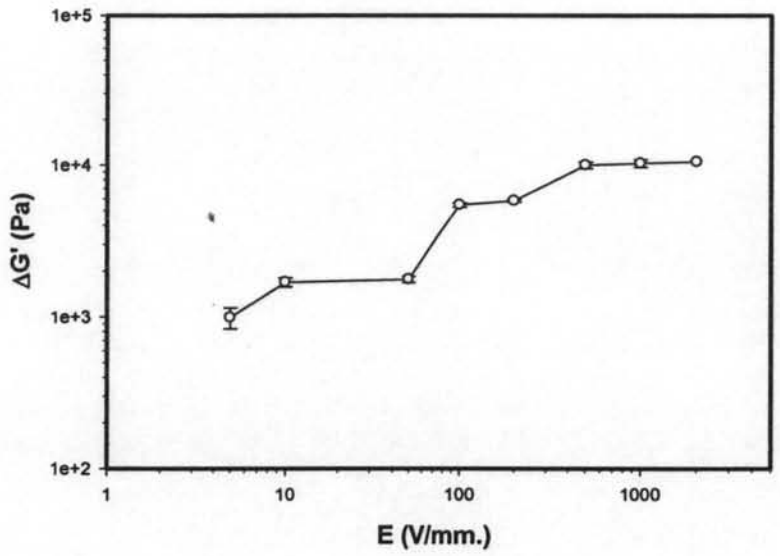

(a)

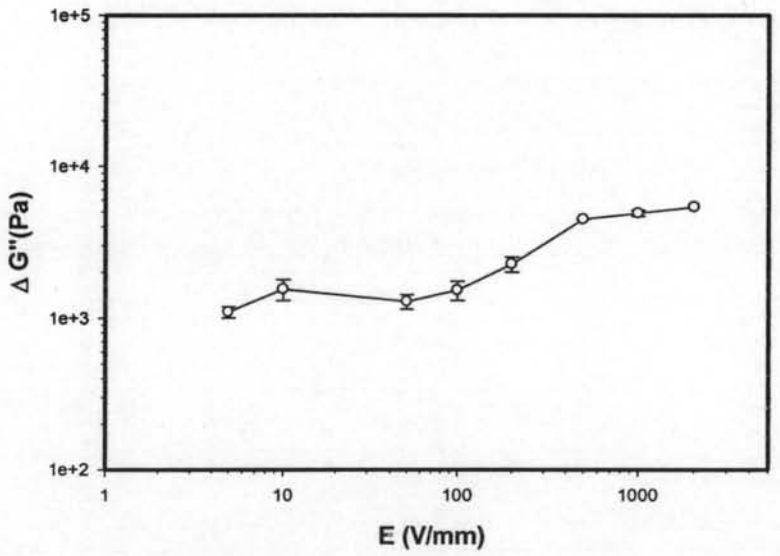

(b)

Figure L9 Responses of the storage and the loss moduli ($\Delta G'(\omega)$ and $\Delta G''(\omega)$) of polymer blend between Ppy and AR70 at 3% v/v of Ppy (AR70:3_un) vs. electric field strength, frequency 1.0 rad/s, strain 1%, gap 0.643 mm at 27^0C: (a) $\Delta G'(\omega)$; (b) $\Delta G''(\omega)$ when $G'_0 = 45{,}020$ Pa and $G''_0 = 21{,}922$ Pa.

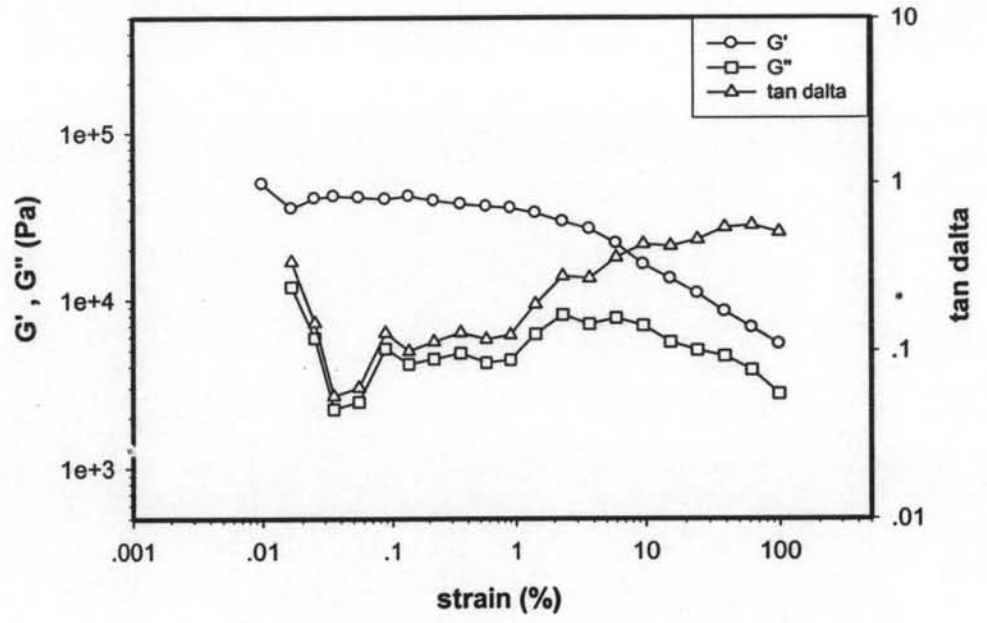

(a)

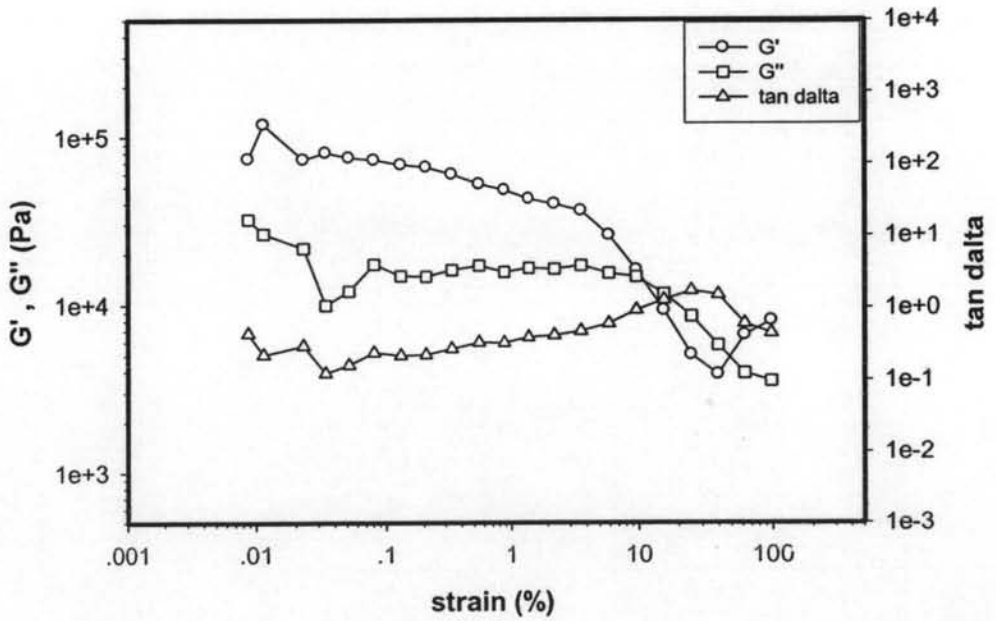

Figure L10 Strain sweep test of polymer blend between Ppy and AR70 at 4 % v/v of Ppy (AR70:4_un), frequency 1.0 rad/s, 27^0 C, gap 0.295 mm at: a) E = 0 V/mm; b) E = 2000 V/mm.

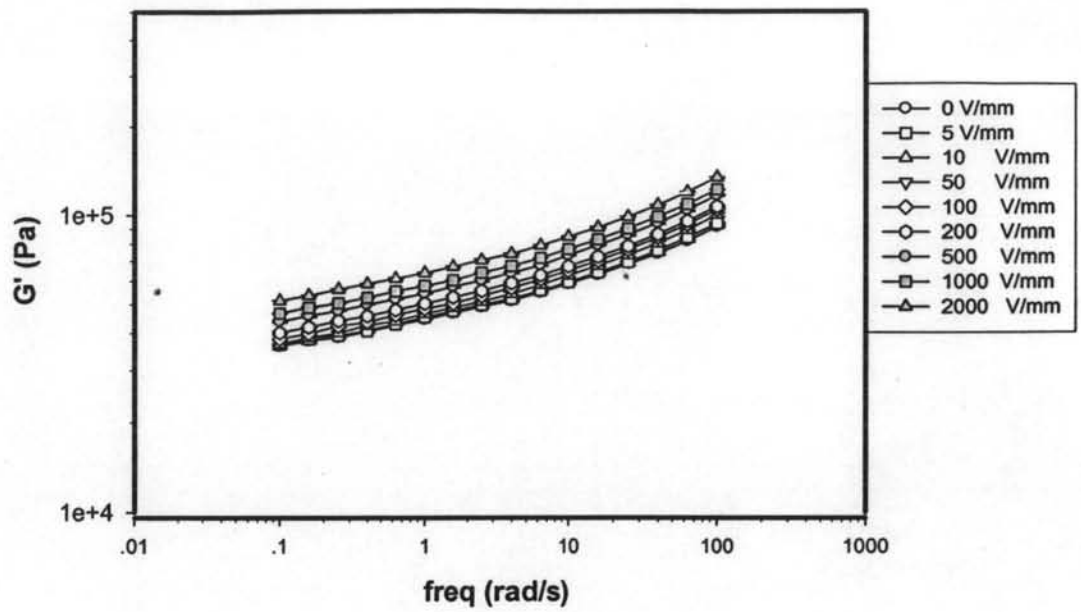

(a)

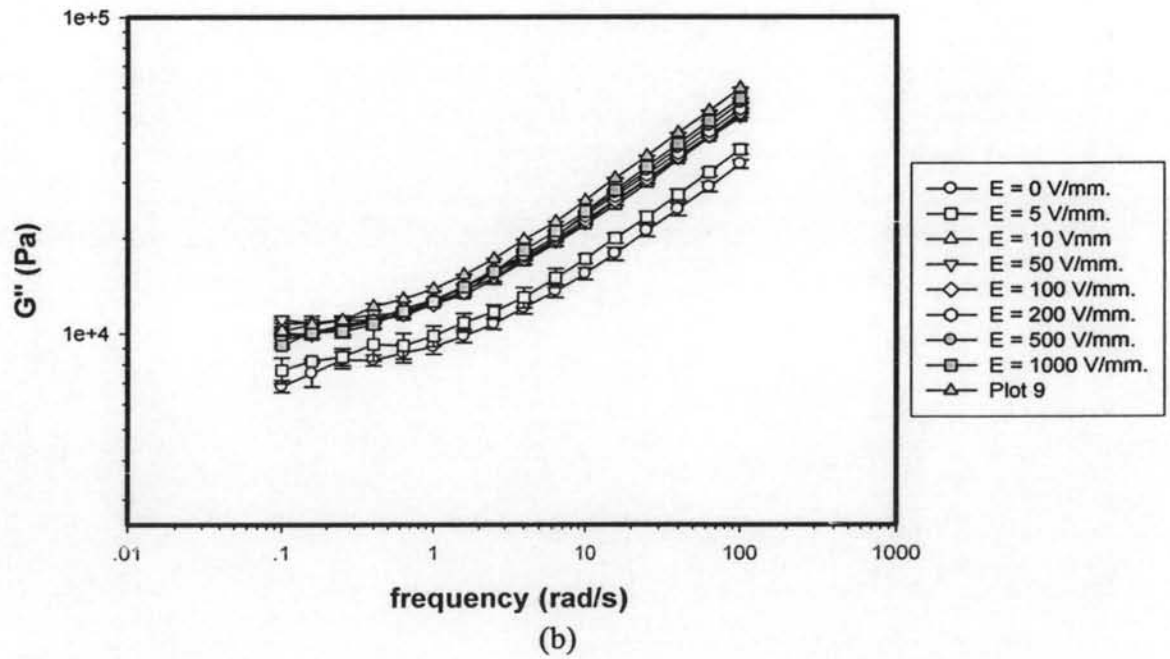

(b)

Figure L11 Frequency sweep test of polymer blend between Ppy and AR70 at 4% v/v of Ppy (AR70:4_un), strain 1%, 27^0 C, gap 0.295 mm at various electric field strengths: a) G'(Pa); b) G" (Pa).

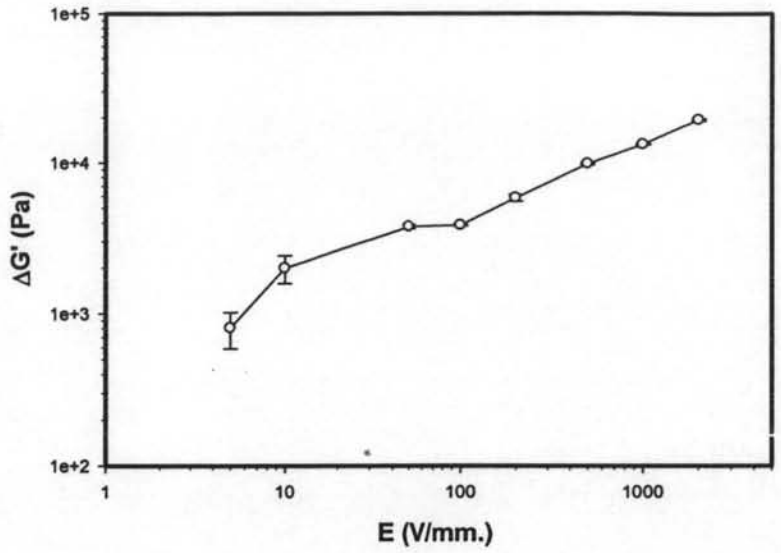

(a)

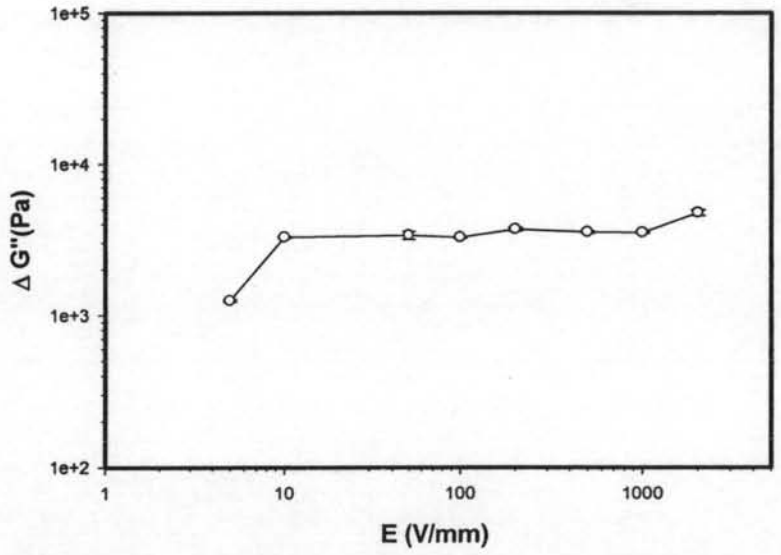

Figure L12 Responses of the storage and the loss moduli ($\Delta G'(\omega)$ and $\Delta G''(\omega)$ of polymer blend between Ppy and AR70 at 4 % v/v of Ppy (AR70:4_un) vs. electric field strength, frequency 1.0 rad/s, strain 1%, gap 0.295 mm at 27^0C: (a) $\Delta G'(\omega)$; (b) $\Delta G''(\omega)$ when $G'_0 = 44{,}658$ Pa and $G''_0 = 9120$ Pa.

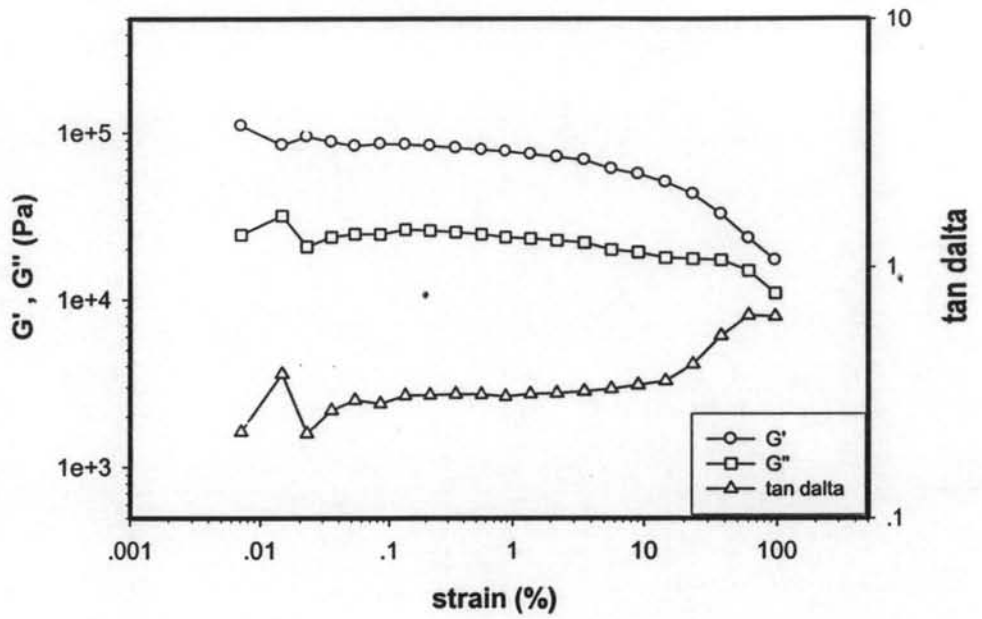

(a)

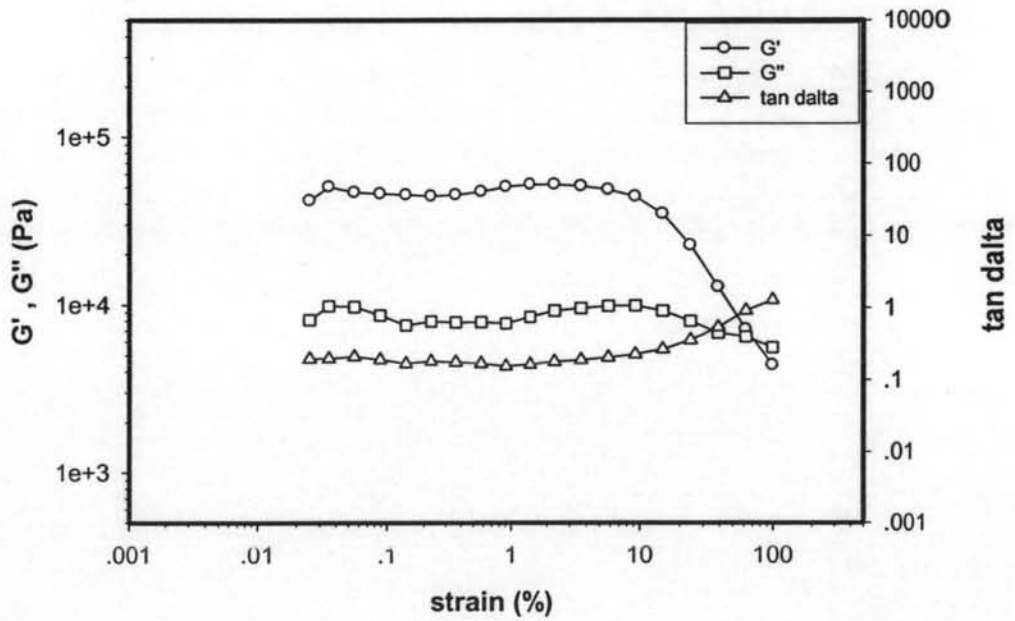

(b)

Figure L13 Strain sweep test of polymer blend between Ppy and AR70 at 5 % v/v of Ppy (AR70:5_un), frequency 1.0 rad/s, 27^0 C, gap 0.560 mm at: a) E = 0 V/mm; b) E = 2000 V/mm.

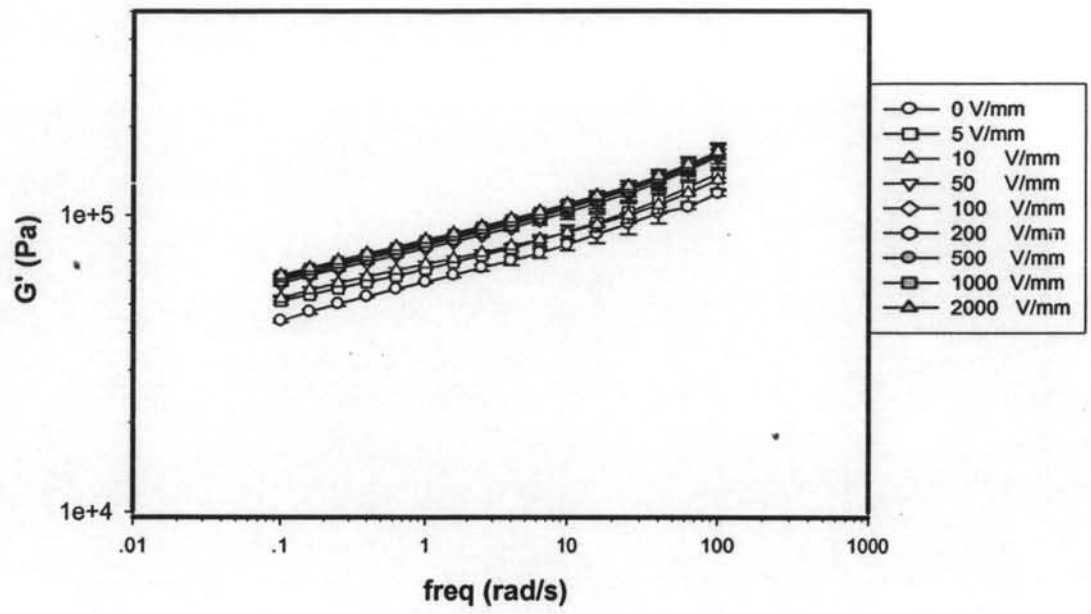

(a)

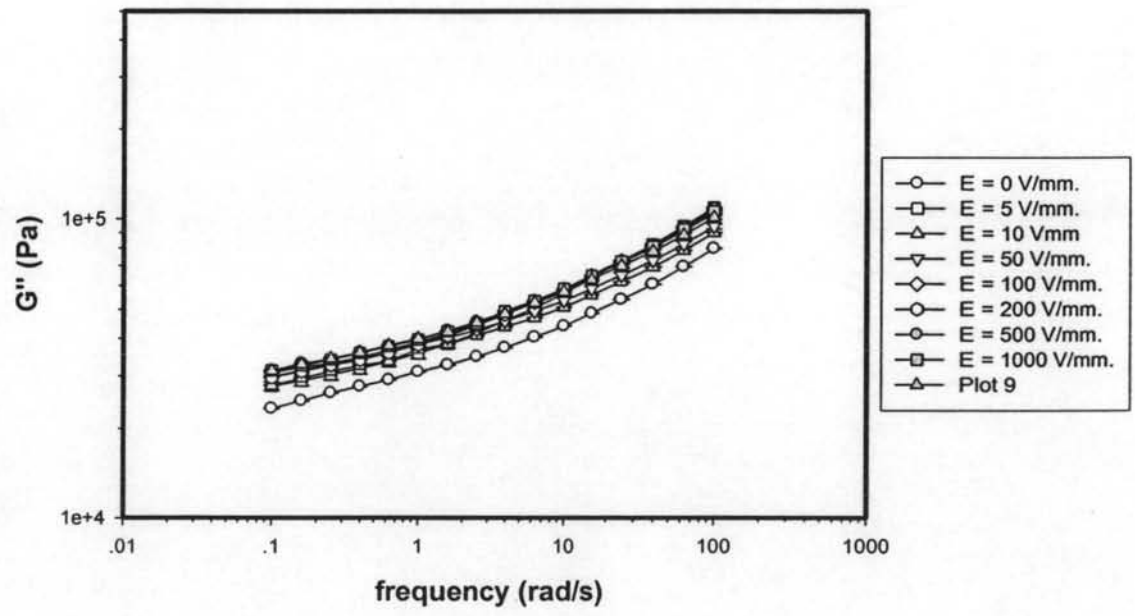

(b)

Figure L14 Frequency sweep test of polymer blend between Ppy and AR70 at 5% v/v of Ppy (AR70:5_un), strain 1%, 27^0 C, gap 0.560 mm at various electric field strengths: a) G'(Pa); b) G" (Pa).

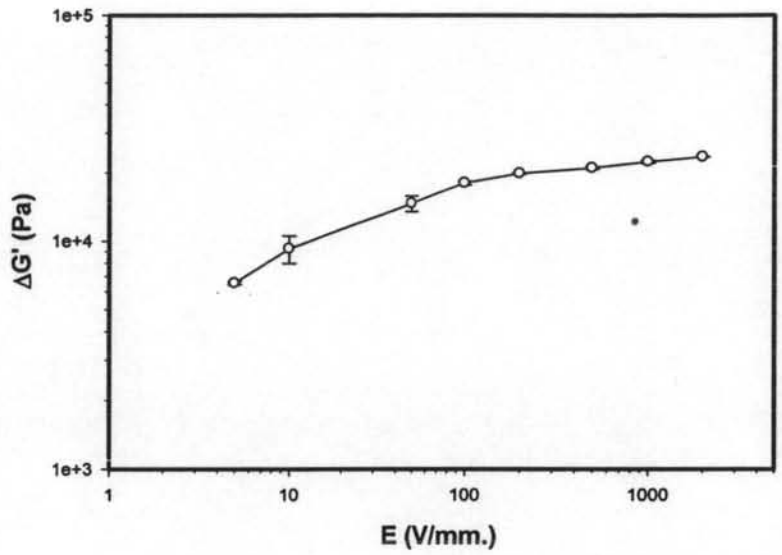

(a)

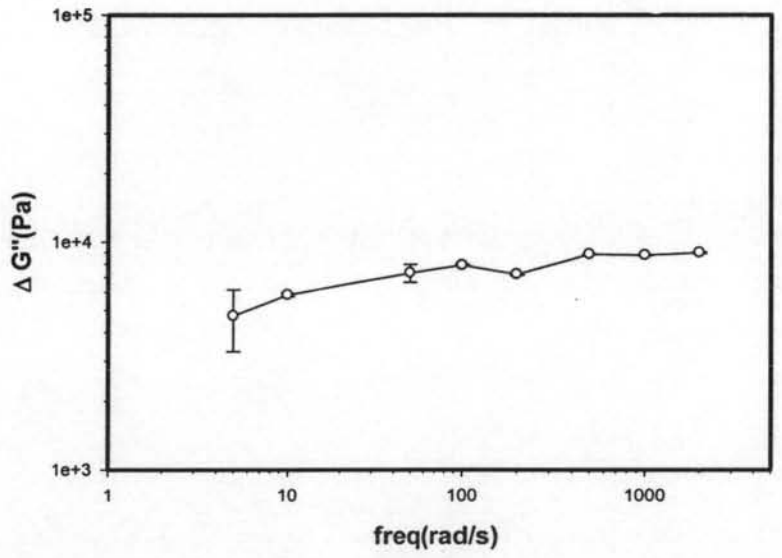

(b)

Figure L15 Responses of the storage and the loss moduli ($\Delta G'(\omega)$ and $\Delta G''(\omega)$ of polymer blend between Ppy and AR70 at 5 % v/v of Ppy (AR70:5_un) vs. electric field strength, frequency 1.0 rad/s, strain 1%, gap 0.560 mm at 27^0C: (a) $\Delta G'(\omega)$; (b) $\Delta G''(\omega)$ when G'_0 = 59,303 Pa and G''_0 = 30,962 Pa

Table L1.Rheology properties of various particle concentrations

Materials	G'_0 (Pa)	G'_{1kV} (Pa)	G'_{2kV} (Pa)	G''_0 (Pa)	G''_{2kV} (Pa)	$\Delta G'_{1KV}$ (Pa)	$\Delta G'_{2kV}$ (Pa)	$\Delta G''_{2kV}$ (Pa)	$\Delta G'_{1kV}/G'_0$	$\Delta G'_{2kV}/G'_0$	$\Delta G''_{2kV}/G''_0$	σ_{dc} (S/cm.)
AR 70	19666	40714	65418	3924.5	18789	21047	45751	14865	1.0702	2.3264	3.7877	9.63E-13
AR70:1_un	29540	43589	54764	6504.5	18954	14049	25224	12449	0.4756	0.8539	1.9139	1.28E-12
AR70:2_un	36526	39958	40763	4963.5	5820.7	3432.5	4237.3	857.20	0.0940	0.1160	0.1727	1.30E-12
AR70:3_un	45020	55392	55635	21922	27314	10372	10615	5393	0.2304	0.2358	0.2460	4.03E-12
AR70:4_un	44658	57993	64032	9120.6	13878	13336	19374	4757	0.2986	0.4338	0.5216	4.94E-12
AR70:5_un	59303	81751	82940	30962	39956	22448	23637	8995	0.3785	0.3986	0.2905	5.33E-12

Specimens were tested at frequency =1 rad/s, strain 1% and, temperature = 27 ^{0}C
Films were formed by water solution casting.
G'_0, and G''_0 is storage and loss modulus without electric field
G'_{1kV} is storage modulus at 1 kV/mm, G'_{2kV} and G''_{2kV} are storage and loss modulus at 2 kV/mm.
$\Delta G'_{1kV}$ is the the storage modulus responses between G'_0 and G'_{1kV}
$\Delta G'_{2kV}$ is the the storage modulus responses between G'_0 and G'_{2kV}
$\Delta G''_{2kV}$ is the the loss modulus responses between G''_0 and G''_{2kV}
$\Delta G'_{1kV}/G'_0$ is sensitivity of the storage modulus at 1 kV
$\Delta G'_{2kV}/G'_0$ is sensitivity of the storage modulus at 2 kV
$\Delta G''_{2kV}/G''_0$ is sensitivity of the loss modulus at 2 kV

Table L1 Induction time and recovery time of pure polyacrylate (AR70) polypyrrole/ polyacrylate(AR70) elastomer blends.

Samples	Electric field	First induction time	Saturated induction time	First recovery time	Saturated recovery time	First $\Delta G'_{ind}$	Saturated $\Delta G'_{ind}$	First $\Delta G'_{rec}$	Saturated $\Delta G'_{rec}$
	(kV/mm)	(τ_{ind}) (s)	(τ_{ind}) (s)	(τ_{rec}) (s)	(τ_{rec}) (s)	(Pa.s)	(Pa.s)	(Pa.s)	(Pa.s)
Pure AR70	1	411	424	135	436	1,824	485	1,549	613
Pure AR70	2	496	433	459	466	4,861	2,995	2,051	2,896
AR71:4_un	1	434	337	65	207	2,555	9,048	160	3,657
AR71:4_un	2	445	309	62	138	23,592	50,022	16,438	47,301

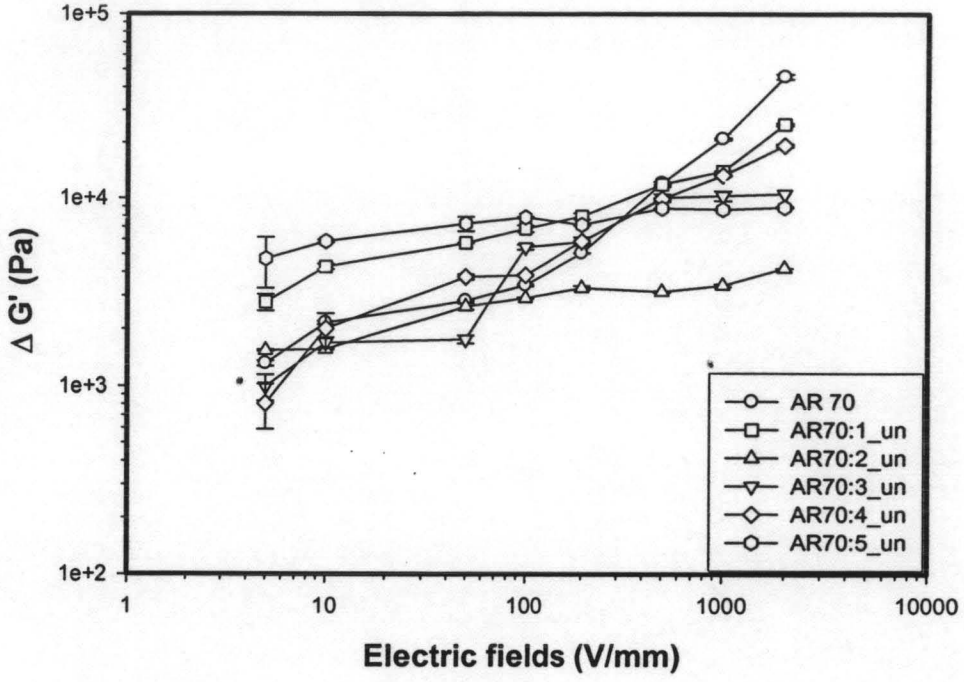

(a)

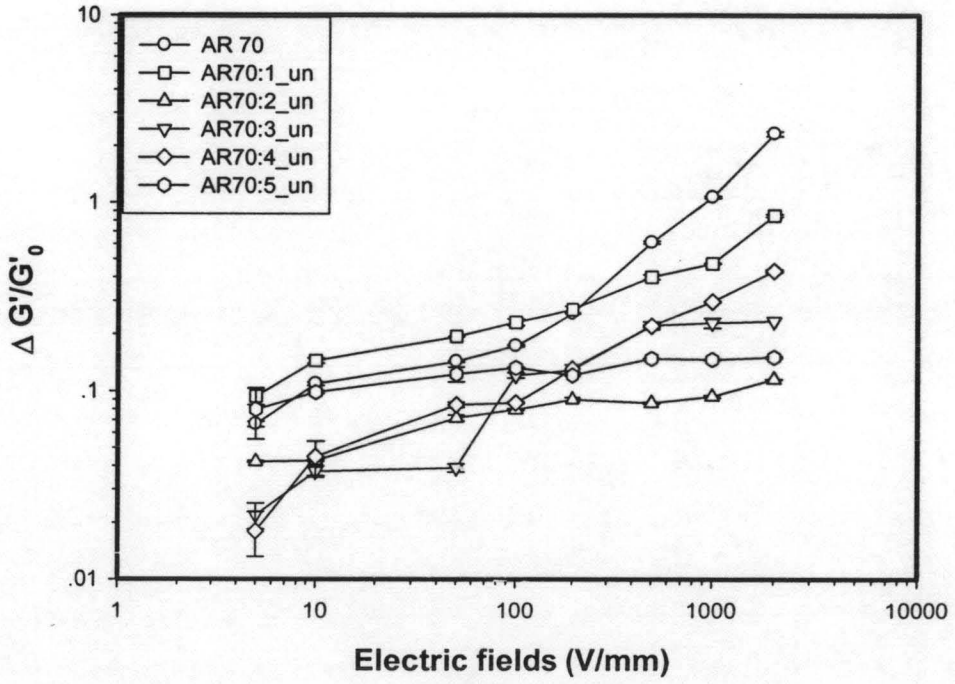

(b)

FigureL16 Effect of paticle on: (a) the storage modulus responses (Δ G') and (b) storage modulus sensitivity ($\Delta G'/G'_0$) vs. electric fields strength: 0 to 2 KV/mm at frequency 1 rad/s, strain 1%, and at 27 ^{0}C.

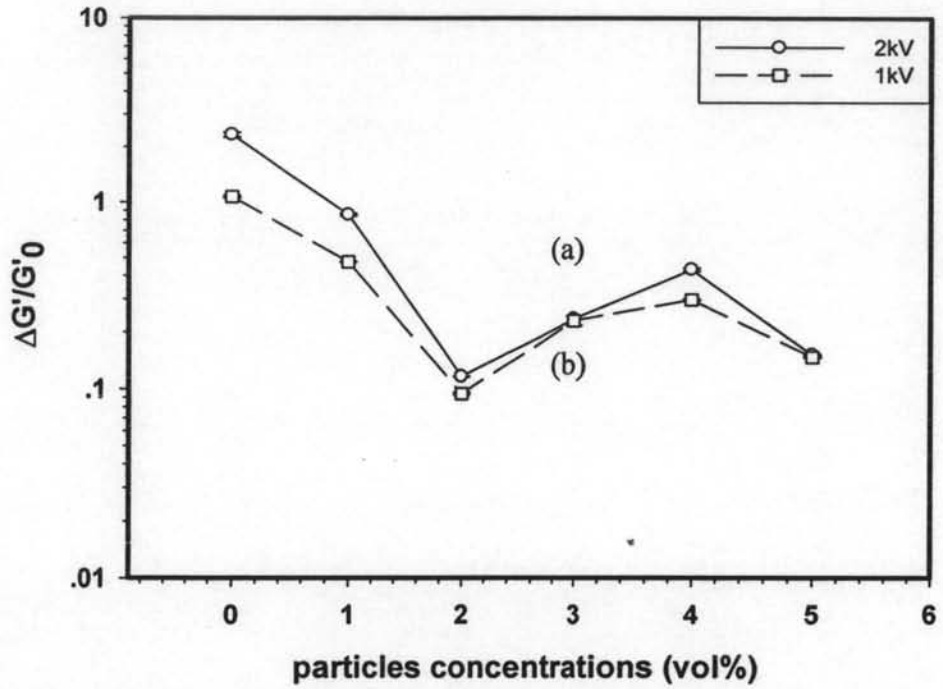

Figure L17 sensitivity vs. particle concentration, strain 1.0%, frequency 1.0 rad/s, and 27 °C: at (a) solid line, 2 kV; (b) dash line, 1 kV.

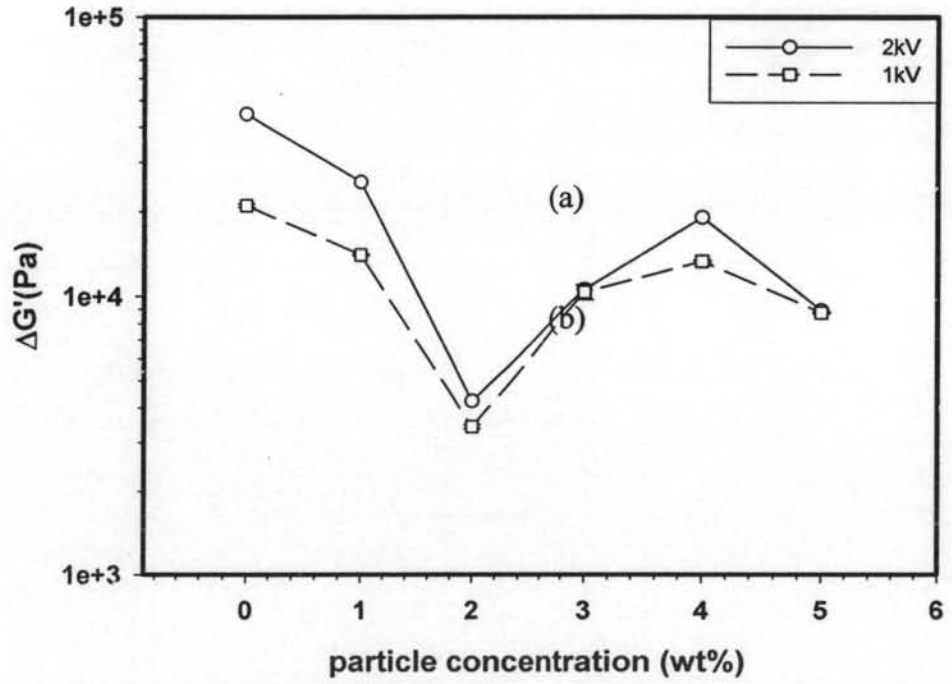

Figure 4.3 the storage modulus responses (ΔG') vs. G'_0 at strain 1.0%, frequency 1.0 rad/s, and 27 °C at: (a) solid line 2 kV; (b) dash line 1 kV.

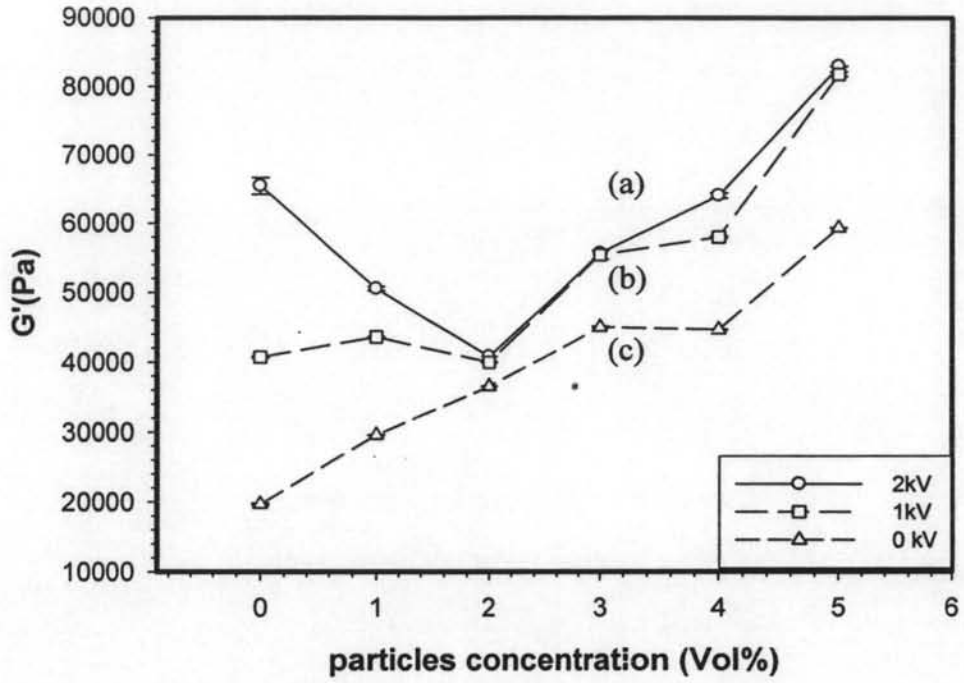

Figure L18 storage modulus (G') vs. particle concentration, strain 1.0%, frequency 1.0 rad/s, and 27 °C: at (a) solid line, 2 kV; (b) long dash line, 1 kV; (c) short dash line, 0 kV.

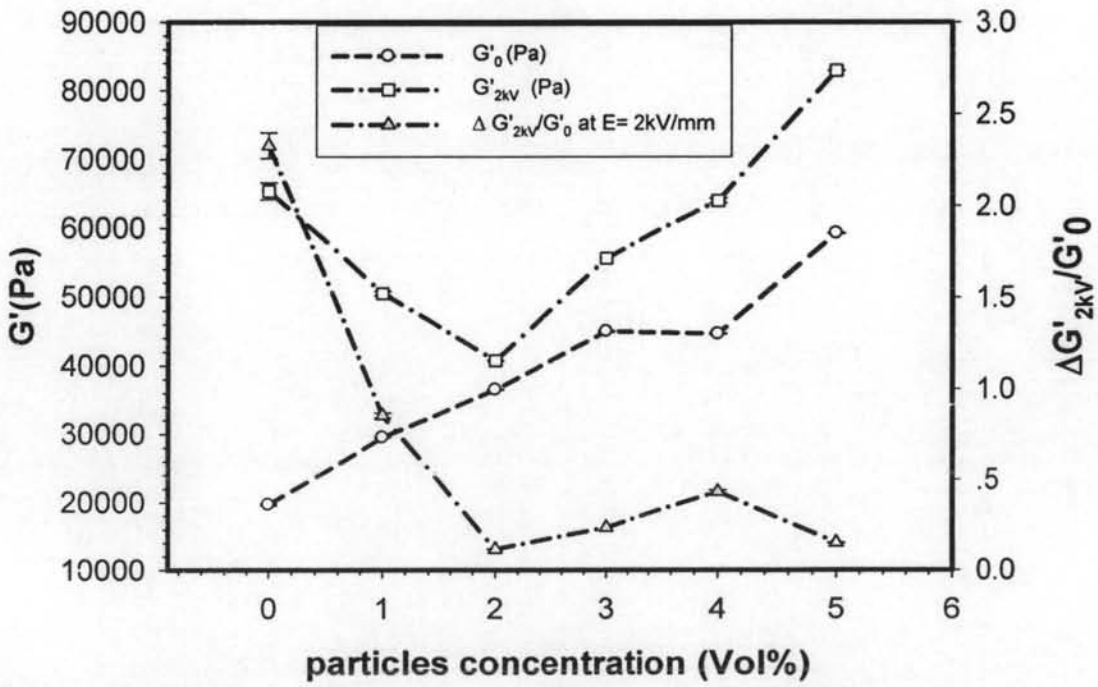

Figure L19 Sensitivity of the polymer blends between AR70 and Ppy (G' and $\Delta G'_{2kV}/G'_0$), versus Ppy various concentrations at 27°C, frequency 1 rad/s.

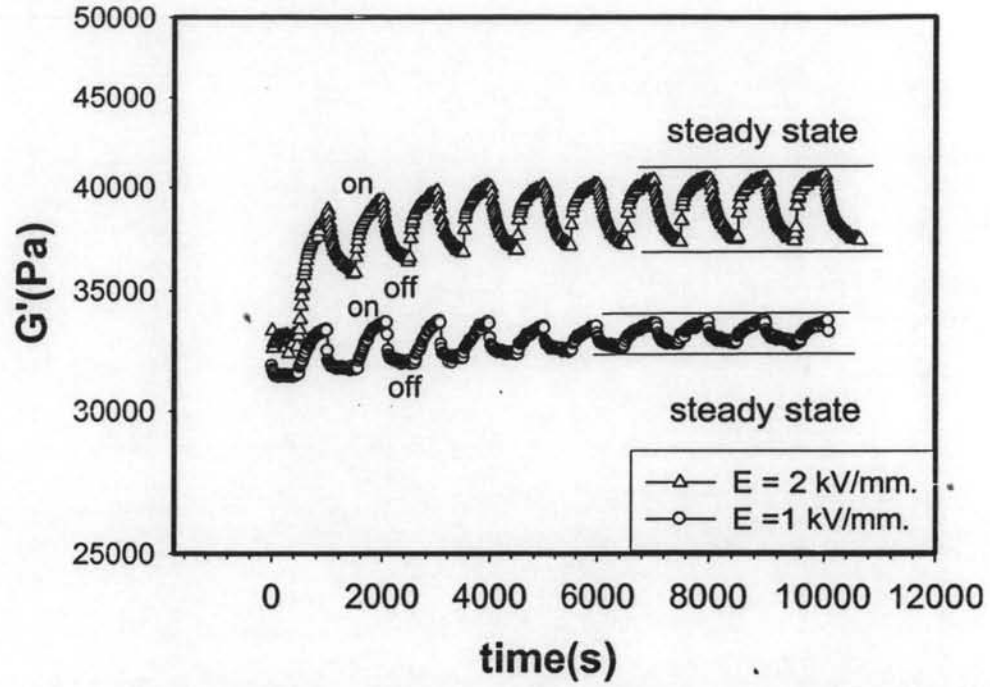

Figure L20 Temporal response of storage modulus (G') of AR70 matrix at electric field strength of 1 and 2 KV/mm, frequency 1.0 rad/s, strain 0.1%, and at 27 ^{0}C.

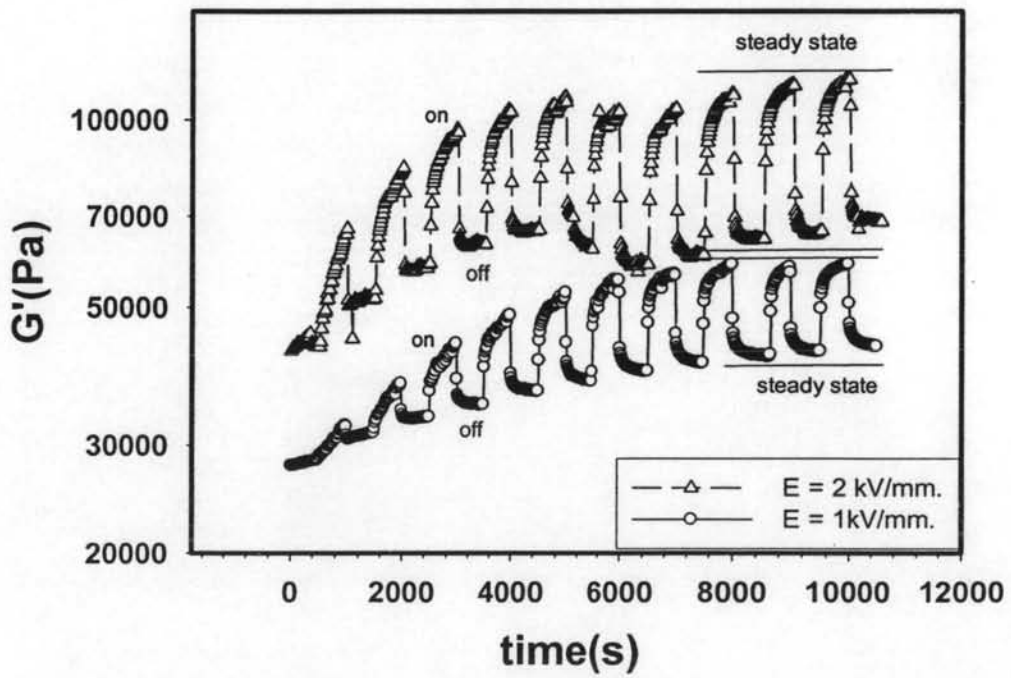

Figure L21 Temporal response of storage modulus (G') of polymer blend between AR70 and undoped Ppy 4% v/v (AR71:4_un) at electric field strength of 1 and 2 KV/mm, frequency 1.0 rad/s, strain 1.0%, and at 27 ^{0}C.

CURRICULUM VITAE

NAME: Mr. Piayalarp Ludeelerd

Date of birth: Feb 18, 1982

Nationality: Thai

University Education

2000-2004 Bachelor Degree of Material Science, Faculty of Science, Chulalongkorn University, Bankok, Thailand